

Elettra Sincrotrone Trieste

Soft X-ray Microscopy

Alessandra Gianoncelli
alessandra.gianoncelli@elettra.eu

Elettra Sincrotrone Trieste, Trieste, Italy

XVIII School on Synchrotron Radiation
"Gilberto Vlaic":
Fundamentals, Methods and Applications
Muggia (Trieste), Italy
21 September – 1 October September 2026

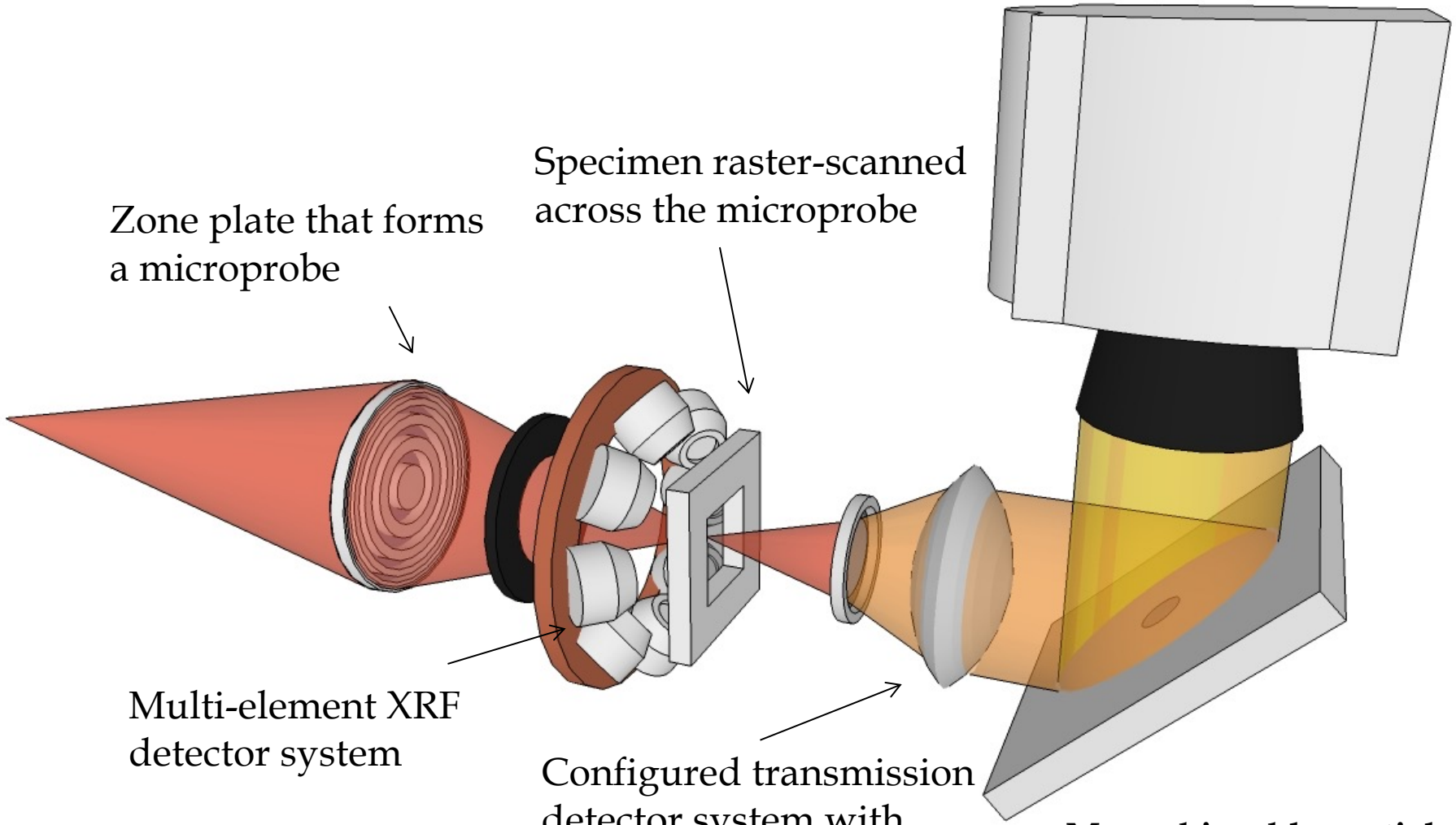
Società Italiana Luce di Sincrotrone

Elettra Sincrotrone Trieste

Elettra Sincrotrone Trieste

TwinMic

• Scanning X-ray microscope (STXM) at Elettra (TwinMic beamline)



Max achievable spatial resolution: 30-50nm

Elettra Sincrotrone Trieste

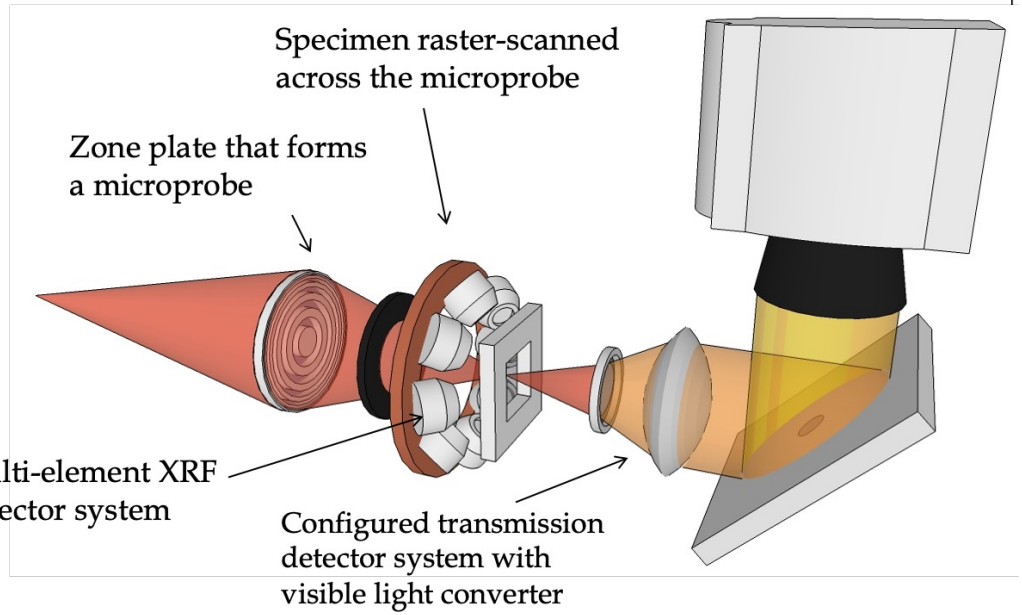
TwinMic

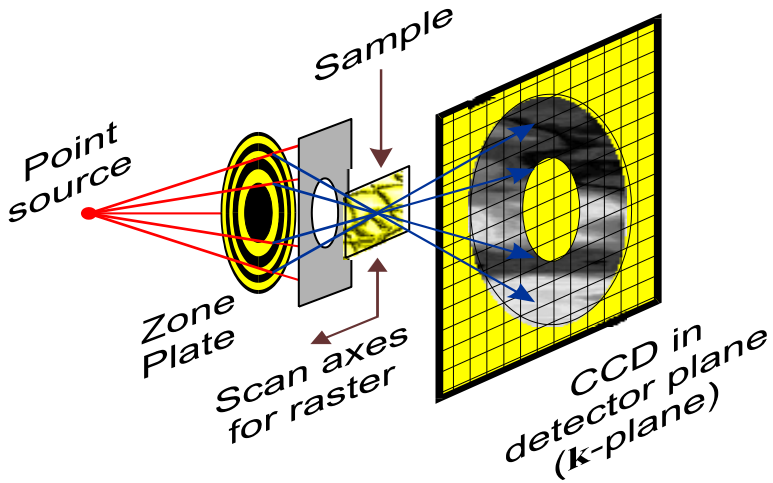
• TwinMic beamline - STXM mode

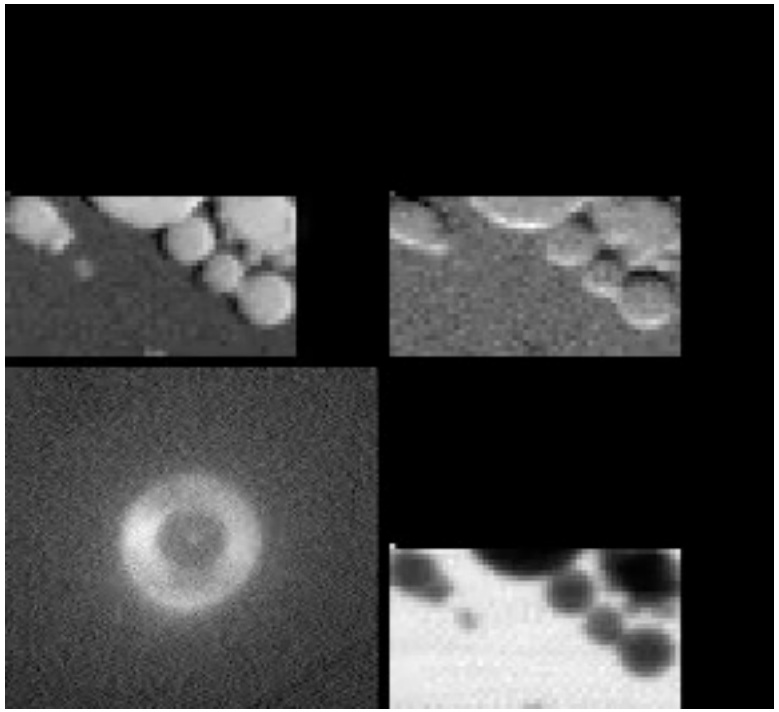
400-2200 eV

In the future 250-4200 eV

High vaccum: 10^{-6} mbar







Simultaneous acquisition of:

- Absorption or transmission
- Differential phase contrast
- Darkfield images

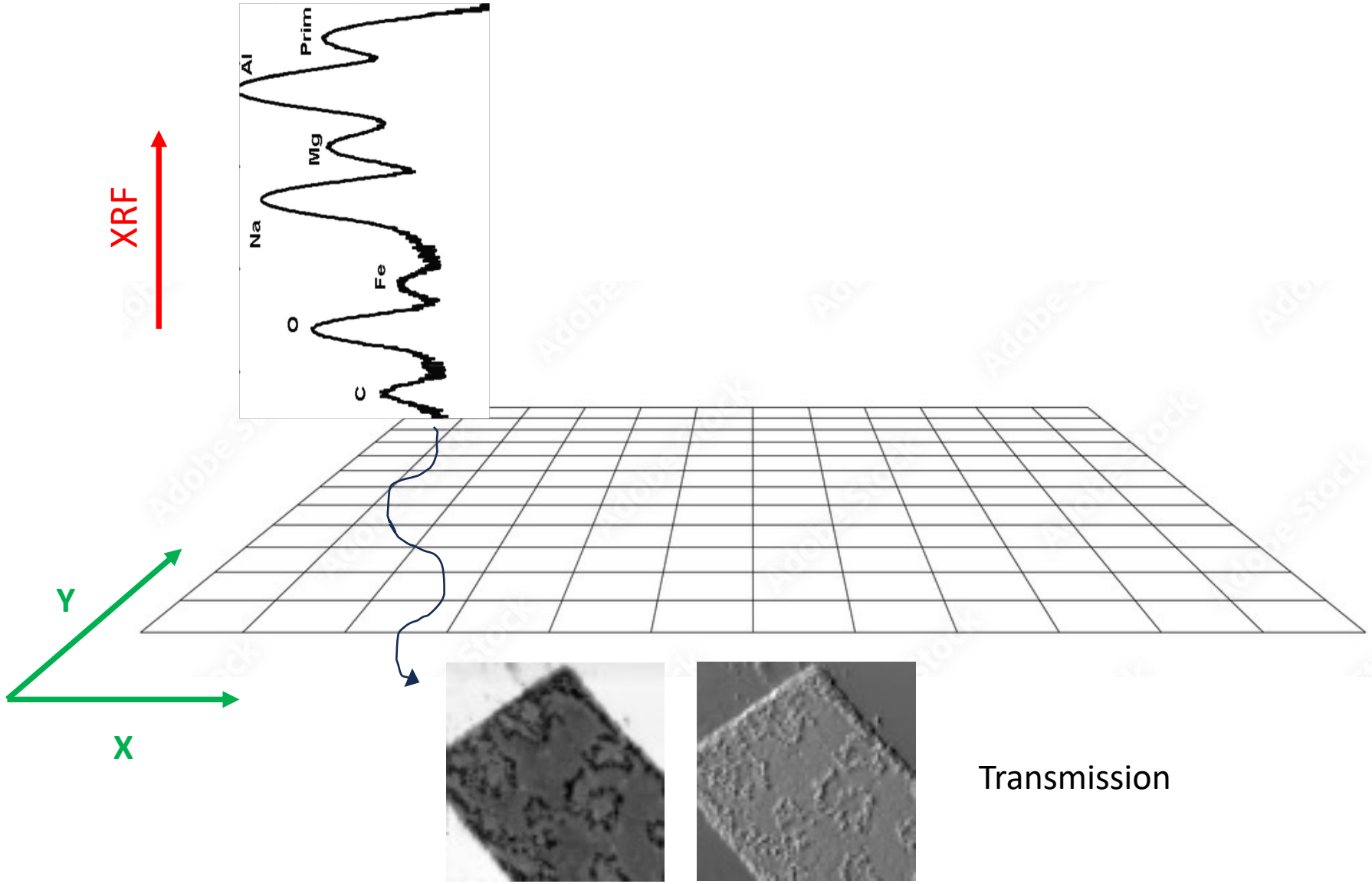
Spatial resolution 50nm-2µm

Morrison, G. et al., IPAP Conf. Series 7, 377-379 (2006)
Gianoncelli A. et al., Appl Phys Lett 89, 251117 (2006)

Elettra Sincrotrone Trieste

TwinMic

• XRF acquisition

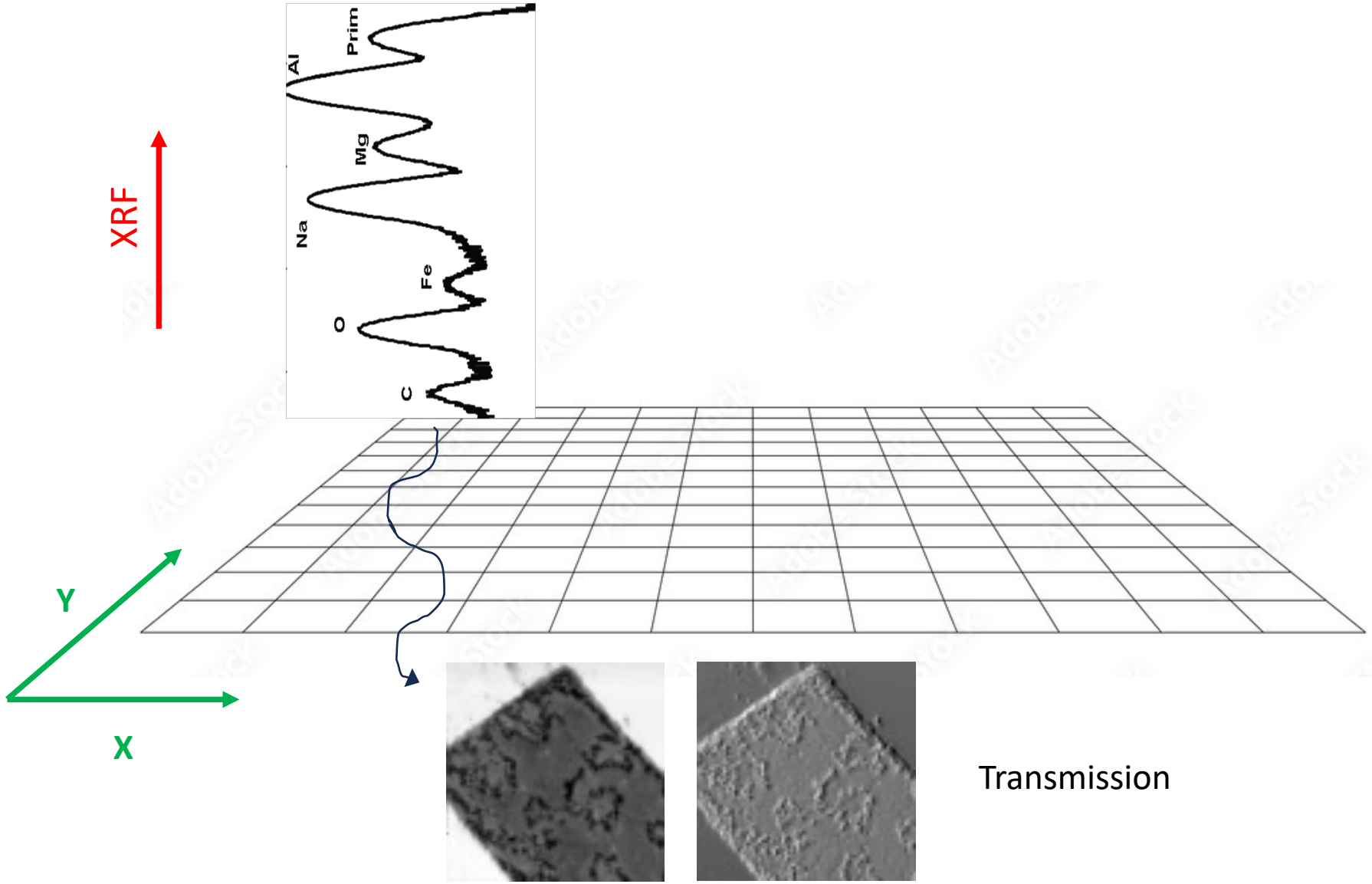


Transmission

Elettra Sincrotrone Trieste

TwinMic

• XRF acquisition

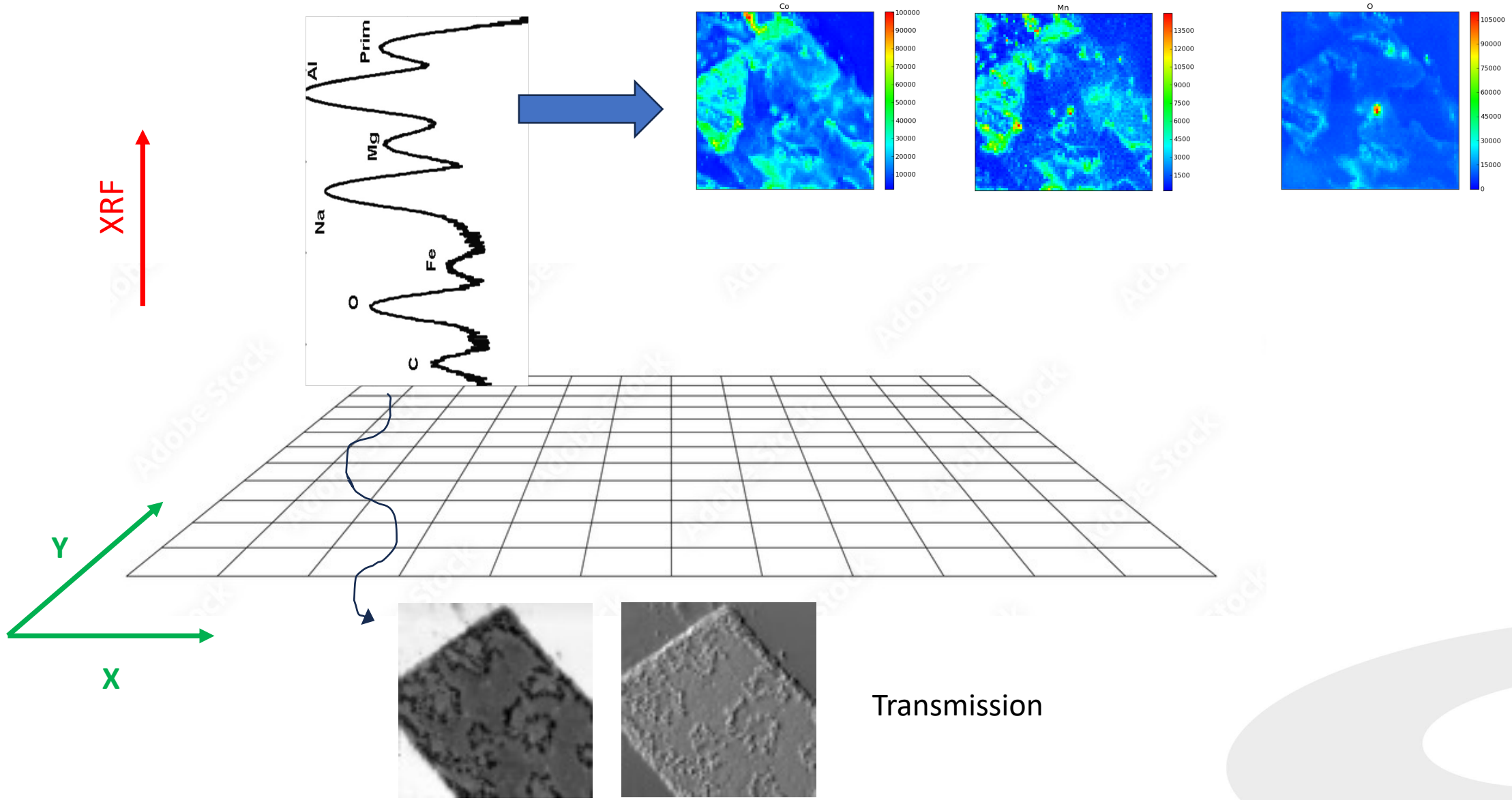


Transmission

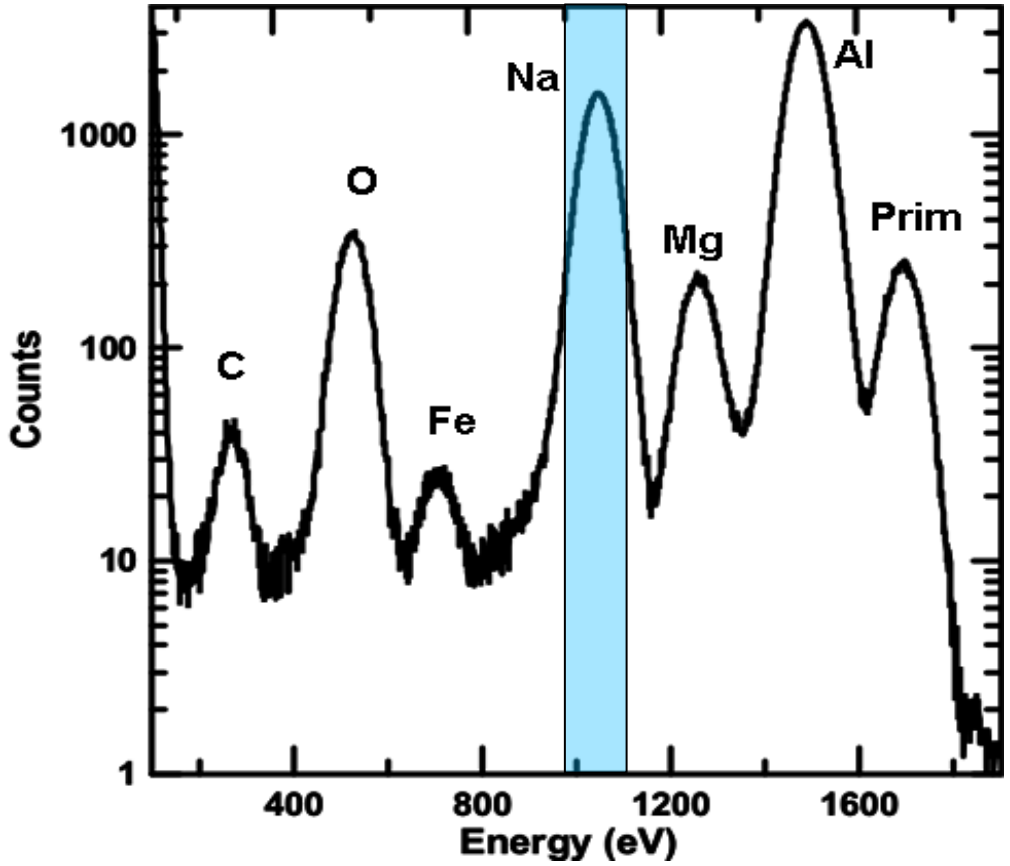
Elettra Sincrotrone Trieste

TwinMic

• XRF acquisition



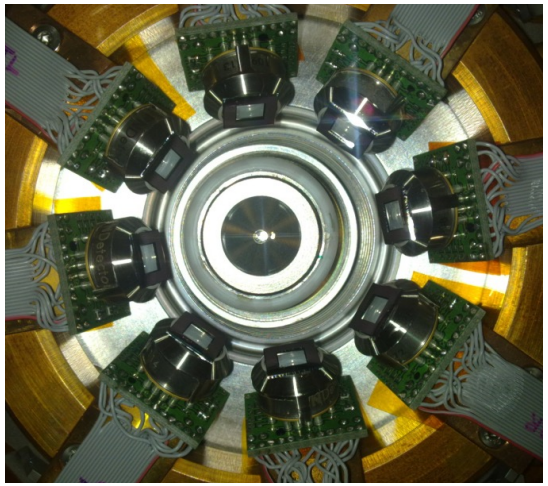
Low-energy X-ray fluorescence:

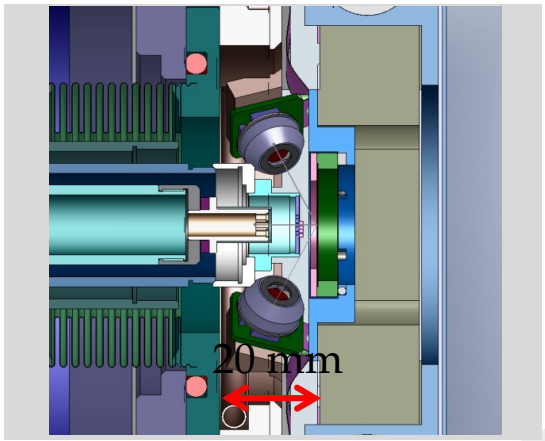


TwinMic LEXRF spectrum with unfocused beam of a test organic matrix on a metal shim

Dynamic range: up to 30 kcounts/s

Average FWHM energy resolution @ C- K edge: 69 eV





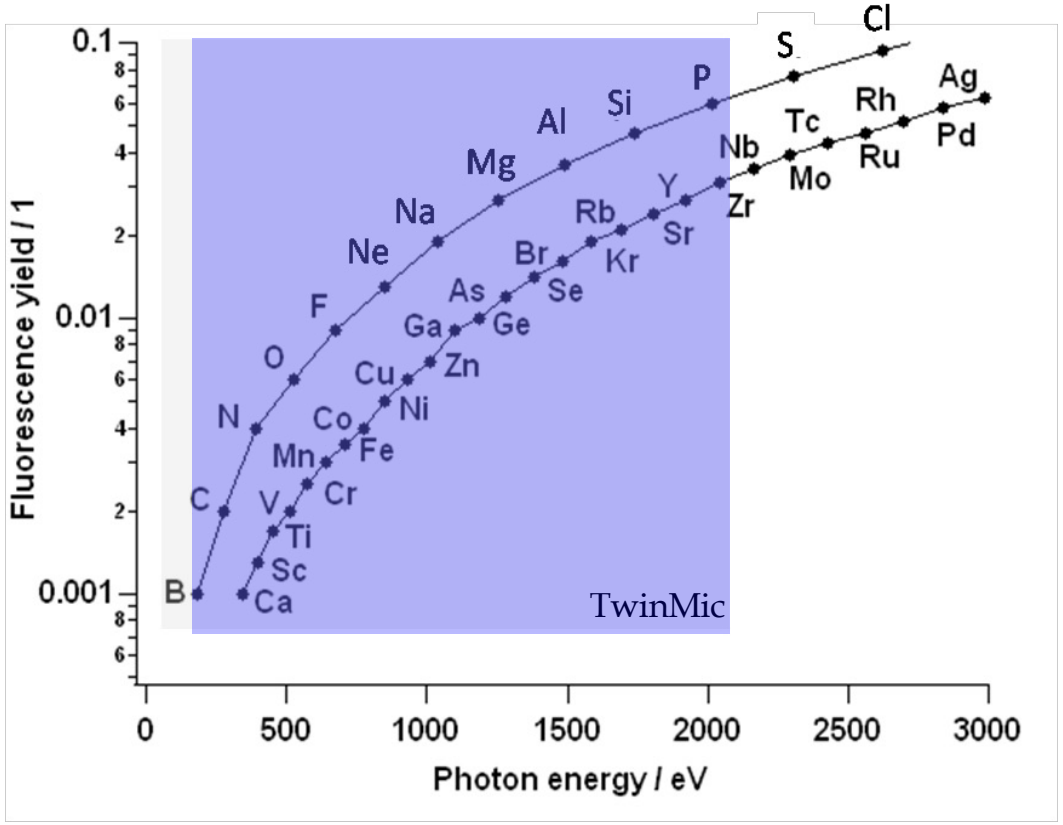
A. Gianoncelli, B. Kaulich, M. Kiskinova, R. Alberti, T. Klatka, A. Longoni, A. de Marco, A. Marcello, Simultaneous Soft X-ray Transmission and Emission Microscopy, Nucl. Instr. and Meth. A 608 (1), 195-198

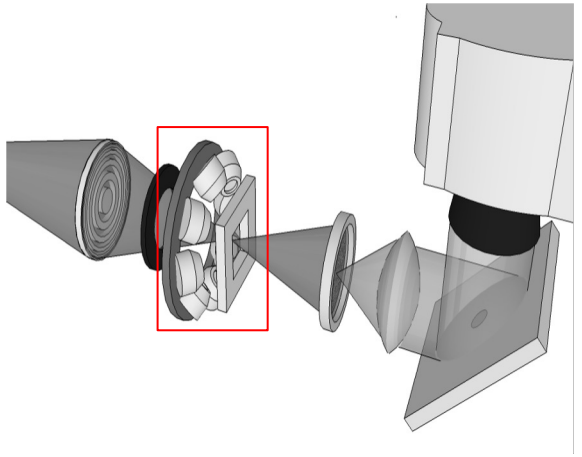
Elettra Sincrotrone Trieste

TwinMic

• LEXRF @TwinMic

Low-energy X-ray fluorescence for elemental analysis:





Detecting trace elements:

X-ray fluorescence: ~1000x better sensitivity than electrons for trace elemental mapping (ion concentrations etc.).

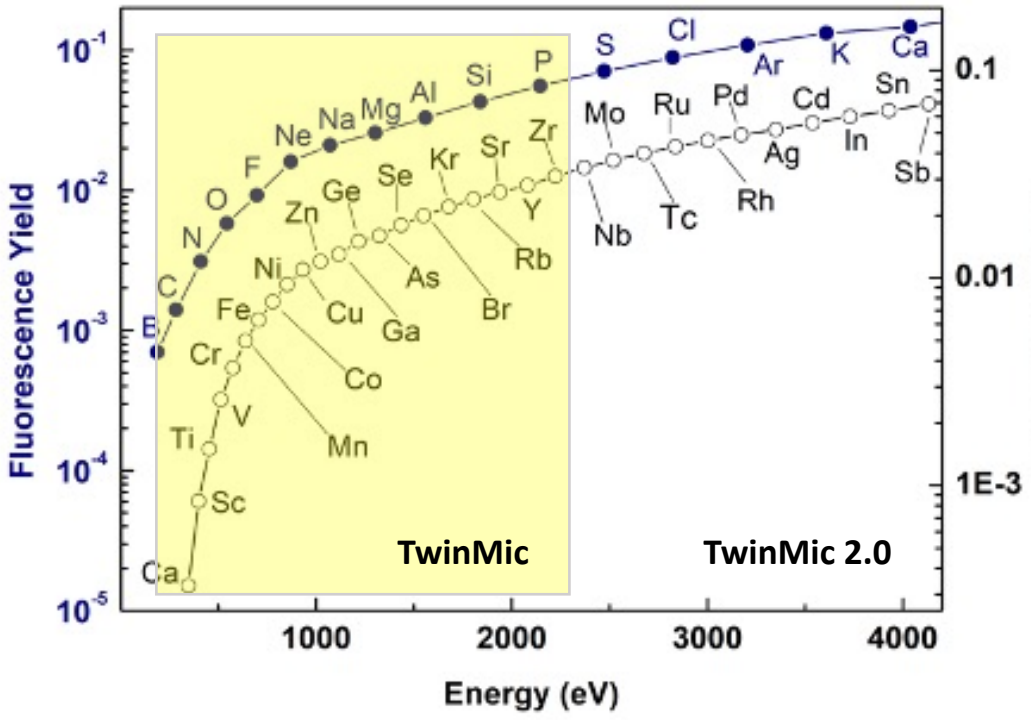
Low fluorescence yields for soft X-rays! !!

A. Gianoncelli, B. Kaulich, M. Kiskinova, R. Alberti, T. Klatka, A. Longoni, A. de Marco, A. Marcello, Simultaneous Soft X-ray Transmission and Emission Microscopy, Nucl. Instr. and Meth. A 608 (1), 195-198

Elettra Sincrotrone Trieste

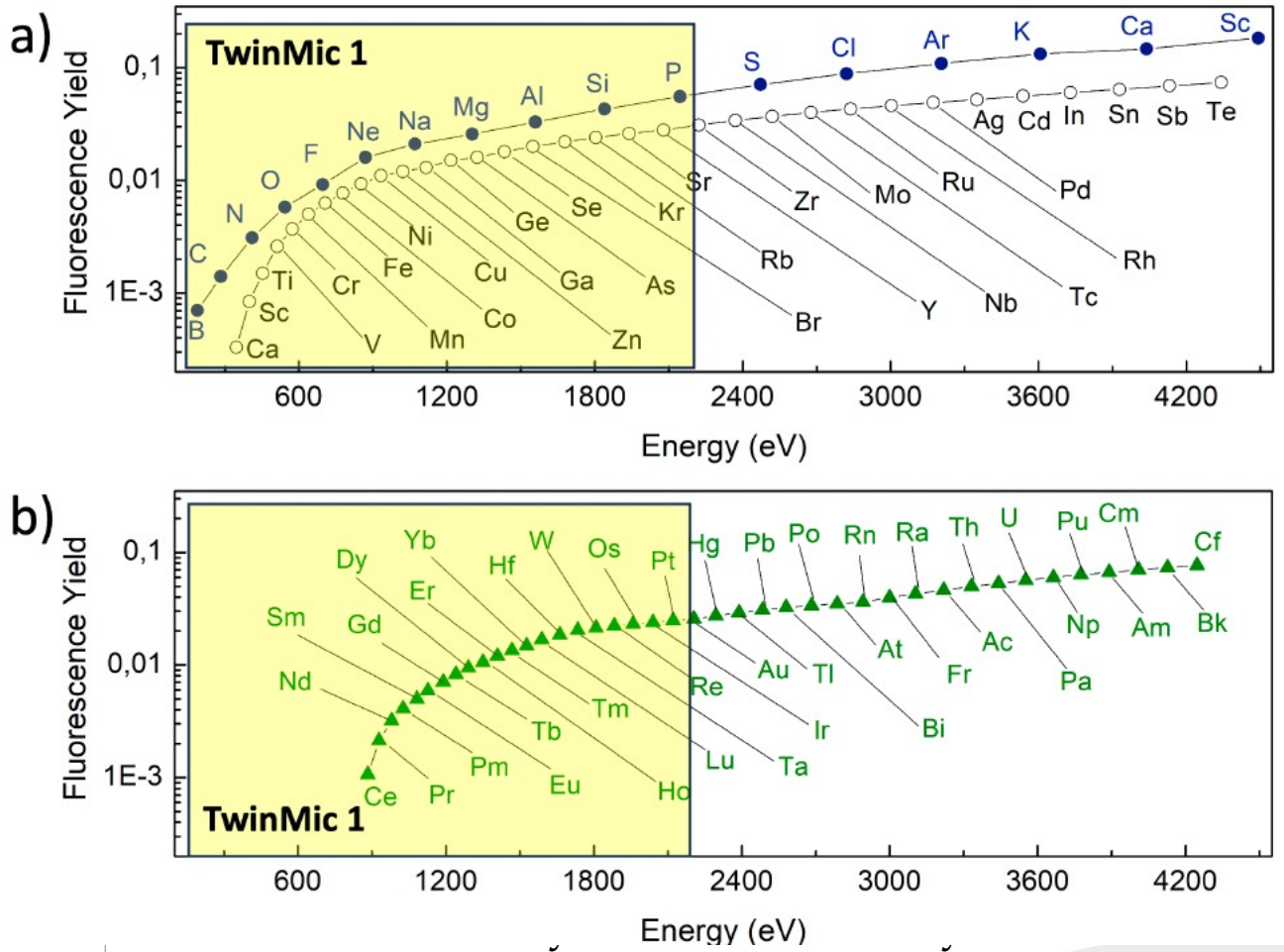
TwinMic

Low-energy X-ray fluorescence for elemental analysis:



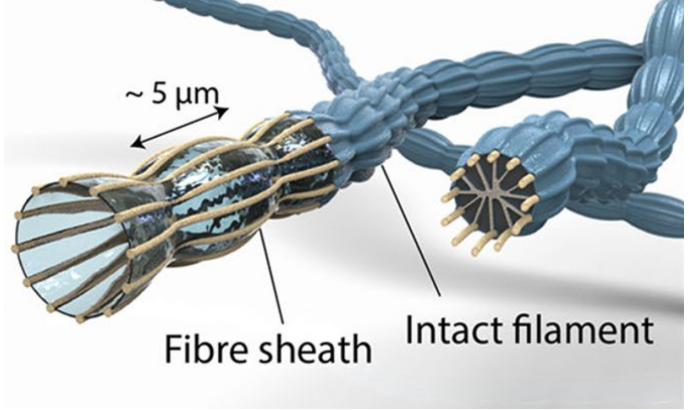
A. Gianoncelli, B. Kaulich, M. Kiskinova, R. Alberti, T. Klatka, A. Longoni, A. de Marco, A. Marcello, Simultaneous Soft X-ray Transmission and Emission Microscopy, Nucl. Instr. and Meth. A 608 (1), 195-198

- LEXRF @ TwinMic2



A. Gianoncelli *et al* 2026 *JINST* **21** C05007**DOI** 10.1088/1748-0221/21/05/C05007

Elettra
Sincrotrone
Trieste



Cable Bacteria

- Long-distance electrical conductance in marine sediment in the ocean floor has been observed since a decade.
- While bacterial nanowires, humus particles and semi-conductive mineral grains were known to conduct electrons over nanometre to micrometre distances, in 2012 it was demonstrated that filamentous bacteria, now called cable bacteria, can transport electrons over centimetre distances, with a conductivity exceptionally high for a biological material.
- LEXRF @ TwinMic, data suggested that Ni is the most likely candidate for the metal contained in the sulfur-ligated group. This conclusion was furtherly supportedby SEM-EDX, ToF-SIMS and high resolution NanoSIM.

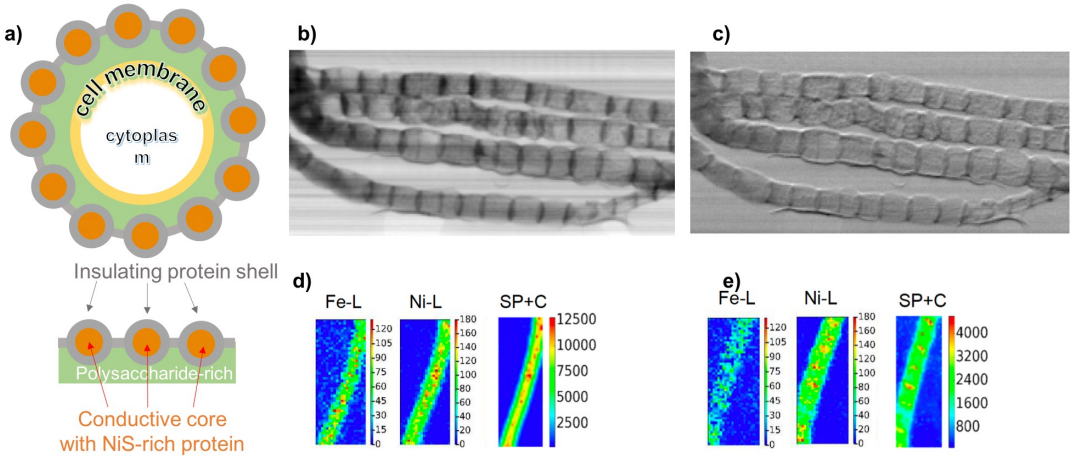
nature COMMUNICATIONS

ARTICLE

https://doi.org/10.1038/s41467-021-24312-4 OPEN

Efficient long-range conduction in cable bacteria through nickel protein wires

Henricus T. S. Boschker[1,2✉], Perran L. M. Cook[3], Lubos Polerecky[4], Raghavendran Thiruvallur Eachambadi[5], Helena Lozano[6], Silvia Hidalgo-Martinez[2], Dmitry Khalenkow[7], Valentina Spampinato[8], Nathalie Claes[9], Paromita Kundu[9], Da Wang[9], Sara Bals[9], Karina K. Sand[10], Francesca Cavezza[11], Tom Hauffman[11], Jesper Tataru Bjerg[2,12,13], Andre G. Skirtach[7], Kamila Kochan[3], Merrilyn McKee[3], Bayden Wood[3], Diana Bedolla[14], Alessandra Gianoncelli[14], Nicole M. J. Geerlings[4], Nani Van Gerven[15,16], Han Remaut[15,16], Jeanine S. Geelhoed[2], Ruben Millan-Solsona[6,17], Laura Fumagalli[18,19], Lars Peter Nielsen[12,13], Alexis Franquet[8], Jean V. Manca[5], Gabriel Gomila[6,17] & Filip J. R. Meysman[1,2✉]



Schematic view of cable bacteria fiber sheath (a); Absorption (b) and differential phase (c) images of a bundle of cable bacteria fiber sheaths; Fe, Ni and scattering peak distribution in intact cable bacteria (d) and B fiber sheaths (e). Panel b, c, d and e were acquired at TwinMic beamline at 1.1 keV, with a spatial resolution of 200nm (b and c) and 400nm (d and e).

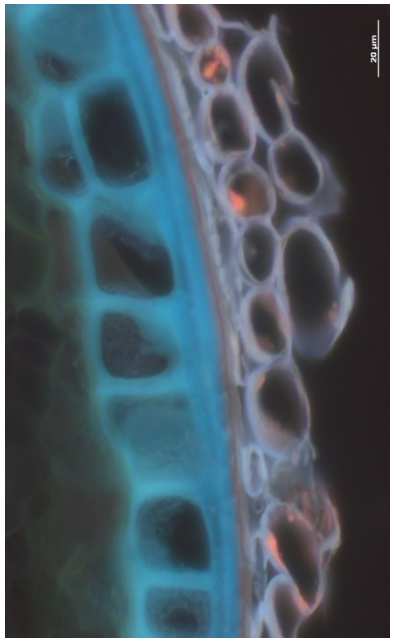
Food Science: Inside the wheat



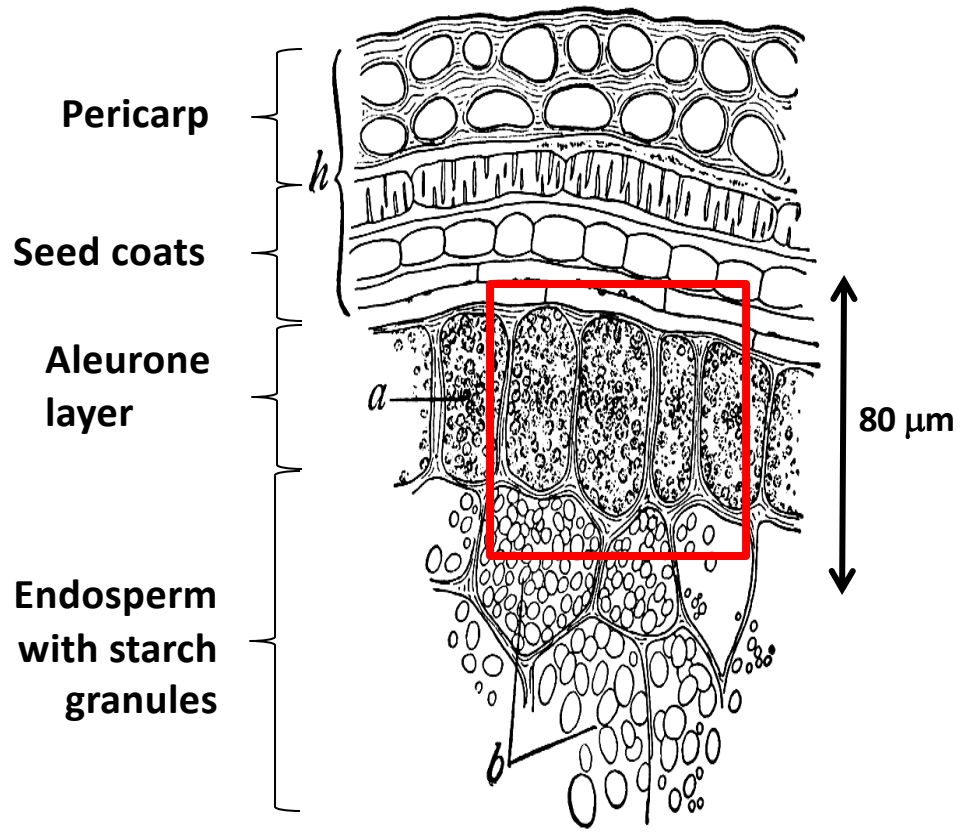
Ivan Kreft,
University Ljubljana

Functionality and toxicity of Zn in wheat and buckwheat analyzed on sub-cellular level





Structure of a wheat grain



M. Regvar, D. Eichert, B. Kaulich, A. Gianoncelli, P. Pongrac, K. Vogel-Mikus, I. Kreft, New insights into globoids of protein storage vacuoles in wheat aleurone using synchrotron soft X-ray microscopy, Journal of Experimental Botany, Vol. 62, No. 11, 3929–3939, 2011.

TwinMic

The twin X-ray microscopy station @ Elettra

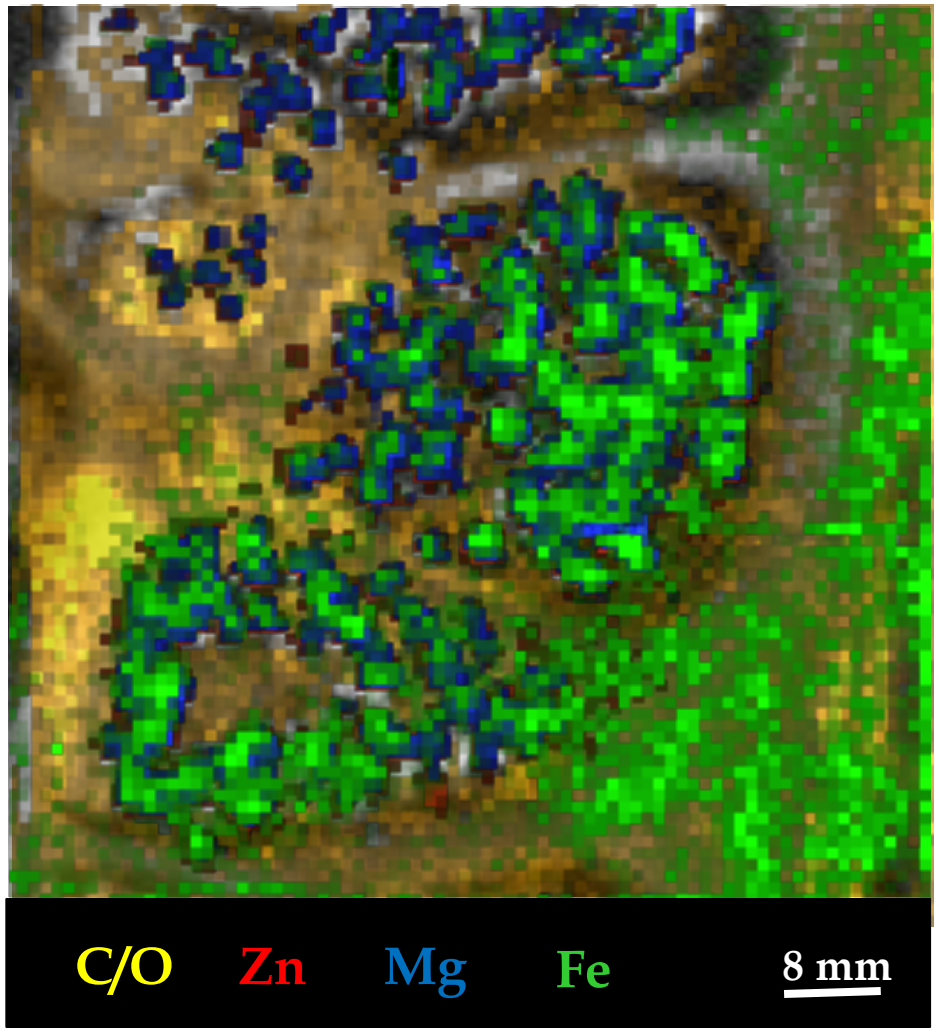


Ivan Kreft,
Fac. of Biotechnology,
University Ljubljana

Functionality and toxicity of Zn in wheat and buckwheat analyzed on sub-cellular level

Healthy control wheat

E=1686 eV
80 x 80 mm^2
80 x 80 px
8 s dwell/ px
1 mm resolution
4 detectors



M. Regvar, D. Eichert, B. Kaulich, A. Gianoncelli, P. Pongrac, K. Vogel-Mikus, I. Kreft, New insights into globoids of protein storage vacuoles in wheat aleurone using synchrotron soft X-ray microscopy, Journal of Experimental Botany, Vol. 62, No. 11, 3929–3939, 2011.

Elettra Sincrotrone Trieste

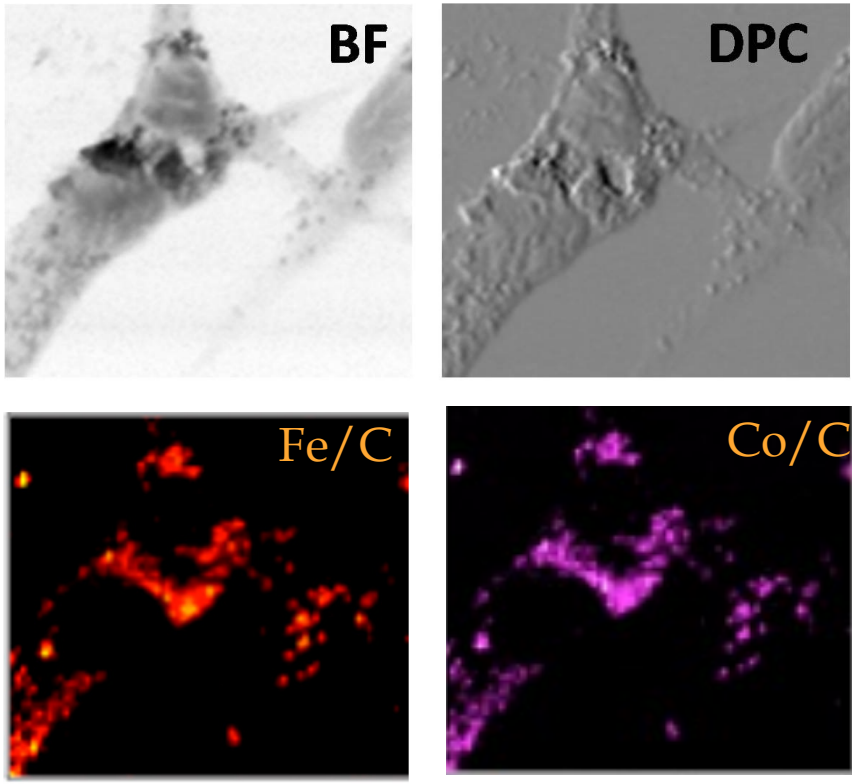
TwinMic

• Nanotoxicology

Cellular distribution and degradation of $CoFe_2O_4$ NPs in Balb/3T3 Fibroblast cells

Localization of engineered nanoparticles (ENPs) inside a cell and on the possible effects on the cell metabolic behaviour

G. Ceccone, P. Marmorato et al., EC Joint Research Center, Ispra, I



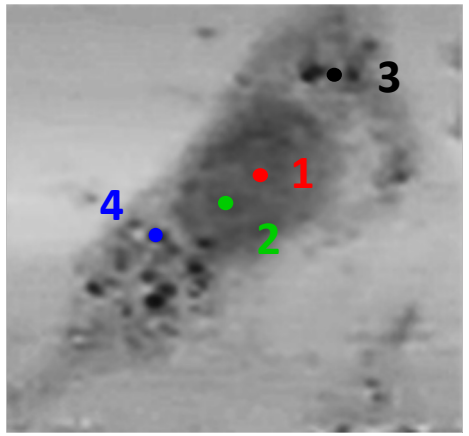
$CoFe_2O_4$ in mouse 3T3 fibroblast cells, E=2019 eV, 60um x 60 um

P. Marmorato, G. Ceccone, A. Gianoncelli, L. Pascolo, J. Ponti, F. Rossi, M. Salomé, B. Kaulich, and M. Kiskinova, *Cellular distribution and degradation of Cobalt Ferrite Nanoparticles in Balb/3T3 Fibroblasts*, Toxicology Letters, 2011, 207 - 2, 128-136.

Elettra Sincrotrone Trieste

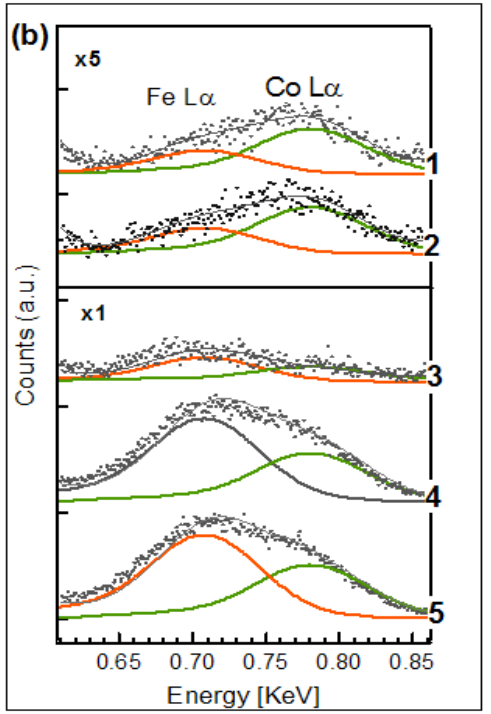
TwinMic

- *Balb/3T3 exposed to 1000mM*

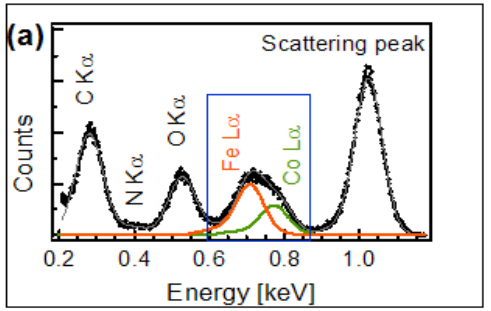


Fe/Co~0.8

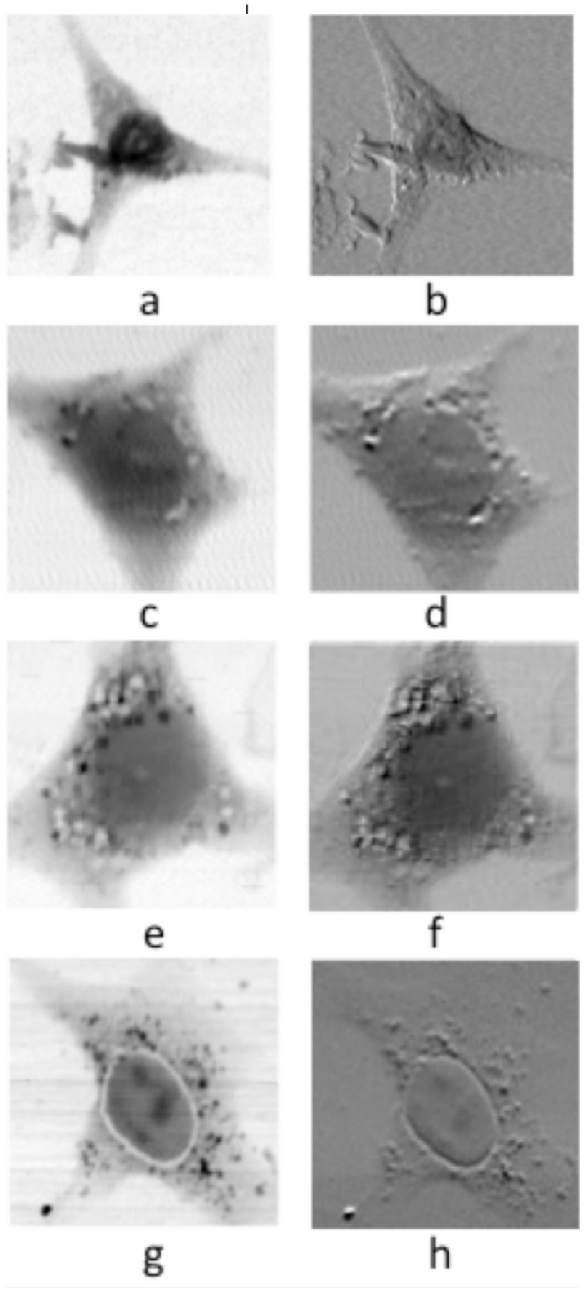
Fe/Co~1.5



Similar behaviour (but less evident) in the nuclear region for 500µM concentration



P. Marmorato, G. Ceccone, A. Gianoncelli, L. Pascolo, J. Ponti, F. Rossi, M. Salomé, B. Kaulich, and M. Kiskinova, *Cellular distribution and degradation of Cobalt Ferrite Nanoparticles in Balb/3T3 Fibroblasts*, Toxicology Letters, 2011, 207 - 2, 128-136.



Control

40 μM

250 μM

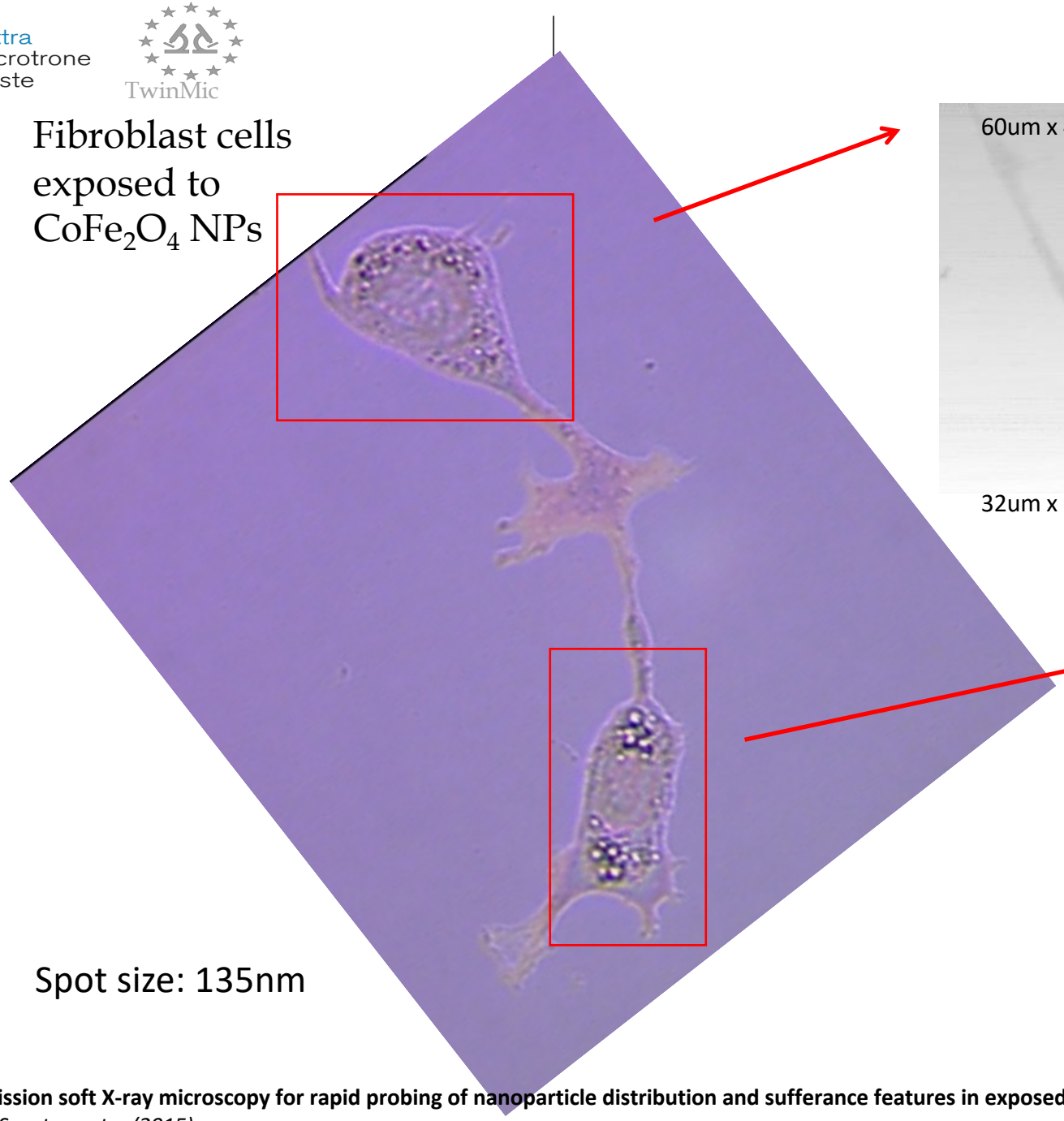
500 μM

High-resolution scanning transmission soft X-ray microscopy for rapid probing of nanoparticle distribution and sufferance features in exposed cells
Kourousias G, Pascolo L, Marmorato P, Ponti J, Ceccone G, Kiskinova M, Gianoncelli A *X-Ray Spectrometry (2015)*

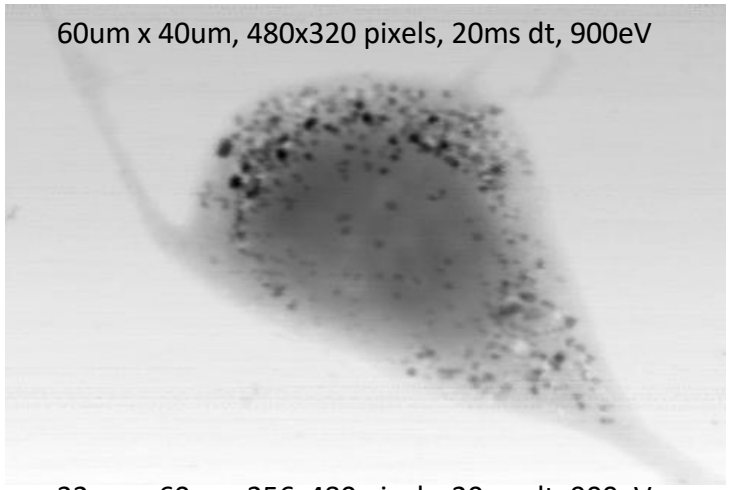
Elettra Sincrotrone Trieste

TwinMic

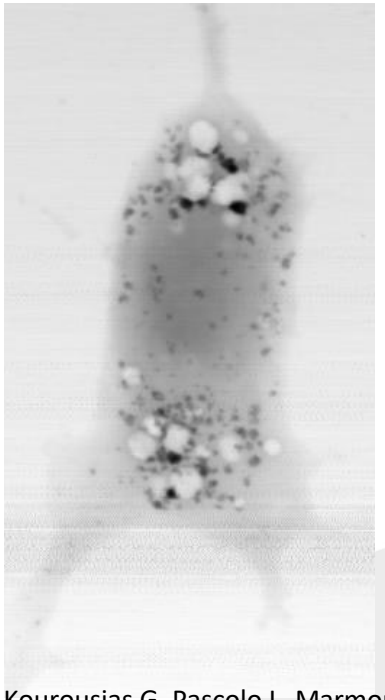
Fibroblast cells exposed to $CoFe_2O_4$ NPs



60um x 40um, 480x320 pixels, 20ms dt, 900eV



32um x 60um, 256x480 pixels, 20ms dt, 900eV

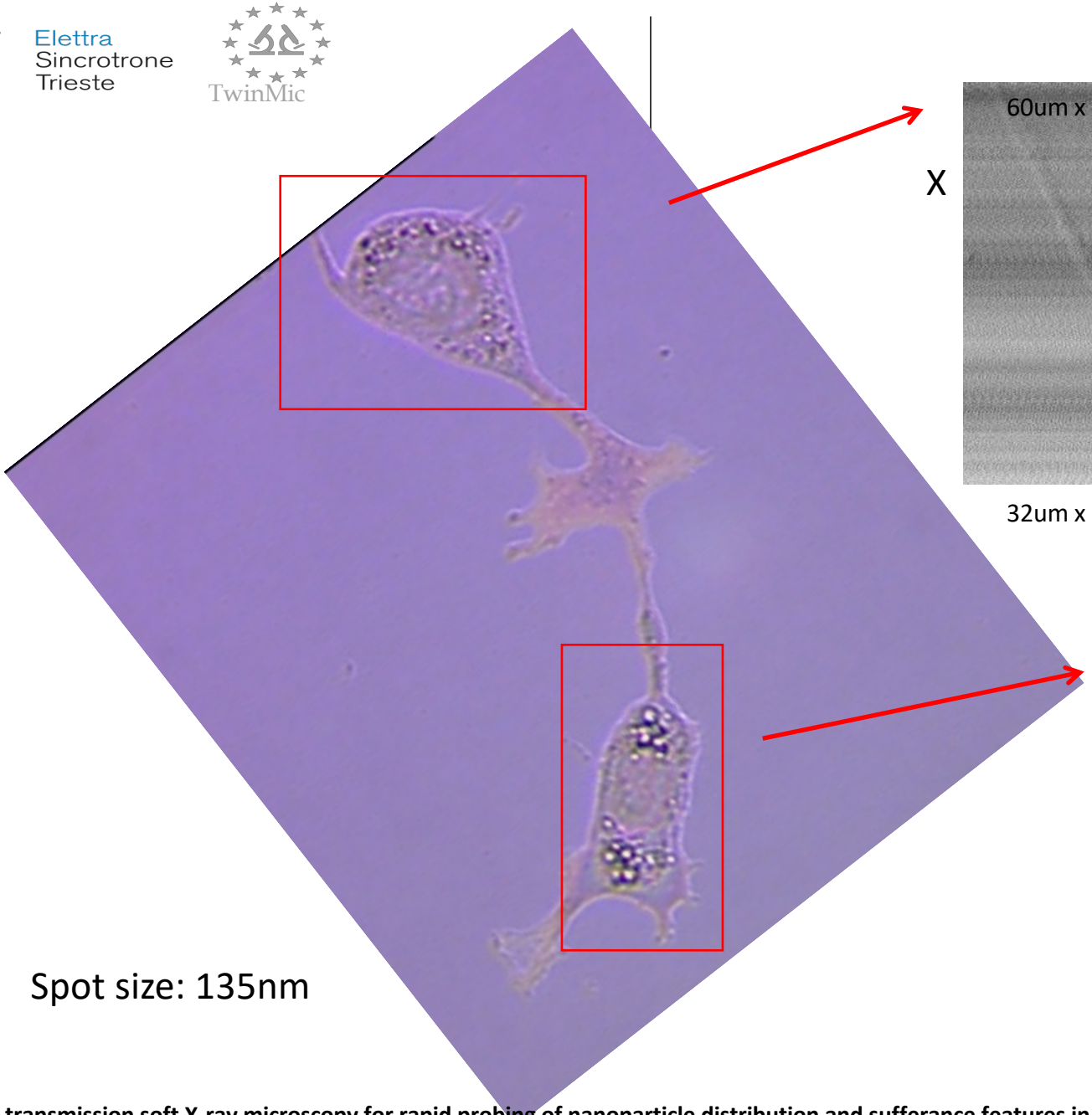


Spot size: 135nm

High-resolution scanning transmission soft X-ray microscopy for rapid probing of nanoparticle distribution and sufferance features in exposed cells Kourousias G, Pascolo L, Marmorato P, Ponti J, Ceccone G, Kiskinova M, Gianoncelli A *X-Ray Spectrometry (2015)*

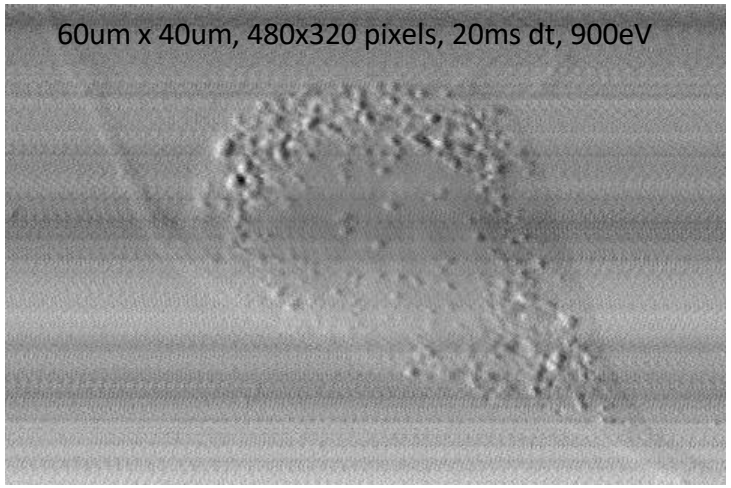
Elettra Sincrotrone Trieste

TwinMic

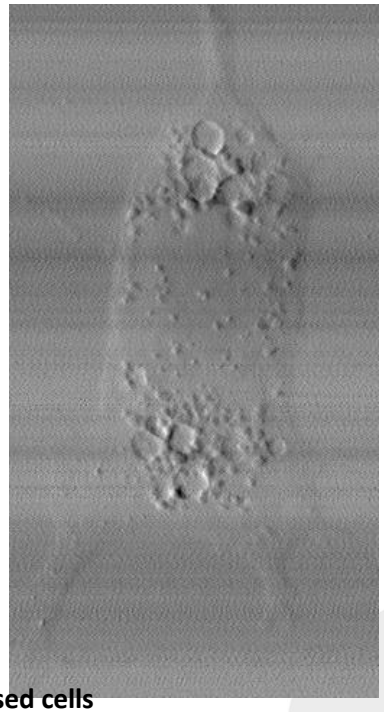


Spot size: 135nm

X



32um x 60um, 256x480 pixels, 20ms dt, 900eV



X

High-resolution scanning transmission soft X-ray microscopy for rapid probing of nanoparticle distribution and sufferance features in exposed cells
Kourousias G, Pascolo L, Marmorato P, Ponti J, Ceccone G, Kiskinova M, Gianoncelli A *X-Ray Spectrometry (2015)*

Red oil solution that specifically stains lipids

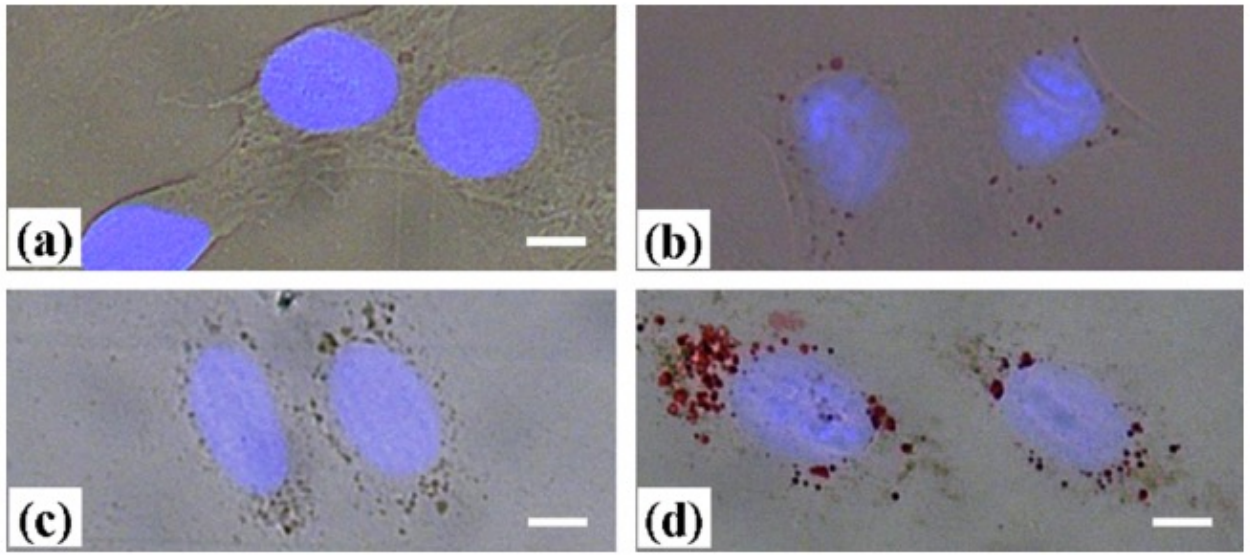
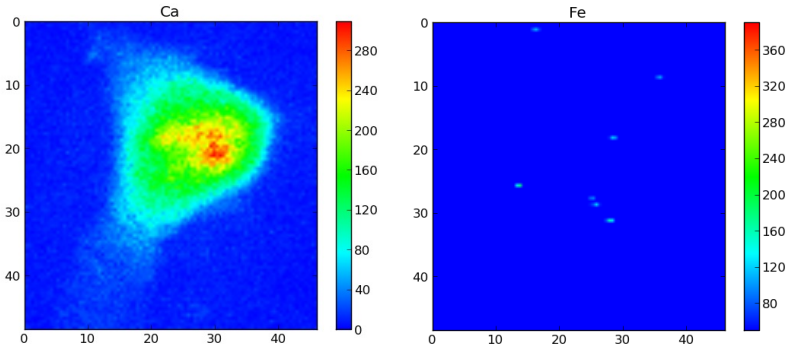


Fig. 6. Optical images of Balb/3T3 control cells (a and b) and incubated for 24 h with 500 μM $CoFe_2O_4$ NPs suspension (c and d). Red spots represent lipids stained by Red Oil O solution (b and d) whilst nuclei are stained in blue by Hoechst. Bar = 10 μm. (For interpretation of the references to color in this figure legend, the reader is referred to the web version of the article.)

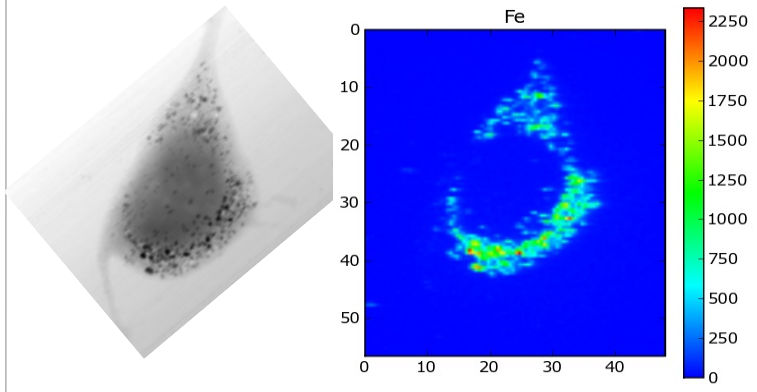
P. Marmorato, G. Ceccone, A. Gianoncelli, L. Pascolo, J. Ponti, F. Rossi, M. Salomé, B. Kaulich, and M. Kiskinova, *Cellular distribution and degradation of Cobalt Ferrite Nanoparticles in Balb/3T3 Fibroblasts*, Toxicology Letters, 2011, 207 - 2, 128-136.

Nanotoxicology: $CoFe_2O_4$ ENPs

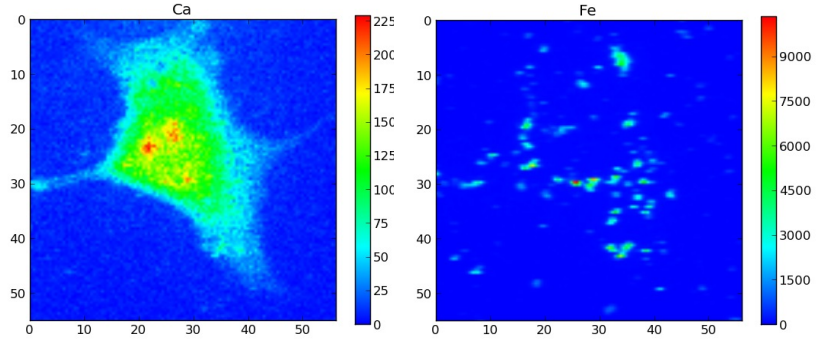
Control



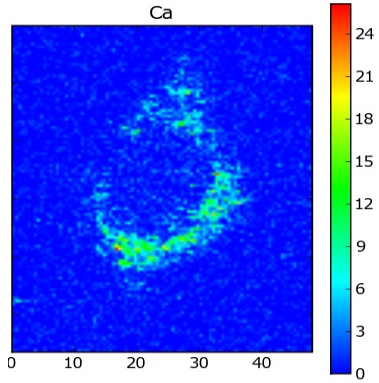
Exposed to 500µM



Exposed to 40µM







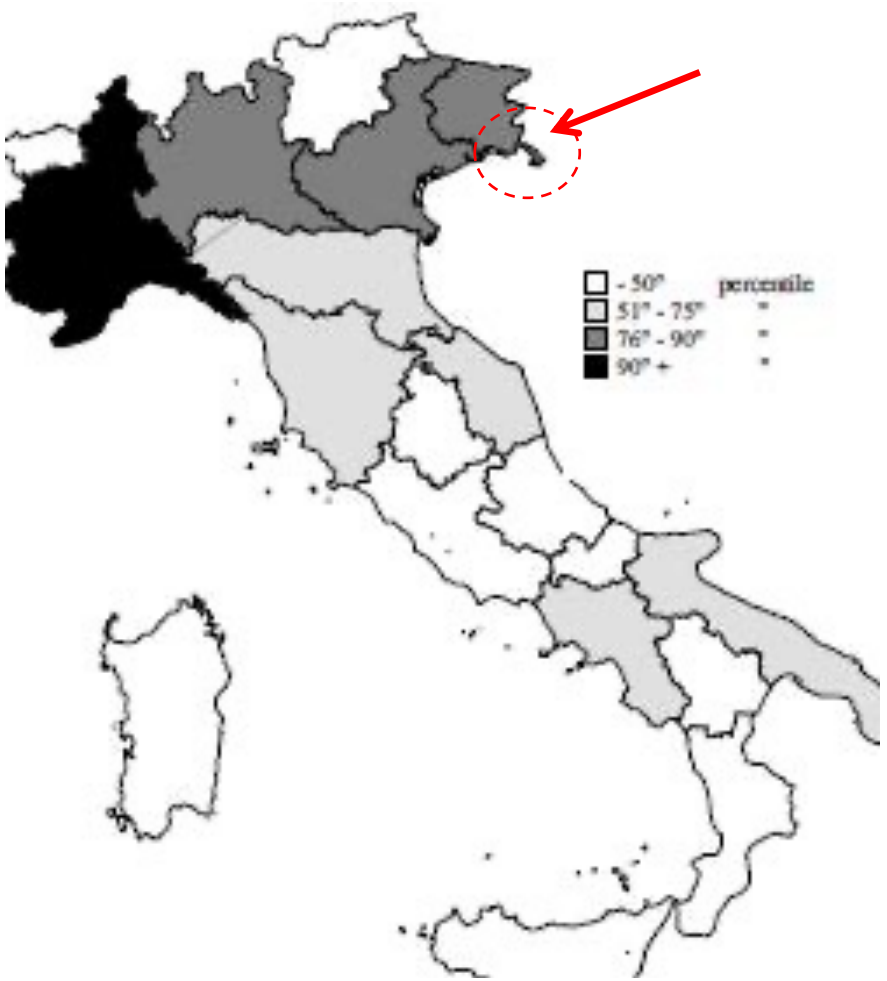
P. Marmorato, G. Ceccone, A. Gianoncelli, L. Pascolo, J. Ponti, F. Rossi, M. Salomé, B. Kaulich, and M. Kiskinova, Cellular distribution and degradation of Cobalt Ferrite Nanoparticles in Balb/3T3 Fibroblasts, in press in Toxicology Letters

Elettra Sincrotrone Trieste

SIMILARLY TO OTHER COUNTRIES, IN ITALY THE MAXIMAL INCIDENCE OF MESOTHELIOMA IS EXPECTED IN THE NEXT 5-10 YEARS

In Italy, many sites of large asbestos-cement factories (eg, Casale Monferrato), and naval shipyards (eg, Monfalcone).
Areas with the highest mortality for asbestos related diseases



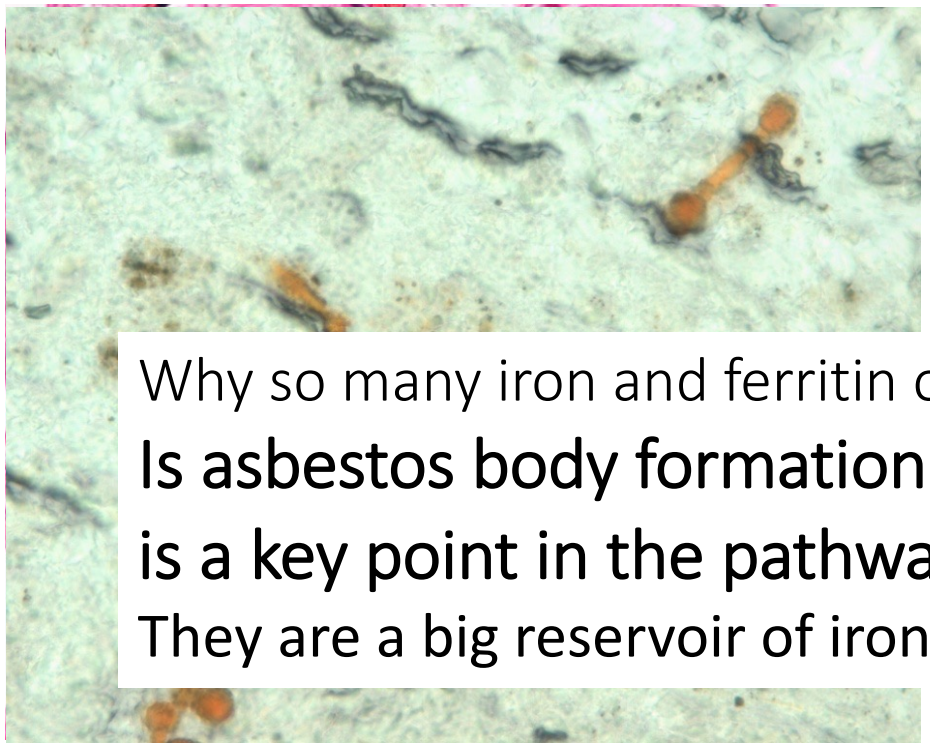


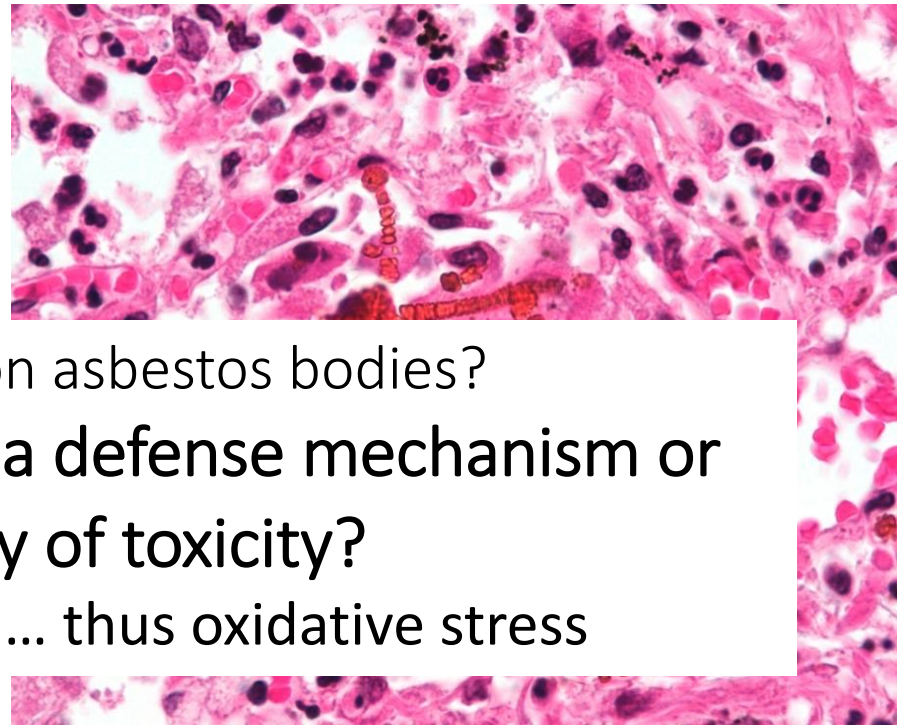
In the hospitals of Monfalcone and Trieste: 60 mesothelioma deaths each year

Courtesy of Prof. Mauro Melato

Elettra
Sincrotrone
Trieste

THE ASBESTOS BODIES
The histopathologic finding in patients exposed to asbestos





Why so many iron and ferritin on asbestos bodies?

Is asbestos body formation a defense mechanism or is a key point in the pathway of toxicity?

They are a big reservoir of iron … thus oxidative stress

Ferruginous bodies are believed to be formed by macrophages that have phagocytized and attempted to digest the fibers.

THREE DIFFERENT SYNCHROTRON FACILITIES, changing incident energy and spatial resolution

Elettra Sincrotrone Trieste

TwinMic -Energy range: 0.25-2.2keV
X-Ray Microscopy and XRF;
Spatial resolution: >300 nm;

1)



2)



ID21 - Energy range: 2-7.3 keV - spatial resolution >200 nm ; **ID22; ID16B** Energy range: 12-25 keV - nano spatial resolution

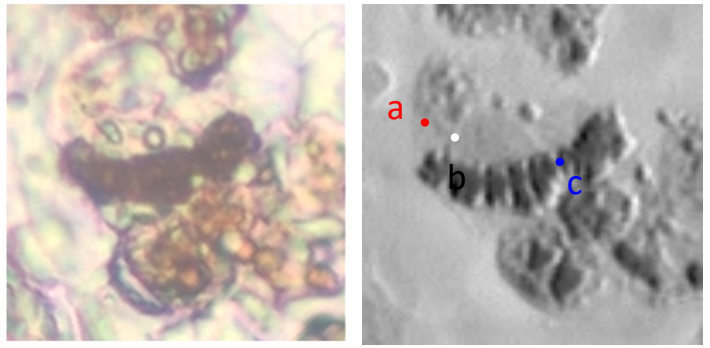
3)

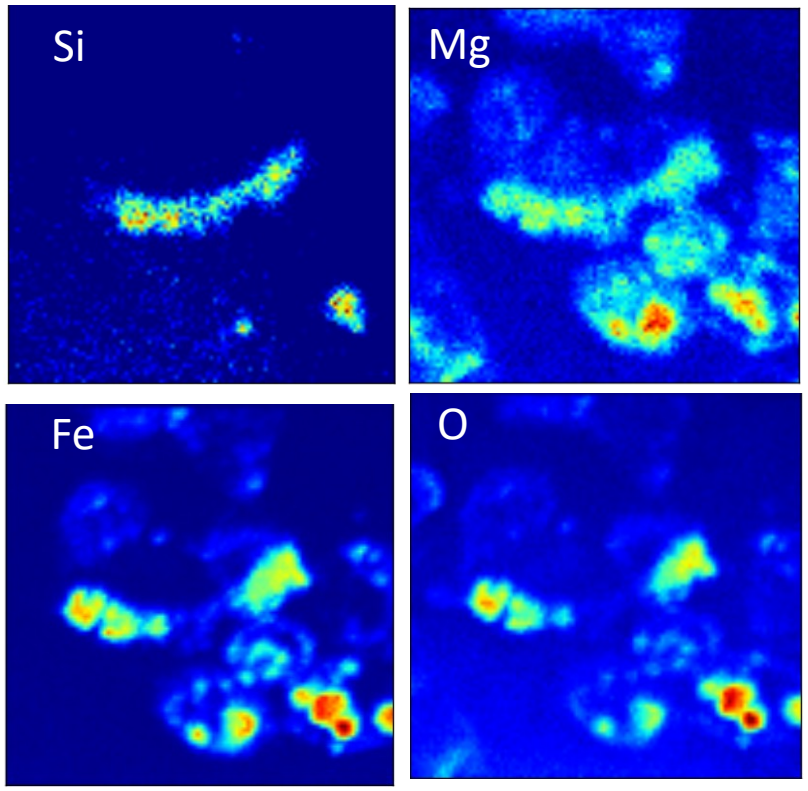


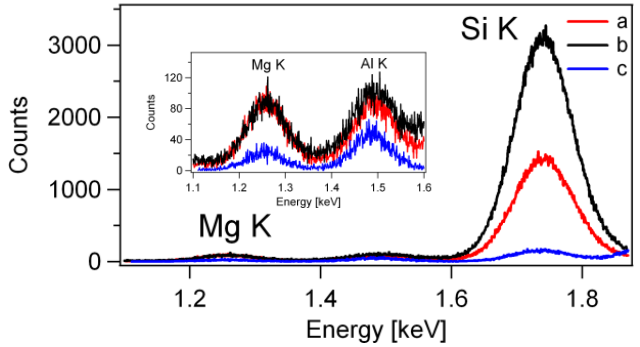
XFM beamline
Energy range: 4-25 keV (12.74 keV)
High speed analyses - large areas
Spatial resolution: 2µm
Maia detector: 384 element array
(Ca, Fe, Zn, Ti, Ni)

Elettra
Sincrotrone
Trieste

TwinMic Analyses: X-ray Microscopy of an ASBESTOS BODY in lung tissue sample







LE-XRF (1.9 and 0.9 kev):
first result combining morfological and

Pascolo *et al. Particle and Fibre Toxicology* 2011, **8**:7
http://www.particleandfibretoxicology.com/content/8/1/7

pft PARTICLE AND FIBRE TOXICOLOGY

RESEARCH Open Access

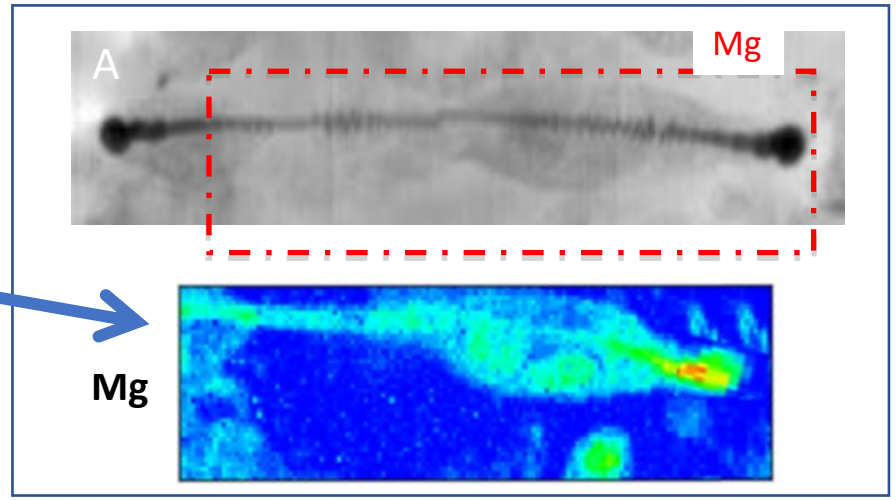
Synchrotron soft X-ray imaging and fluorescence microscopy reveal novel features of asbestos body morphology and composition in human lung tissues

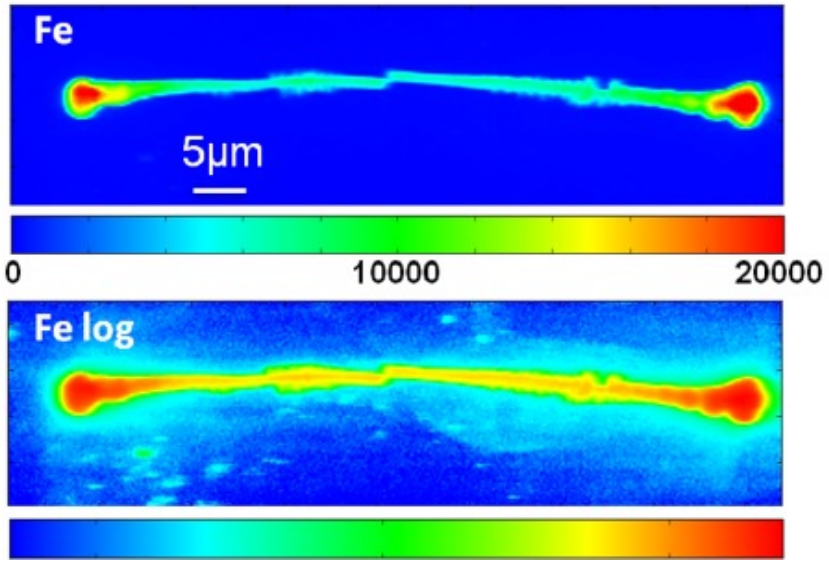
Lorella Pascolo[1*], Alessandra Gianoncelli[1], Burkhard Kaulich[1], Clara Rizzardi[2,3], Manuela Schneider[2], Cristina Bottin[2], Maurizio Polentarutti[1], Maya Kiskinova[1], Antonio Longoni[4], Mauro Melato[2,3,5]

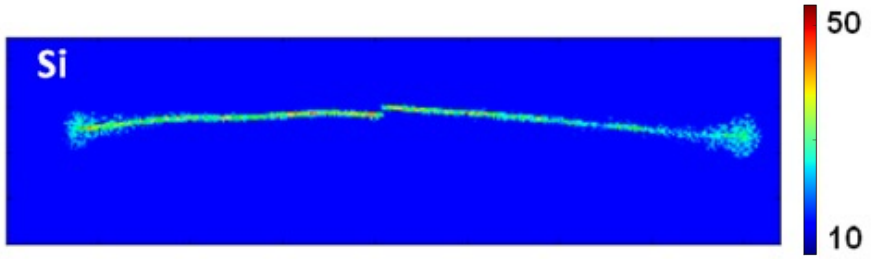
Elettra
Sincrotrone
Trieste

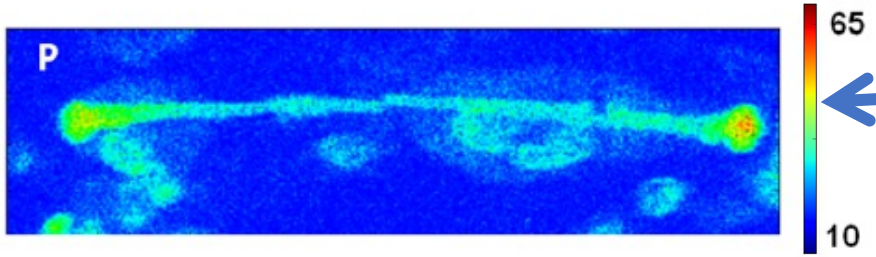
LE-XRF at TwinMIC (1.9 Kev) and XRF at ID21 (7.3)

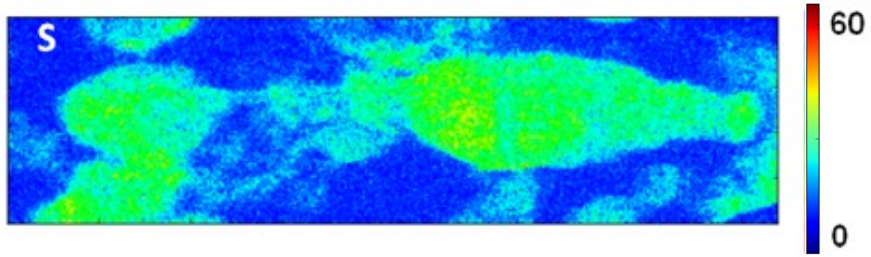
ASBESTOS BODY FORMATION MECHANISMS: IRON AND OTHER CHEMICAL ELEMENTS

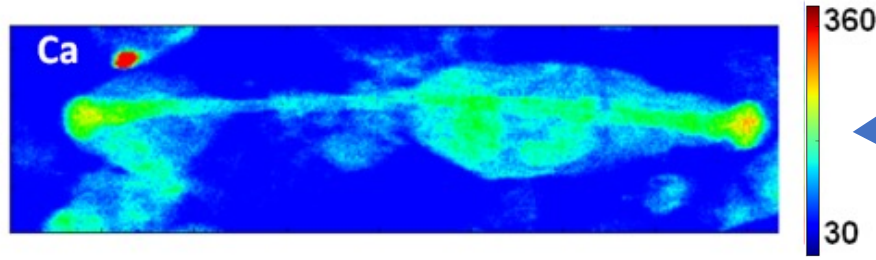






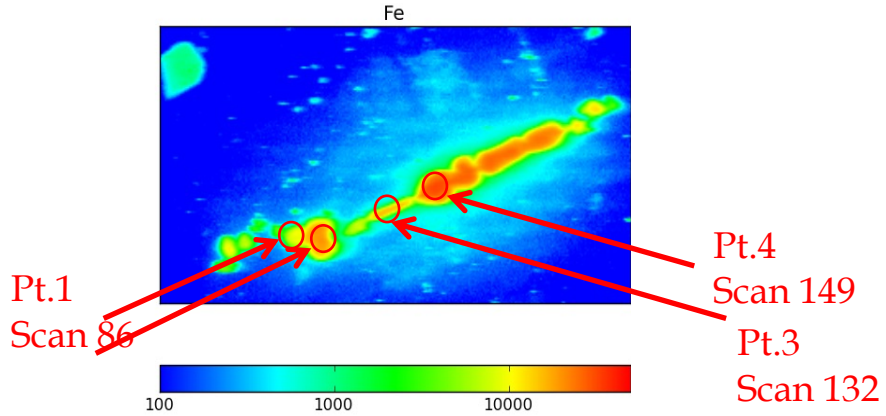


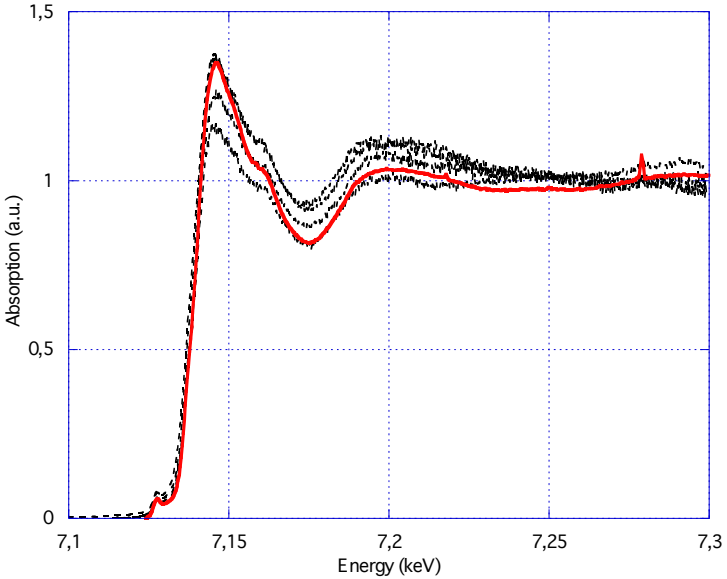




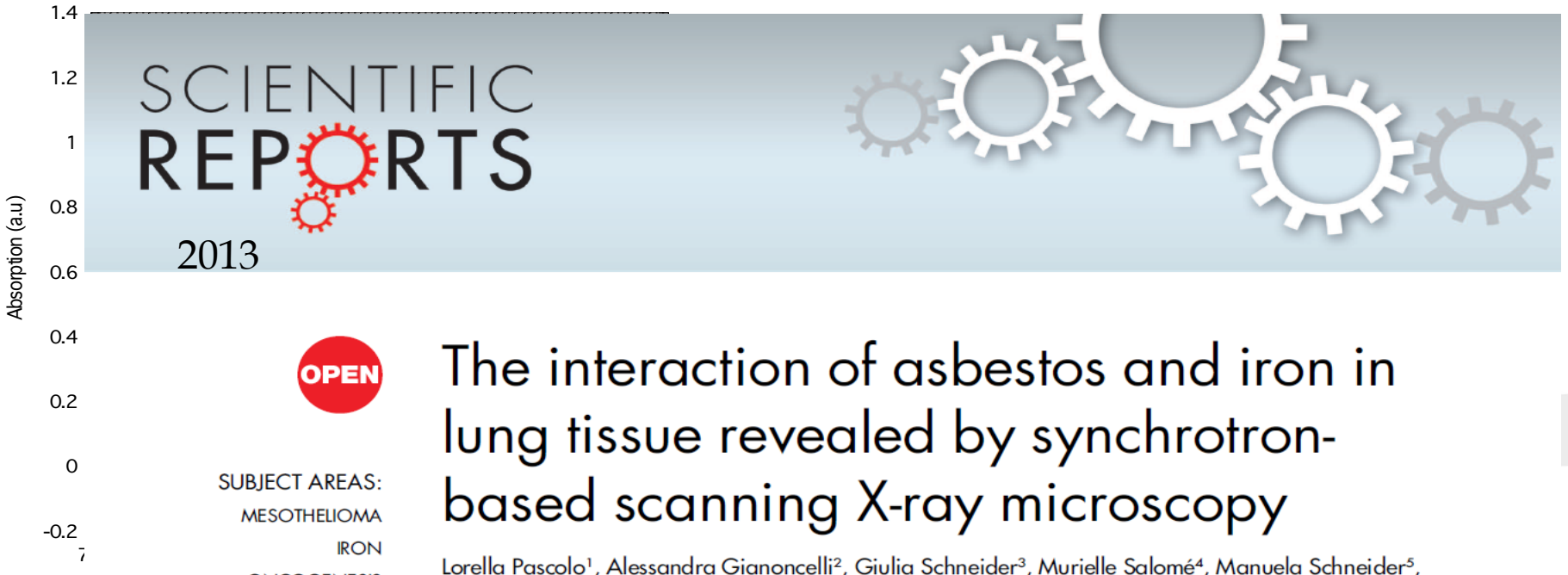
Elettra
Sincrotrone
Trieste

µXANES analyses under XRF set-up @ ID21 (ESRF)





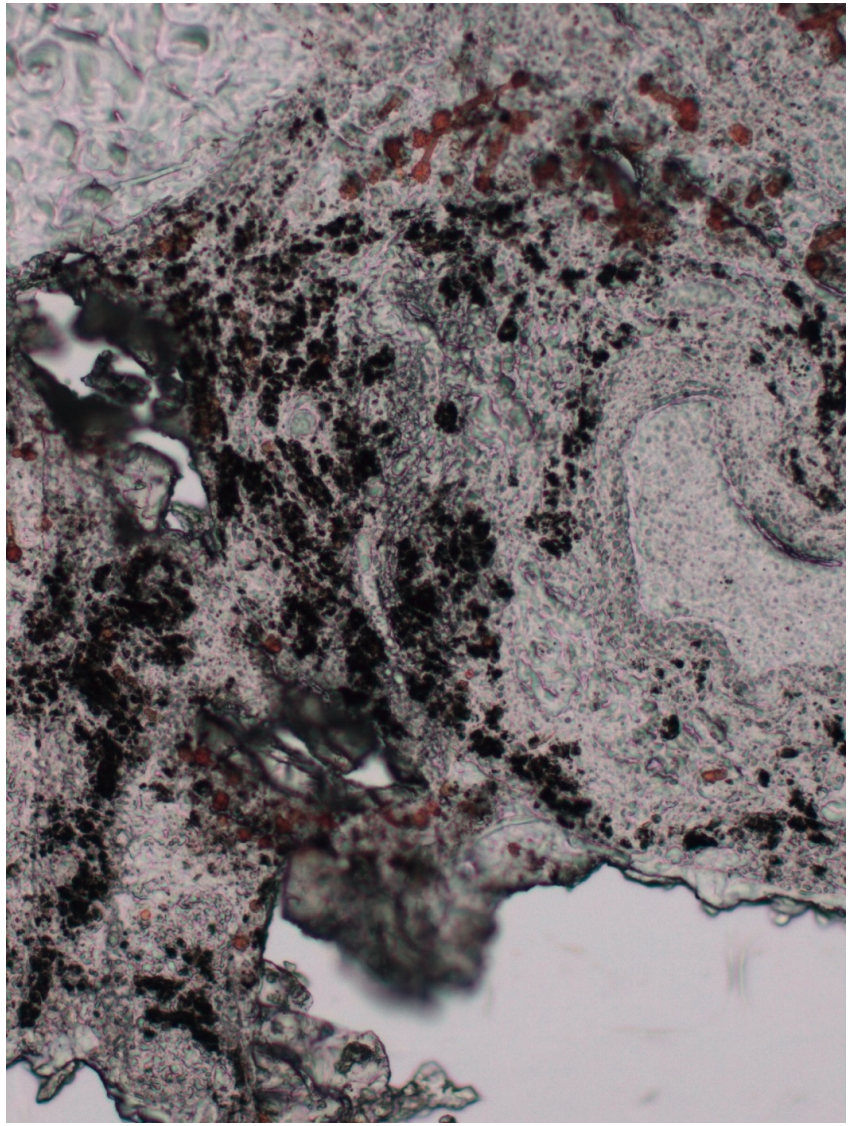
Micro-spot absorption spectroscopy



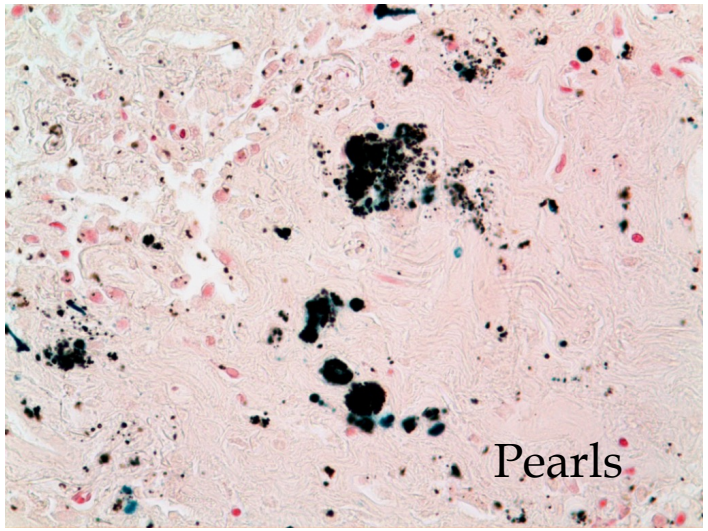
Elettra
Sincrotrone
Trieste

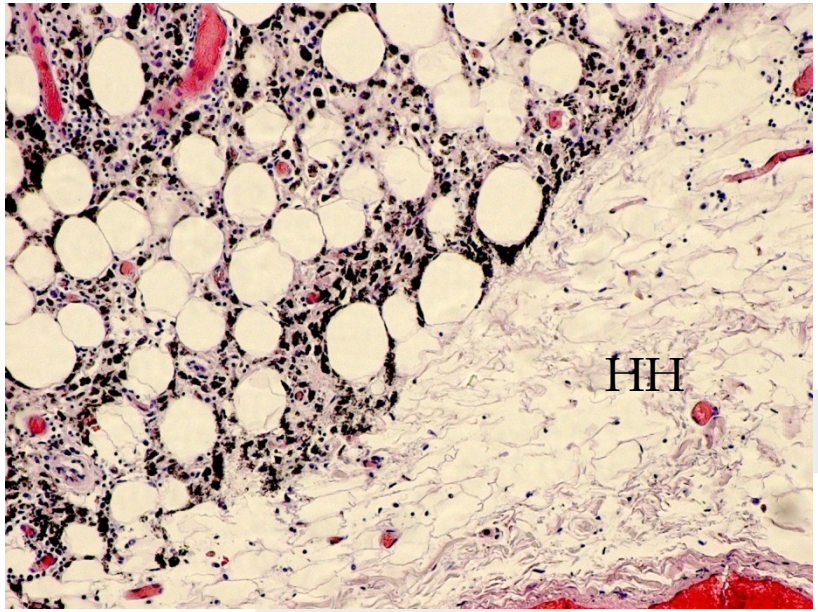
COMPARING WITH OTHER POLLUTANTS IN LUNG

ASBESTOSIS



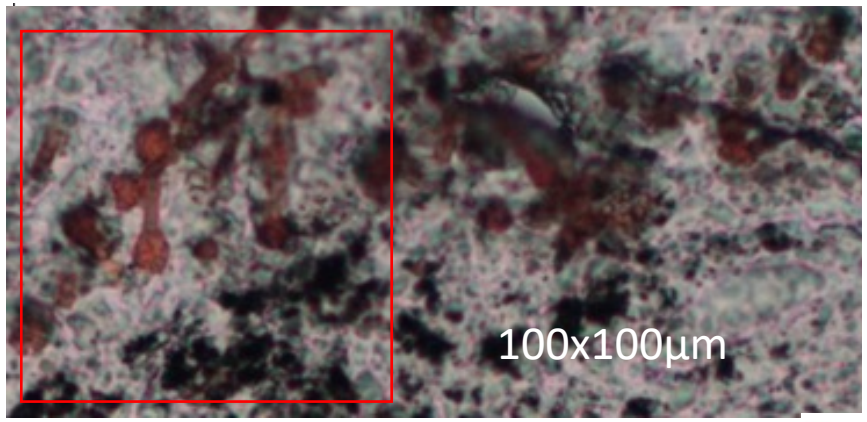
ANTHRACOSI S

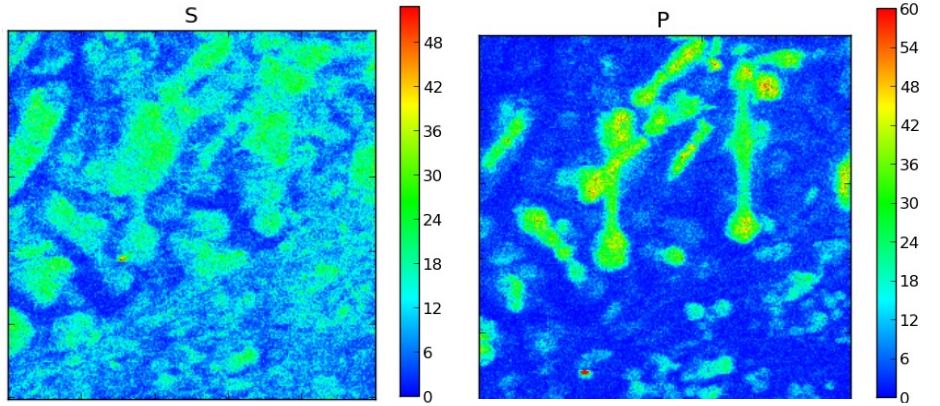


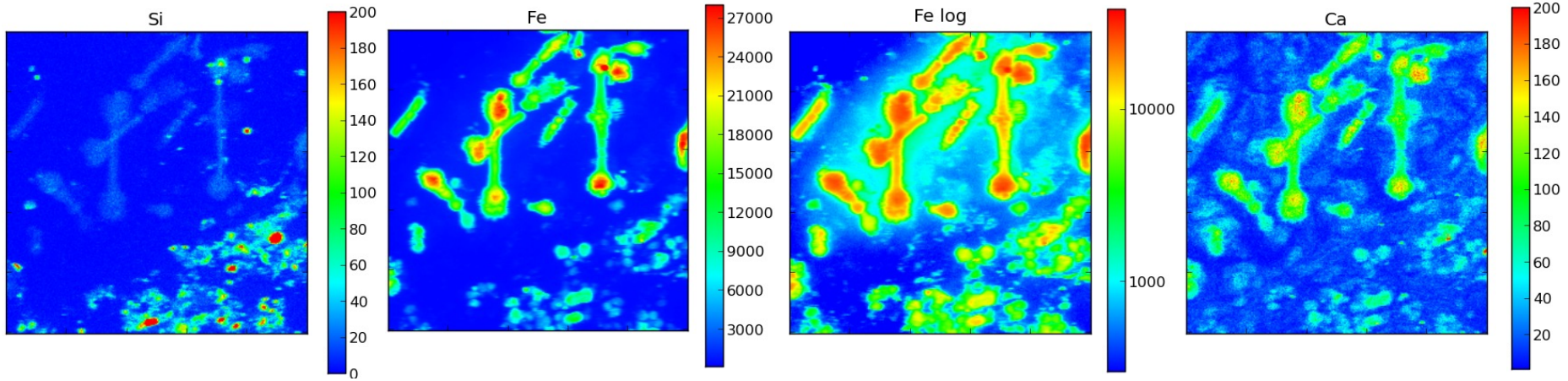


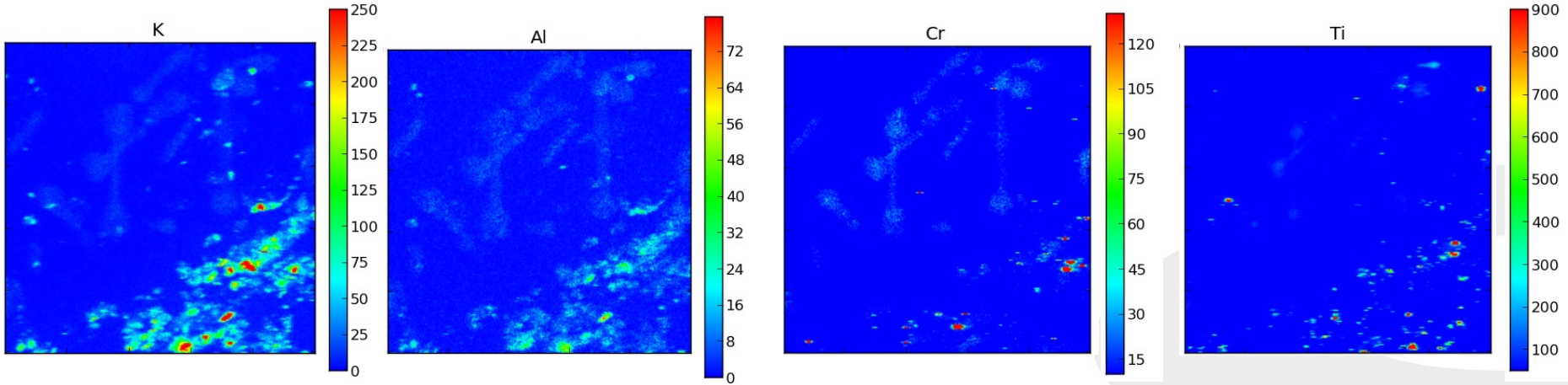
Analysis with XRF (7.3 keV) on asbestos and anthracosis (particulate)

Elettra
Sincrotrone
Trieste



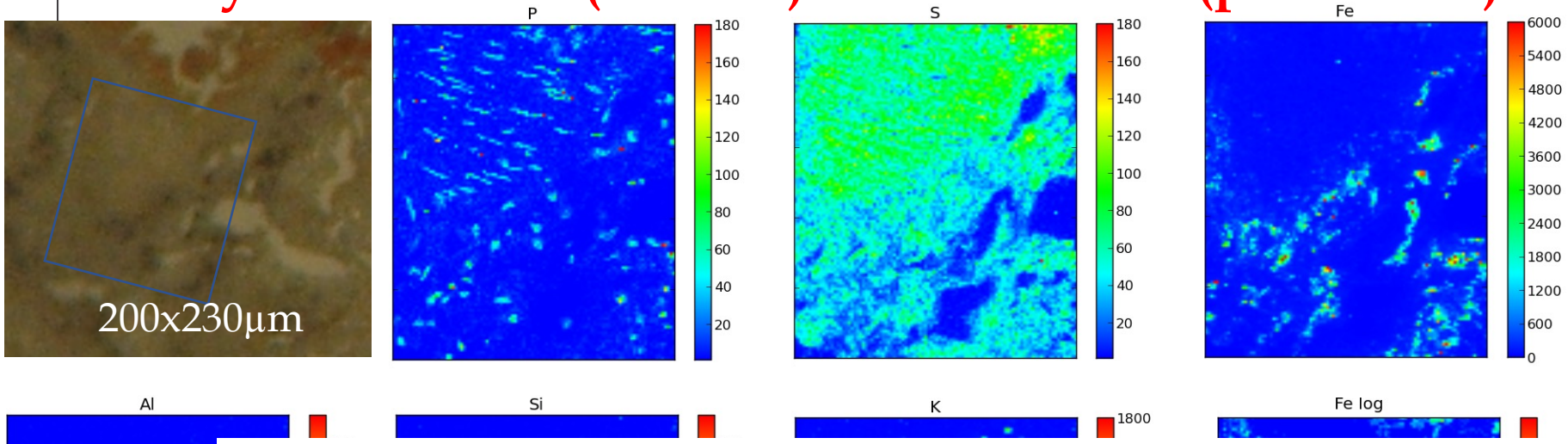




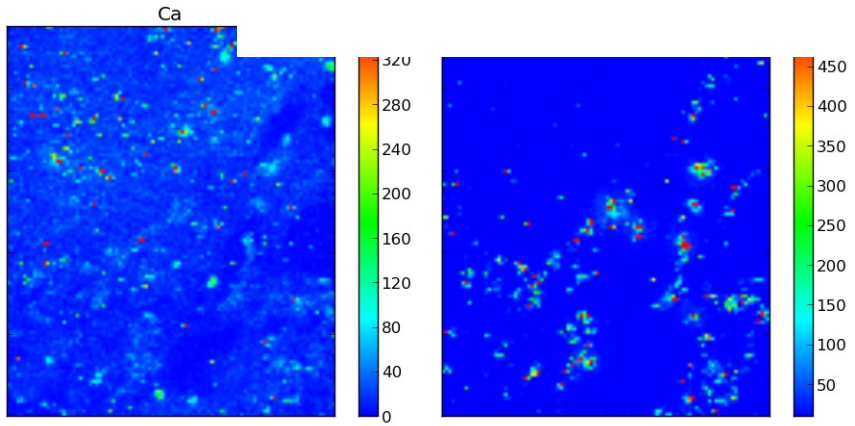


Analysis with XRF (7.3 keV) on anthracosis (particulate)

Elettra Sincrotrone Trieste



Particulate is heterogeneous (aggregation of different materials)
Contains Fe (less than asbestos bodies)
May alter Fe homeostasis of Fe in the tissue
Contains high K and Si (traces of Cr, Ti)
Doesn't causes calcification processes (very low Ca and P co-localization)



SCIENTIFIC REPORTS

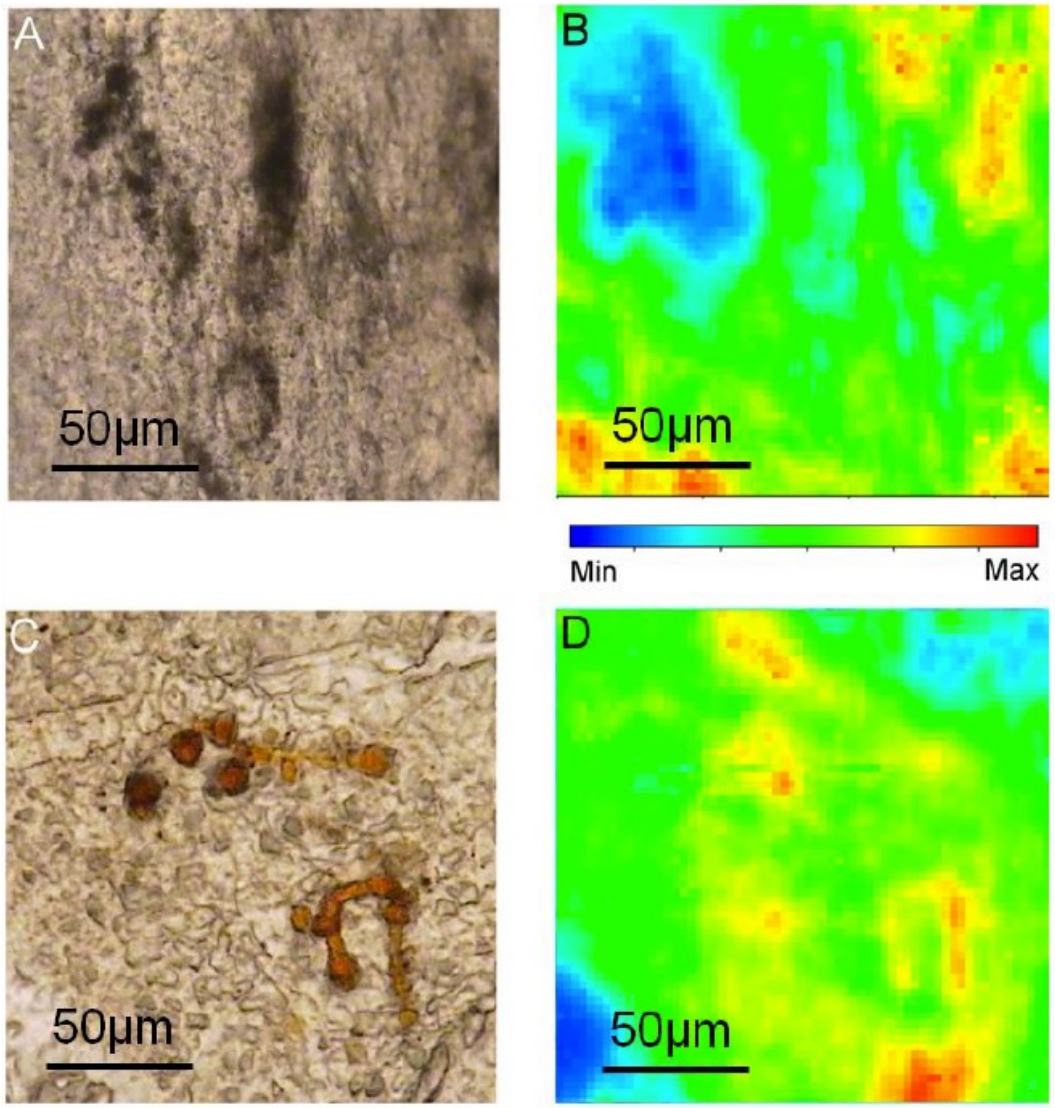
OPEN

Differential protein folding and chemical changes in lung tissues exposed to asbestos or particulates

Received: 19 March 2015
Accepted: 16 June 2015
Published: 10 July 2015

Lorella Pascolo[1], Violetta Borelli[2], Vincenzo Canzonieri[3], Alessandra Gianoncelli[4], Giovanni Birarda[4,5], Diana E. Bedolla[4,6], Murielle Salomé[7], Lisa Vaccari[4], Carla Calligaro[8], Marine Cotte[7], Bernhard Hesse[7], Fernando Luisi[9], Giuliano Zabucchi[2], Mauro Melato[1] & Clara Rizzardi[10]

FTIR spectro-microscopy
@ Elettra (SISSI) and ESRF (ID21)



Sensitive, label-free and non-damaging technique for the characterization of biomolecules

Particularly useful for the study of proteins, the so called Amide I (~ 1700-1600 cm^{-1}) and Amide II (~ 1580-1480 cm^{-1}) bands, from the C=O stretching and N-H bending vibrations of the peptide backbone

L. Pascolo, V. Borelli, V. Canzonieri, A. Gianoncelli et al, **Differential protein folding and chemical changes in lung tissues exposed to asbestos or particulates**, Scientific Reports 5, 12129 (2015)

Elettra
Sincrotrone
Trieste

FTIR spectro-microscopy
@ Elettra (SISSI) and ESRF (ID21)

The evaluation of the total protein contribution (as Amide I and Amide II) can discriminate asbestos bodies from dust particles.

- Marginal protein content on the dark particles of anthracosis;
- A quite high presence characterizes asbestos bodies (in agreement with the well-known participation of ferritin in the asbestos body formation).

- Proteins of the asbestos coating have a high percentage of **β-folded protein** domains (unexpected, since ferritin, the principal protein of the asbestos body coating, is an α-helix protein)

- β-structure folding may be related to conformational changes occurring over the time in tissues surrounding asbestos fibres and bodies (response to the long permanence of the asbestos bodies?) Conversely, the protein transition to β-sheets could be a specific chemical mechanism of the asbestos body formation.

L. Pascolo, V. Borelli, V. Canzonieri, A. Gianoncelli et al, **Differential protein folding and chemical changes in lung tissues exposed to asbestos or particulates**, Scientific Reports 5, 12129 (2015)

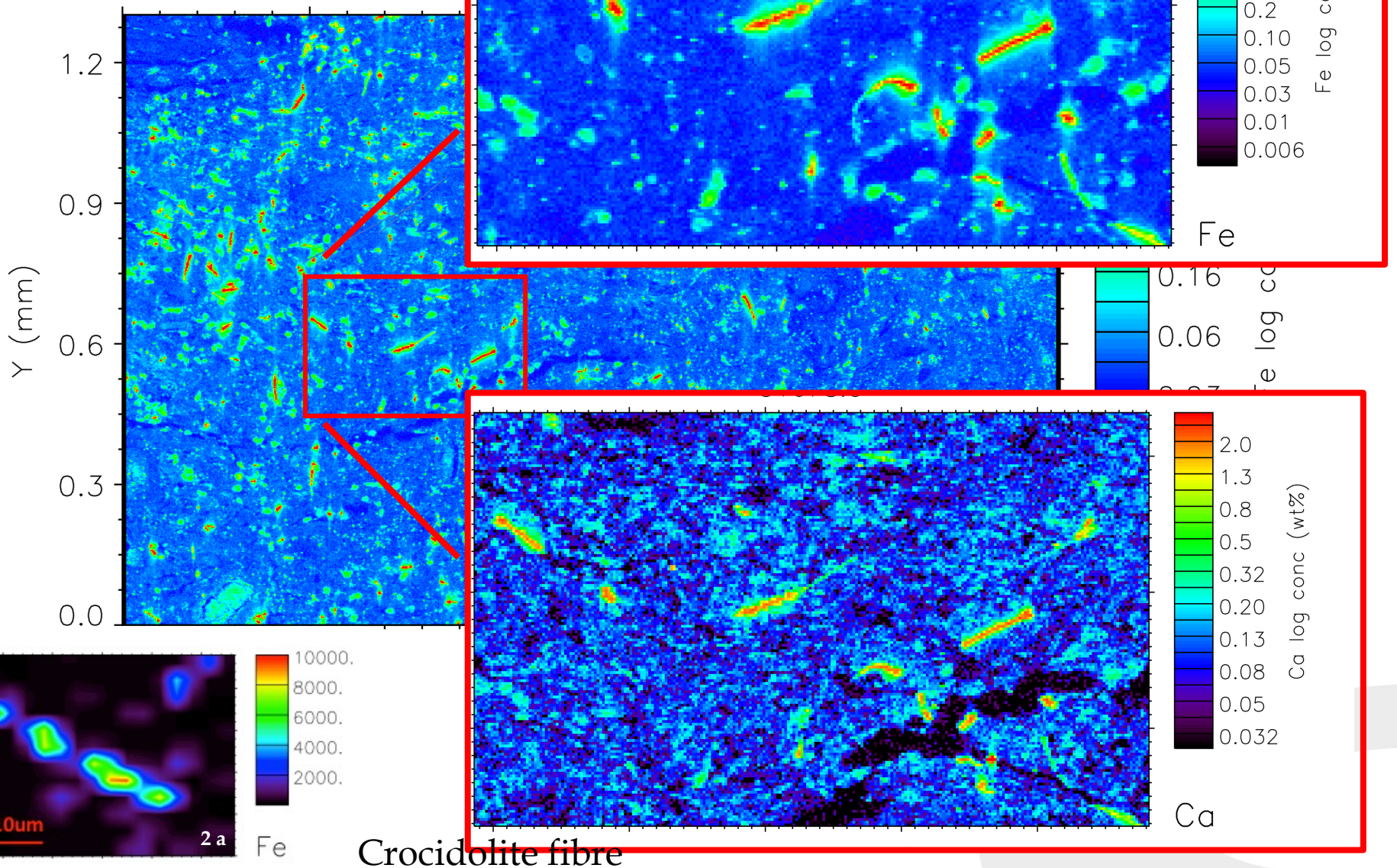
Elettra
Sincrotrone
Trieste

Focused X-Ray Hi

1) MICRO XRF at t

Journal cover!!

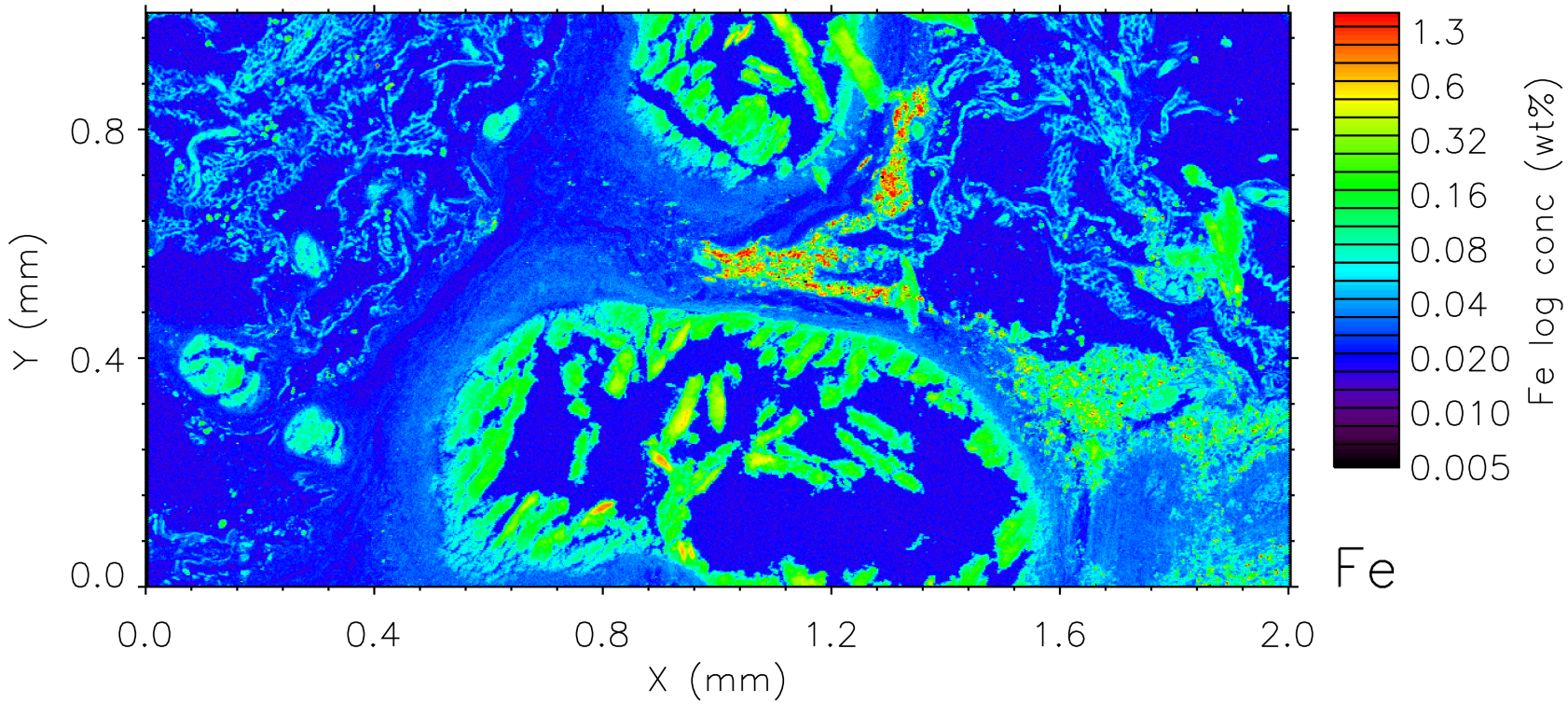


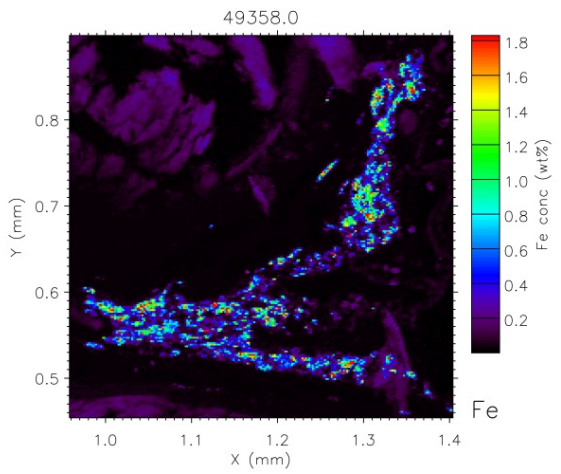


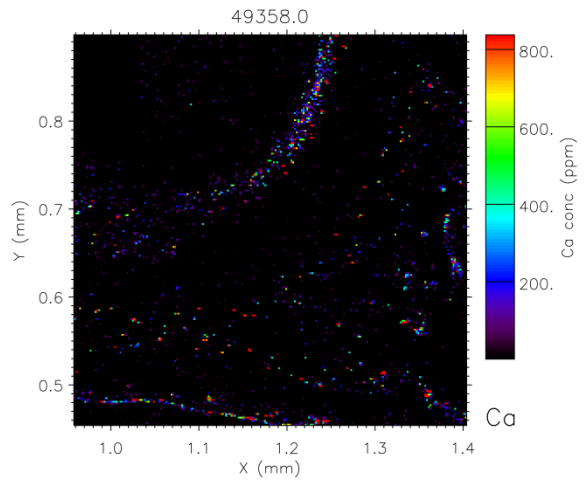
Crocidolite fibre

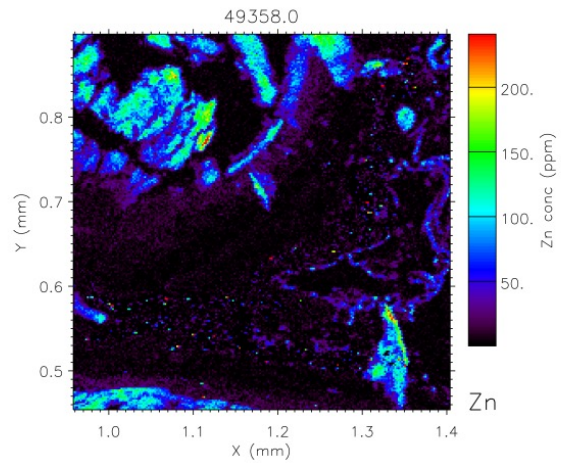
Elettra
Sincrotrone
Trieste

Particulate (anthracosis)- unexposed patient



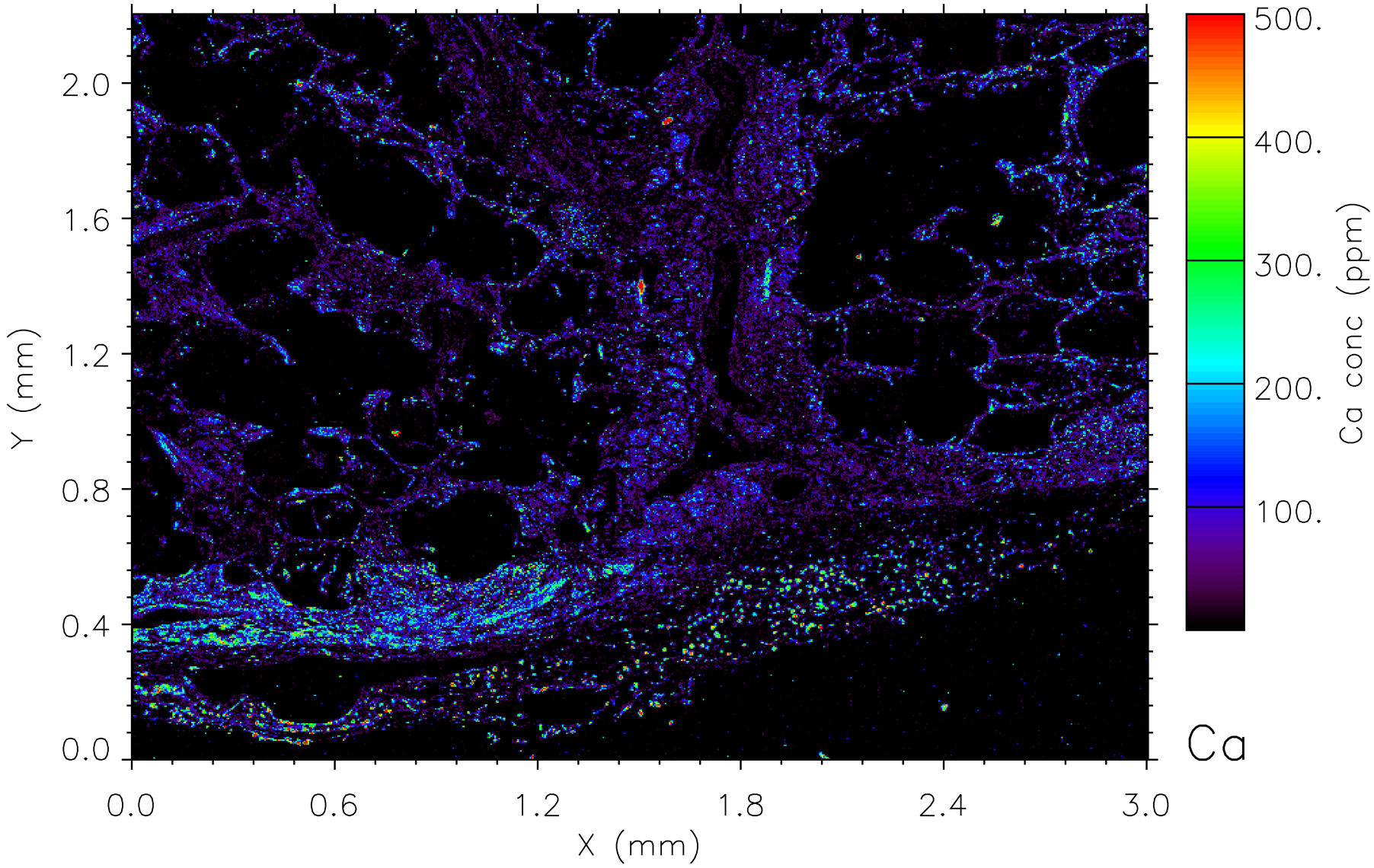






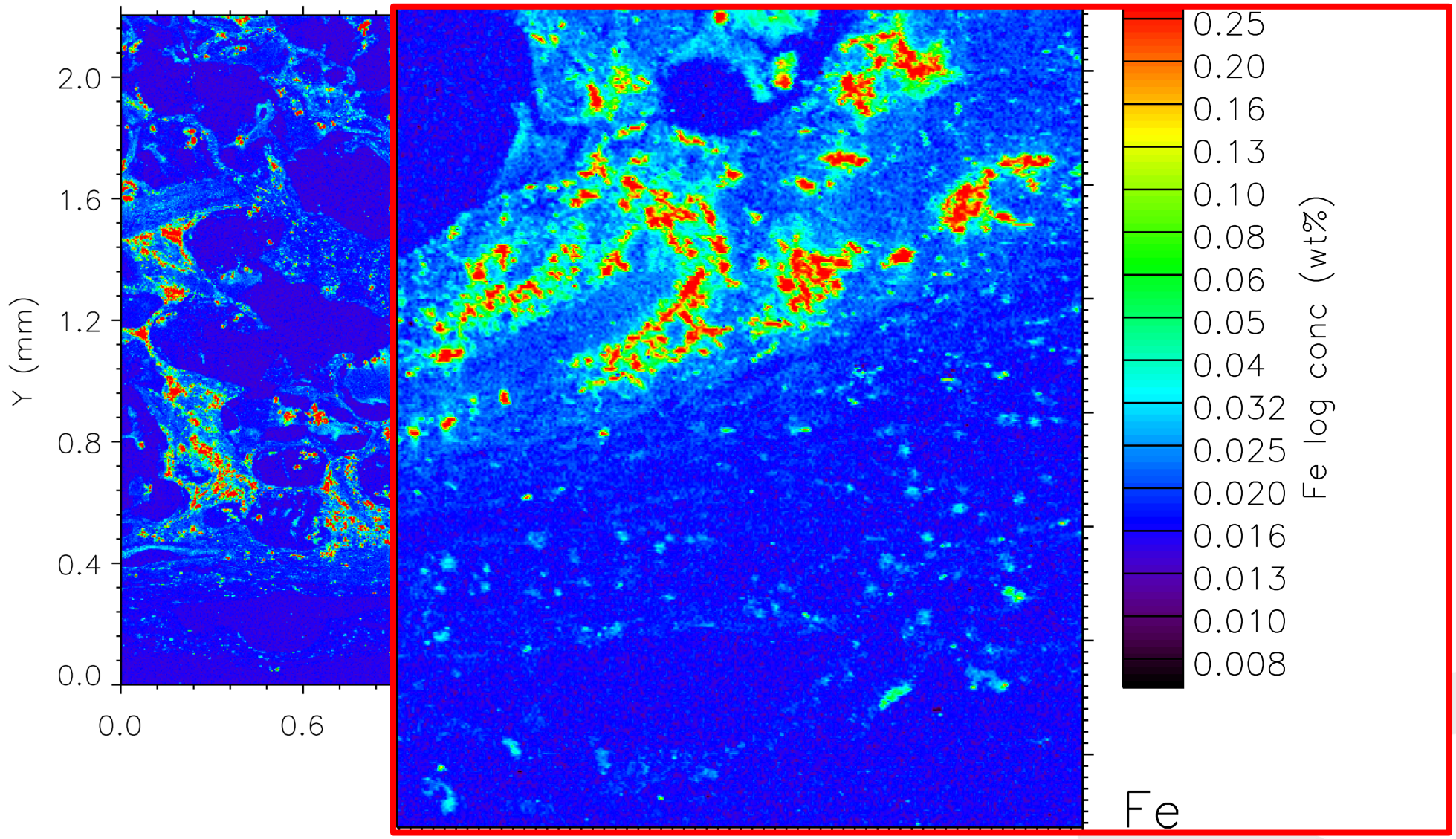
Elettra
Sincrotrone
Trieste

LUNG AND INFLAMED PLEURA



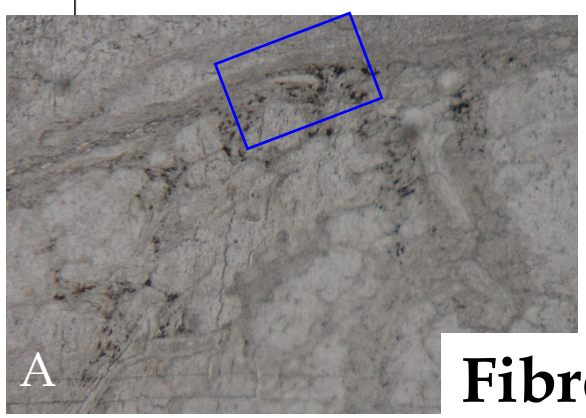
Elettra
Sincrotrone
Trieste

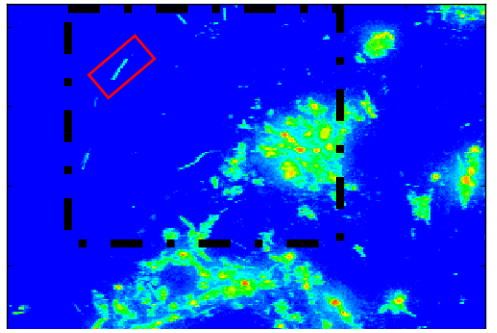
LUNG AND INFLAMED PLEURA

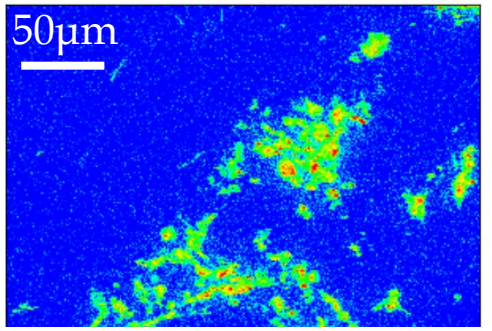


2) µXRF at ID21–ESRF & 3) TwinMic-Elettra

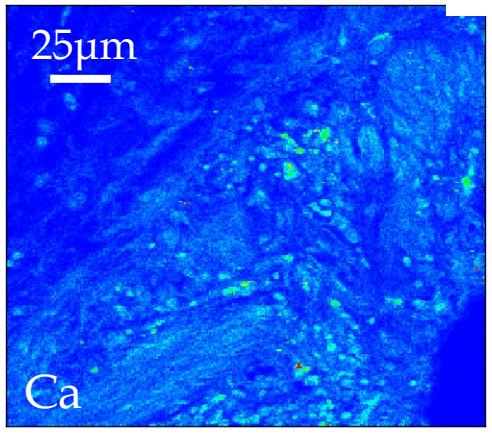
Elettra Sincrotrone Trieste

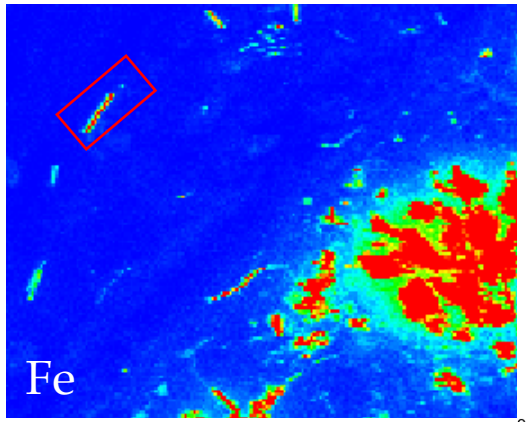


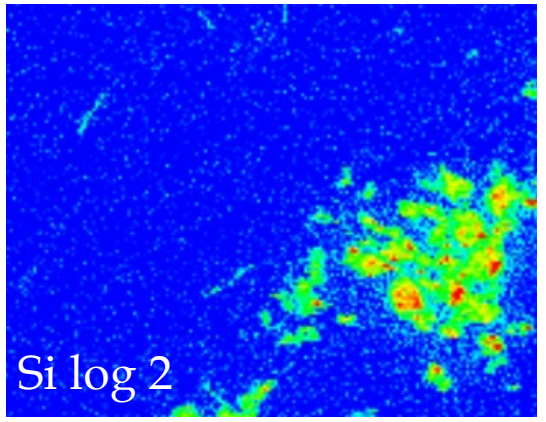




Fibres in the pleural space are from 2 to 20 µm
Contain iron









75 years 1942-2017 MSA Microscopy Society of America — Advancing Microscopy and Microanalysis

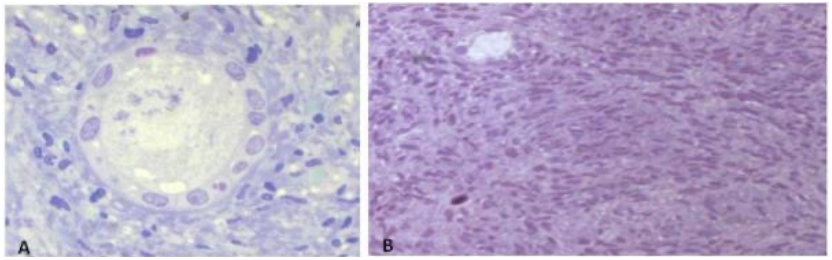
(2016) Focused X-Ray Histological Analyses to Reveal Asbestos Fibers and Bodies in Lungs and Pleura of Asbestos-Exposed Subjects Lorella Pascolo , Alessandra Gianoncelli , Clara Rizzardi , Martin de Jonge , Daryl Howard, David Paterson , Murielle Salomé , Paolo De Paoli, Mauro Melato , Vincenzo Canzonieri

Morphological and chemical changes in vitrified ovarian tissues

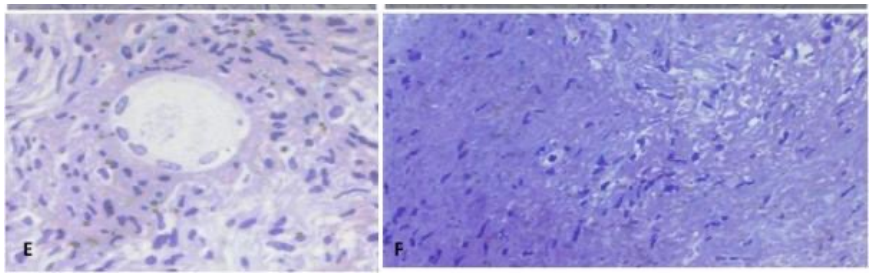
- Before cancer therapy and in other clinical circumstances the cryopreservation of ovary tissue is the unique option to preserve the reproduction potential of young women and pre-pubertal girls.
- The success of future assisted fertilization depends on the preservation state, thus needing appropriate protocols to reduce the morphological and structural damages caused by freeze-thaw processes.
- To further improve the evaluation and to investigate the underlying biochemical mechanism, we combined light and electron microscopy (TEM) to synchrotron X-ray Fluorescence (XRF) microscopy at different incident energies to analyze fresh and cryopreserved human ovarian tissues.
- We also used μCT for the first time to image ovarian tissue structures

L. Pascolo, I. Venturin, A. Gianoncelli, R. Bortul, G. Zito, E. Giolo, M. Salomé, D.E. Bedolla, M. Altissimo, M. Zweyer, G. Ricci, *Reproductive BioMedicine Online*, 37 - 2, 153-162 (2018)
L. Pascolo , I. Venturin , A. Gianoncelli , M. Salomé , M. Altissimo , D.E. Bedolla , E. Giolo , M. Martinelli , S. *Journal of Instrumentation*, 13 - 06, C06003 (2018)

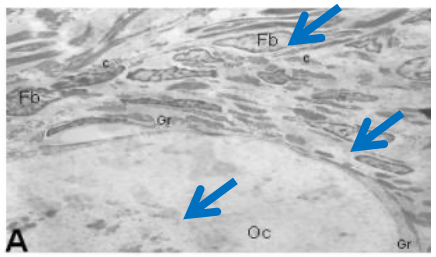
VL and TEM imaging



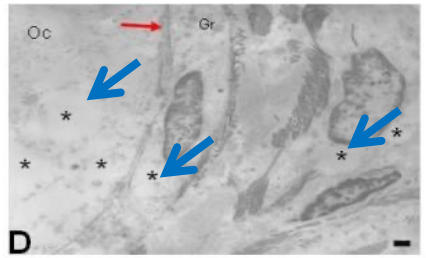
Control (fresh) tissue



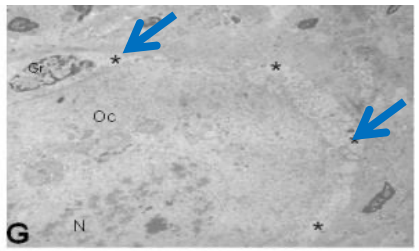
Vitrified tissue



Control tissue



Slow freezing tissue



Vitrified tissue

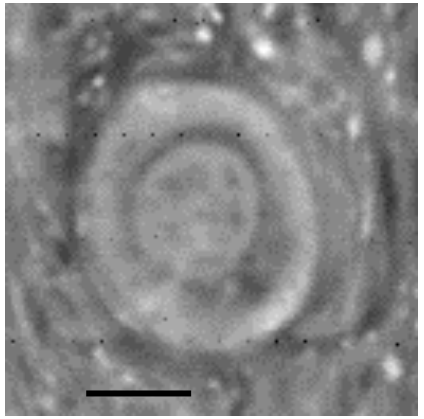
Visible light and TEM microscopies are the standard tools for evaluating follicles' and tissue' morphology and integrity

L. Pascolo, I. Venturin, A. Gianoncelli, R. Bortul, G. Zito, E. Giolo, M. Salomé, D.E. Bedolla, M. Altissimo, M. Zweyer, G. Ricci *Reproductive BioMedicine Online*, 37 - 2, 153-162 (2018)
L. Pascolo , I. Venturin , A. Gianoncelli , M. Salomé , M. Altissimo , D.E. Bedolla , E. Giolo , M. Martinelli , S. *Journal of Instrumentation*, 13 - 06, C06003 (2018)

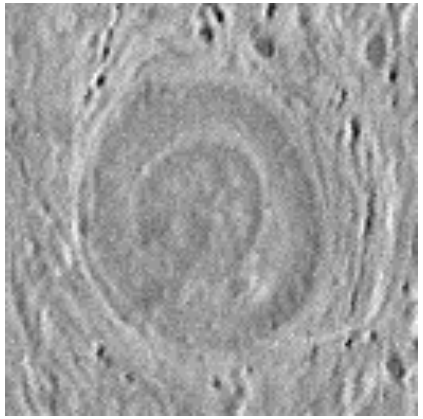
STXM imaging

Control tissue

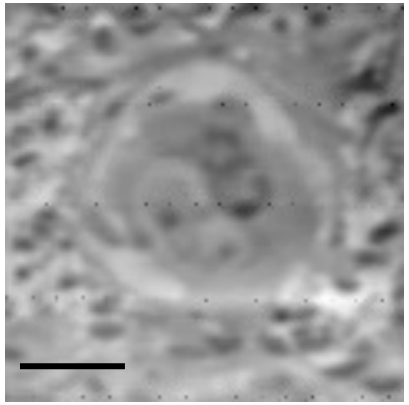
Vitrified tissue



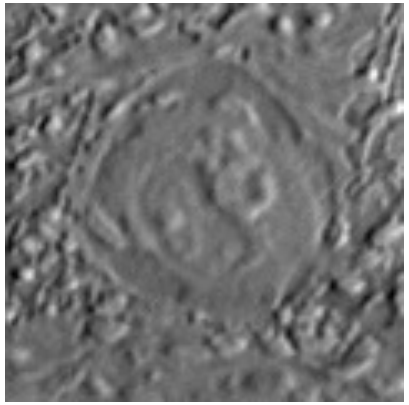
Absorption



Differential Phase Contrast



Absorption



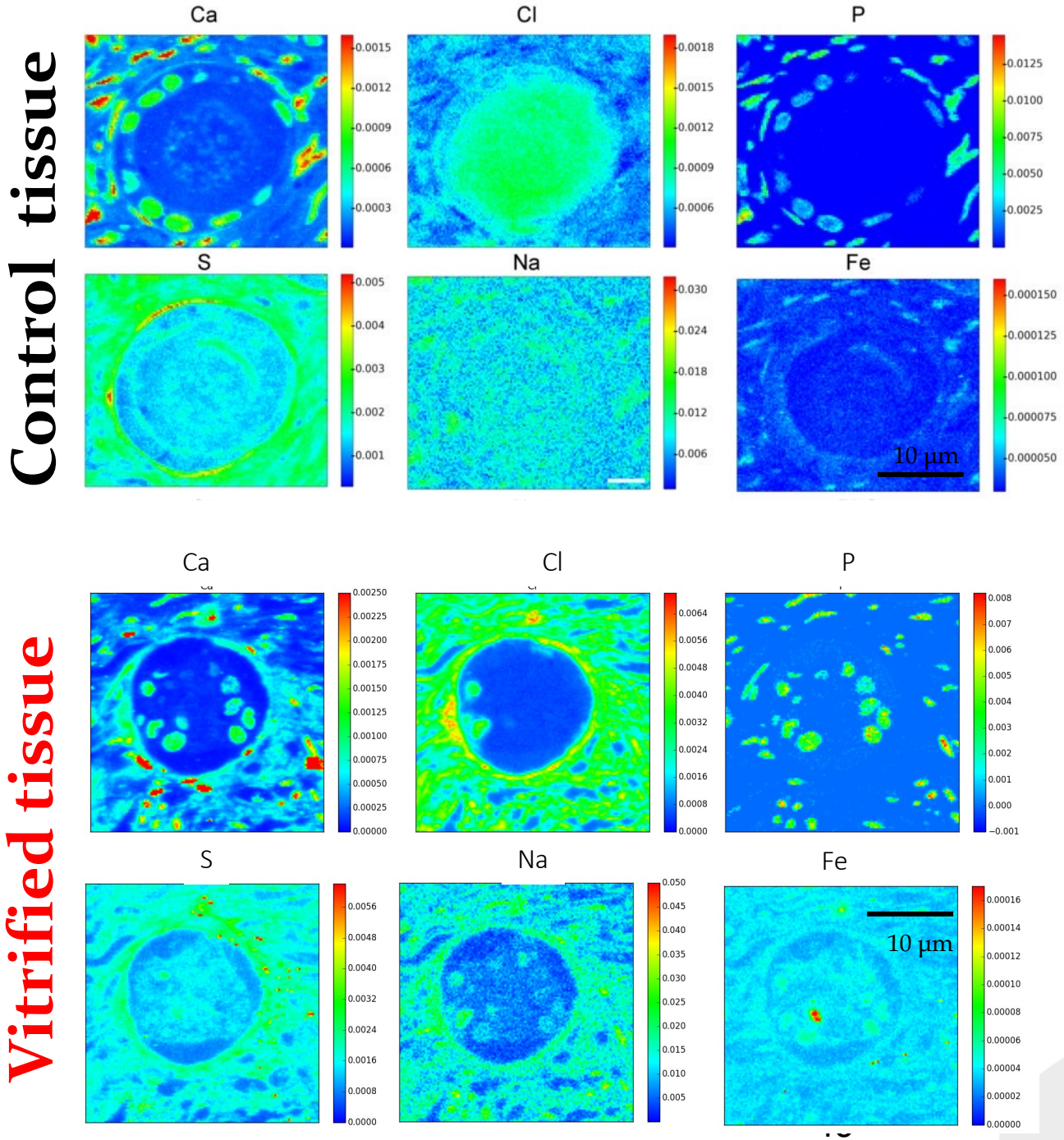
Differential Phase Contrast

The absorption and phase contrast images collected at 1.5 keV at TwinMic beamline. Step size of 400 nm. Scale bar is 10 µm.
A clear difference in the apparence is revealed, probably related to the integrity of extracellular matrix.

L. Pascolo, I. Venturin, A. Gianoncelli, R. Bortul, G. Zito, E. Giolo, M. Salomé, D.E. Bedolla, M. Altissimo, M. Zweyer, G. Ricci *Reproductive BioMedicine Online*, 37 - 2, 153-162 (2018)
L. Pascolo , I. Venturin , A. Gianoncelli , M. Salomé , M. Altissimo , D.E. Bedolla , E. Giolo , M. Martinelli , S. *Journal of Instrumentation*, 13 - 06, C06003 (2018)

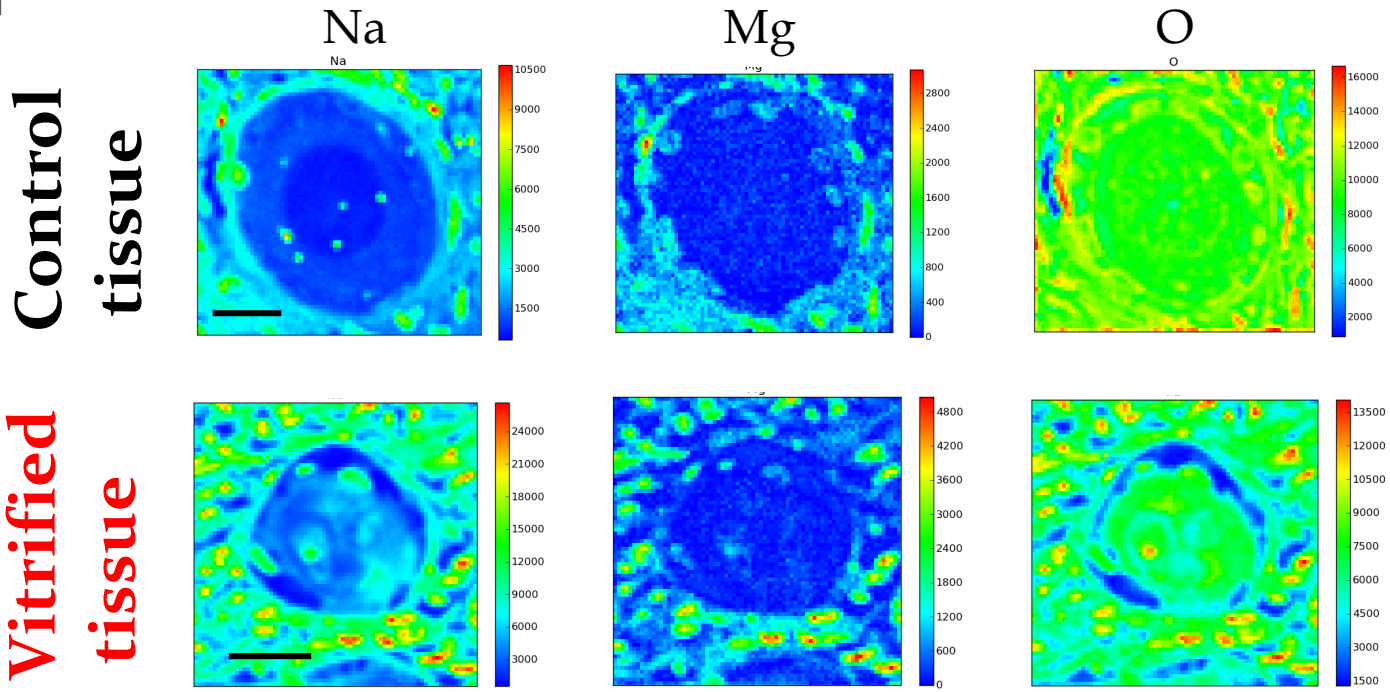
Elettra
Sincrotrone
Trieste

XRF @ ID21 (ESRF synchrotron)



L. Pascolo, I. Venturin, A. Gianoncelli, R. Bortul, G. Zito, E. Giolo, M. Salomé, D.E. Bedolla, M. Altissimo, M. Zweyer, G. Ricci *Reproductive BioMedicine Online*, 37 - 2, 153 (2018)

Soft X-ray Microscopy at TwinMic



- Sulphur distribution seems to be an indicator of the extracellular components changes in the stromal tissues of freeze-stored samples, better revealed by TEM analyses as vacuolarization

- Low quality follicles in vitrified tissues show increased Na in the ooplasm, high Ca at the basal membrane, altered distribution of Cl and Fe.

L. Pascolo, I. Venturin, A. Gianoncelli, R. Bortul, G. Zito, E. Giolo, M. Salomé, D.E. Bedolla, M. Altissimo, M. Zweyer, G. Ricci *Reproductive BioMedicine Online*, 37 - 2, 153 (2018)

MicroPlastics Exposure

PhD project of Federica Zingaro - UniTS

AIM TO UNRAVEL THE NANOPARTICULATE TOXICOLOGICAL ACCUMULATION
IN VITRO AND RELATED IMPACTS ON HUMAN HEALTH AND FERTILITY

Toxicity towards organisms still poorly understood

Detection of polymeric particles lacks techniques (small size, concentration,..)

Model MNPs are required



Toxicology 458 (2021) 152850

Contents lists available at ScienceDirect

TOXICOLOGY

Environment International 146 (2021) 106274

Contents lists available at ScienceDirect

Journal of Hazardous Materials 426 (2022) 127804

Contents lists available at ScienceDirect

Journal of Hazardous Materials

journal homepage: www.elsevier.com/locate/jhazmat

ELSEVIER

HAZARDOUS MATERIALS

Check for updates

Identification and characterisation of individual nanoplastics by scanning transmission X-ray microscopy (STXM)

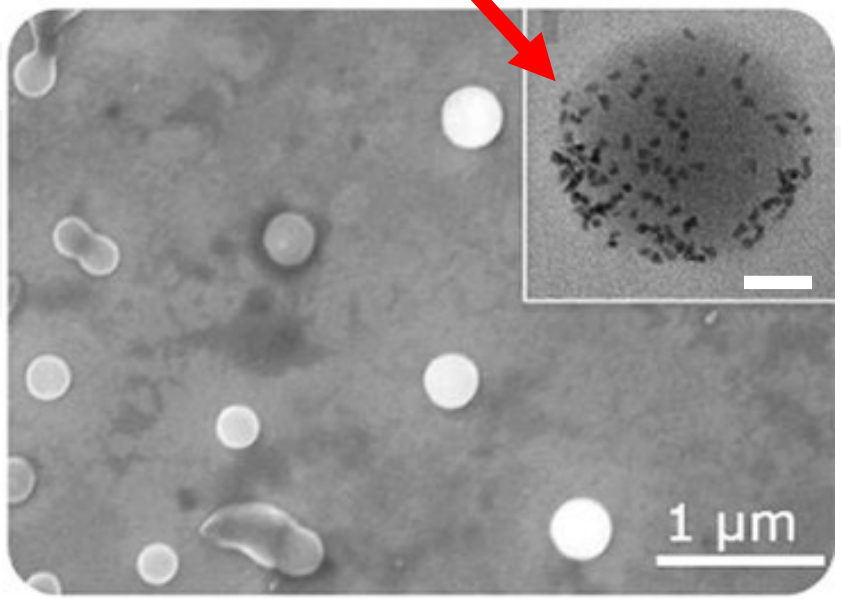
Alexandra Foetisch [a], Montserrat Filella [b], Benjamin Watts [c], Laure-Hélène Vinot [a], Moritz Bigalke [a,*]

UNIVERSITÀ DEGLI STUDI DI TRIESTE

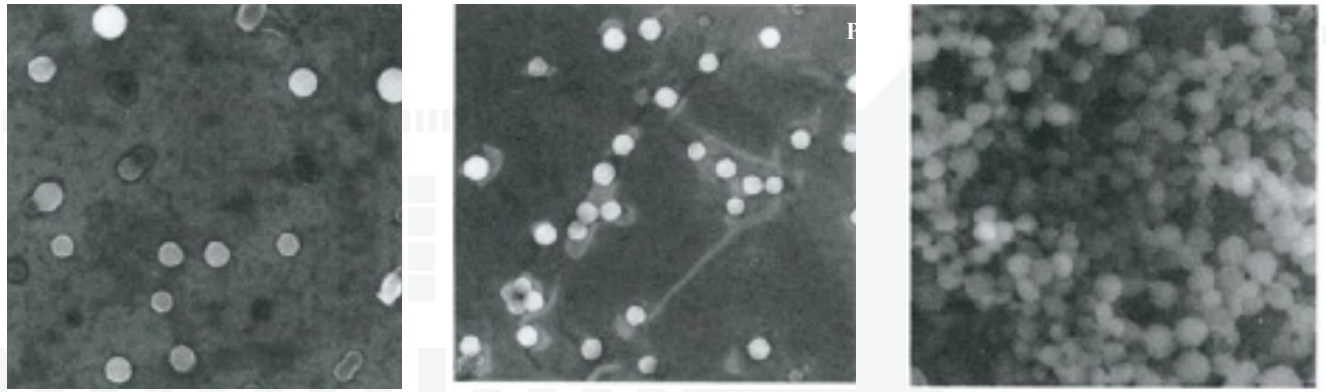
CADMIUM SELENIDE QUANTUM DOTS NANOPLASTICS (NPS) SYNTHETIZED AT JRC

- **Novel synthesis via oil-in-water emulsion precipitation**

Spherical shape $50\ \text{nm} < d < 350\ \text{nm}$ (DLS, SEM imaging)



Transmission electron microscopy (TEM) image of PP-QDs NPs



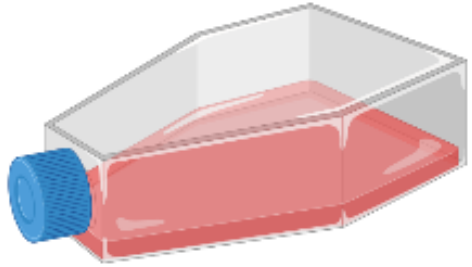
Scanning transmission electron microscopy (SEM) images of QDs -NPs

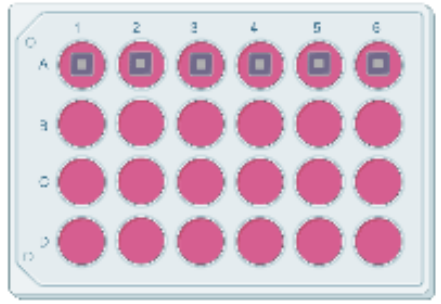
- **The most common polymers in the environment**
- **Polystyrene beads in laboratory studies**

D. Cassano et al. ACS Appl. Nano Mater., 4, (2), 1551–1557, 2021

IN VITRO STUDIES

- ❖ THP-1 cell line, macrophages surrogate
- ❖ Immune frontline of defense
- ❖ M1 phenotype (pro-inf.), M2 (anti-inf.)











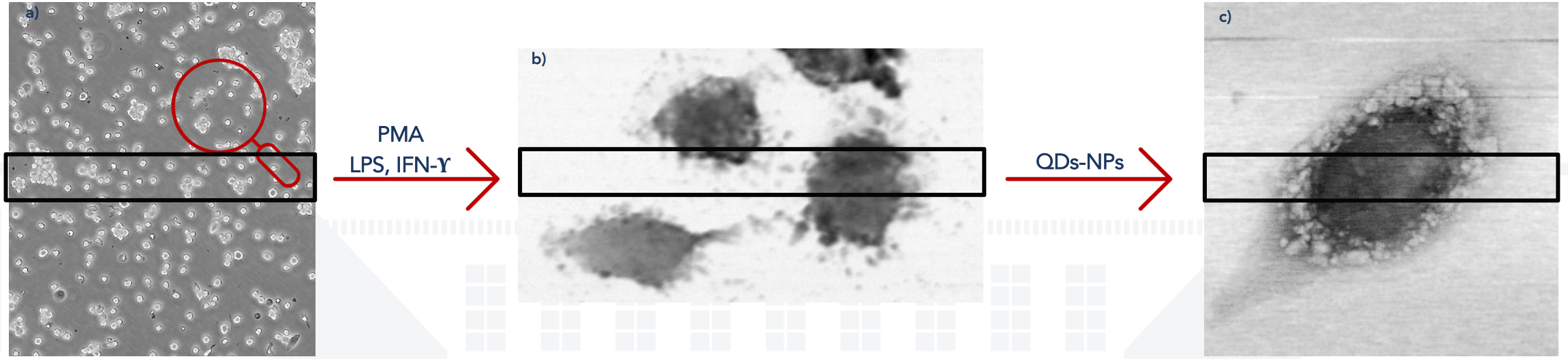
Schematic phagocytosis of NPs by macrophage cells

L. Rubio et al., Journal of Hazardous Materials, 398, 122900, 2020

soft X-ray microscopy TwinMic XRF | STXM | Ptychography | Fullfield | CDI

CERIC Central European Research Infrastructure Consortium

CELL ANALYSIS AT ELETTRA SINCROTRONE



$3 \cdot 10^5$ THP-1 cells/mL

M1-phenotype macrophage

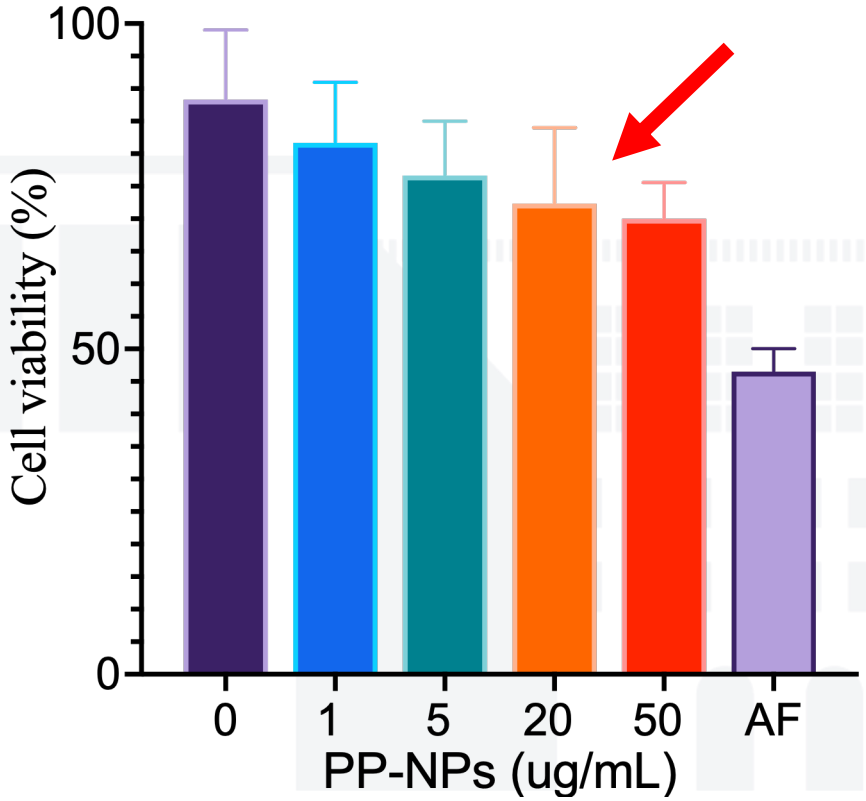
M1-phenotype macrophage exposed to 20 mg/mL QDs-PP

Figures b, c - High resolution STXM images were acquired at TwinMic Beamline at ELETTRA Synchrotron Trieste at 1.2 keV excitation energy, 80 mm x 40 mm, 200nm spatial resolution, and 72 mm x 63 mm, 450 nm spatial resolution, respectively.

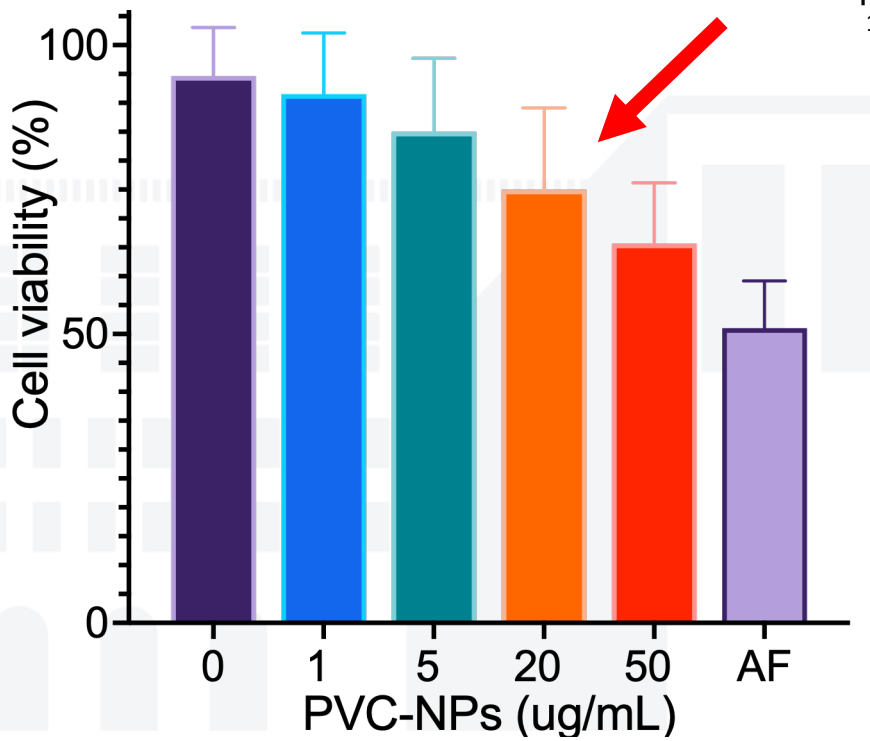
UNIVERSITÀ DEGLI STUDI DI TRIESTE

CITOTOXICOLOGICAL STUDIES RESULTS

MTT assay confirmed the NPs concentration (20 μg/mL) used for experimental analyses assured a high cell viability.



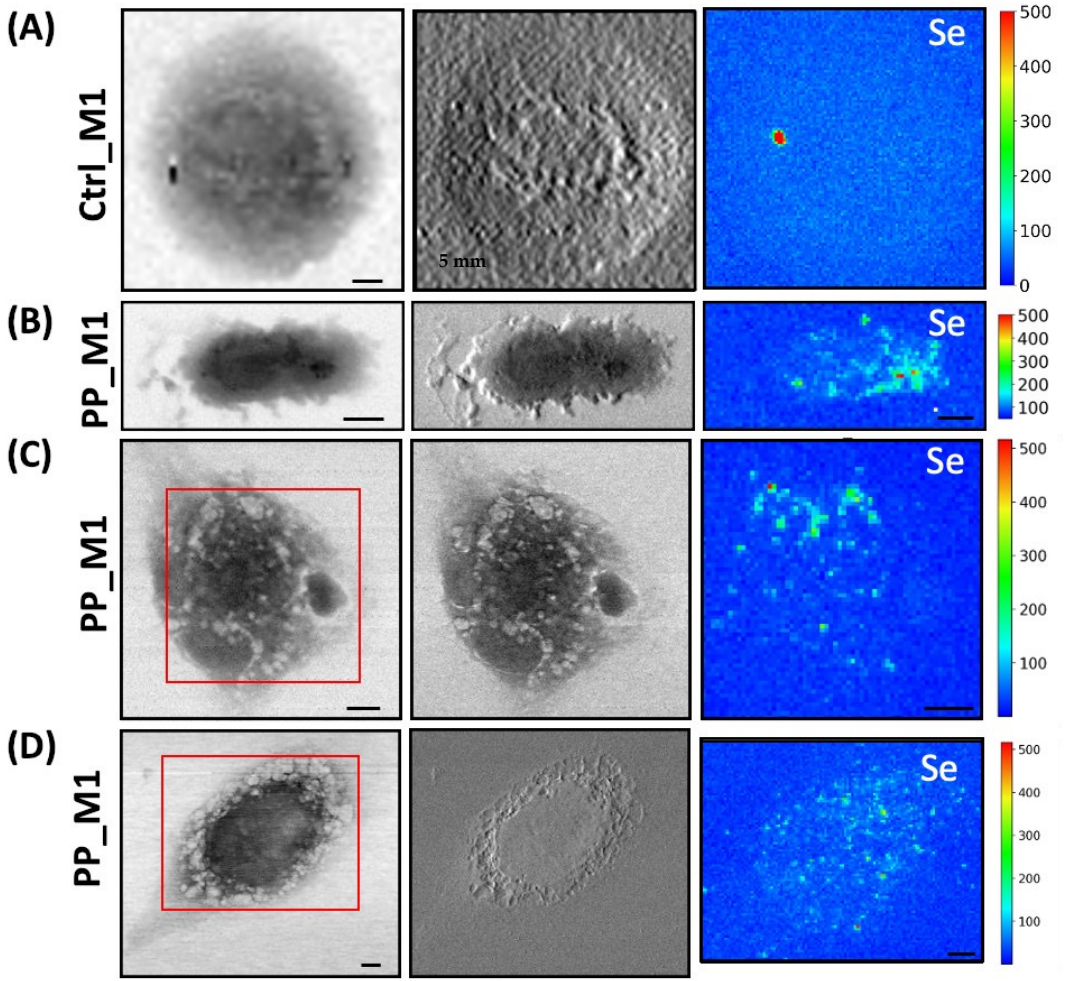
AF: Apoptotic Factor
Steurosporine (2 μM)
1:200



Graphs depicting the cell viability percentage as a function of NPs concentration

Cellular Morphological Changes in PP-NPs Treated Cells

CdSE QDS-labelled Micro- And Nano-plastics



- STXM revealed a more absorbing nuclear region in unexposed macrophages
- PP-NPs treated cells showed to form lipid droplets localized perinuclearly and at the plasma membrane
- LEXRF analyses at 1.7 keV able to track Se L line for NPs identification, and other low-Z elements (C, O, Na, and Mg) for cellular integrity.

Zingaro F., et al., Original Research, Front. Immunol. – Molecular Innate Immunity, Volume 14, **(2023)**

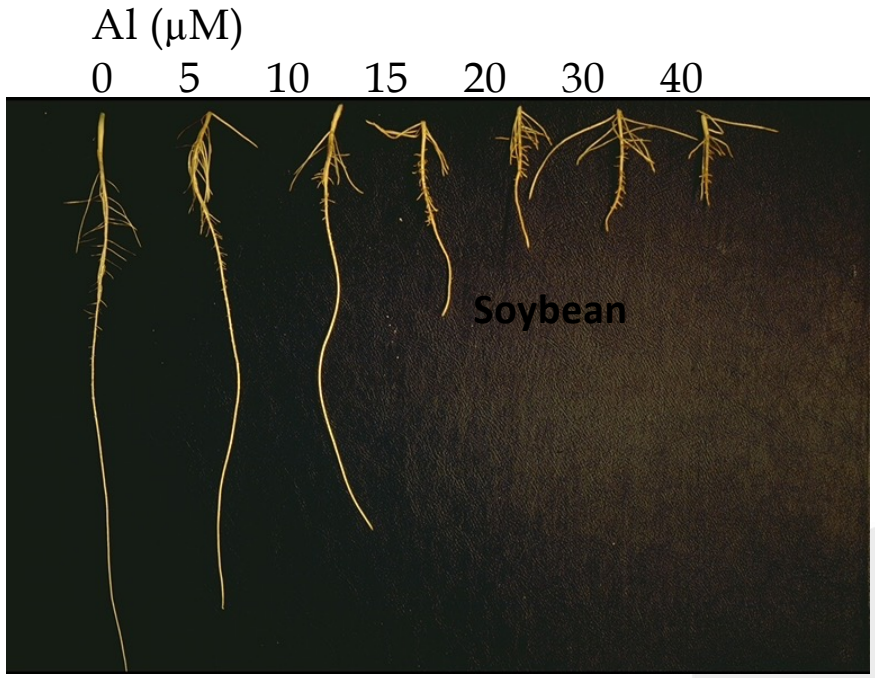
•Aluminium toxicity

Soluble Al – "the most important growth-limiting factor for plants in most strongly acid soils and mine spoils" **Foy (1984)**

Acid soils occupy ~ 40 billion hectares (~ 30 %) of the world's ice free land area
von Uexküll and Mutert (1995)

In Australia alone, acid soils cost $1.5 billion p.a. in lost productivity





Elettra Sincrotrone Trieste

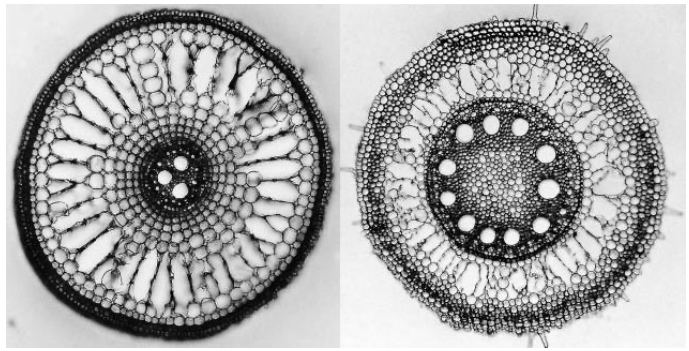
TwinMic

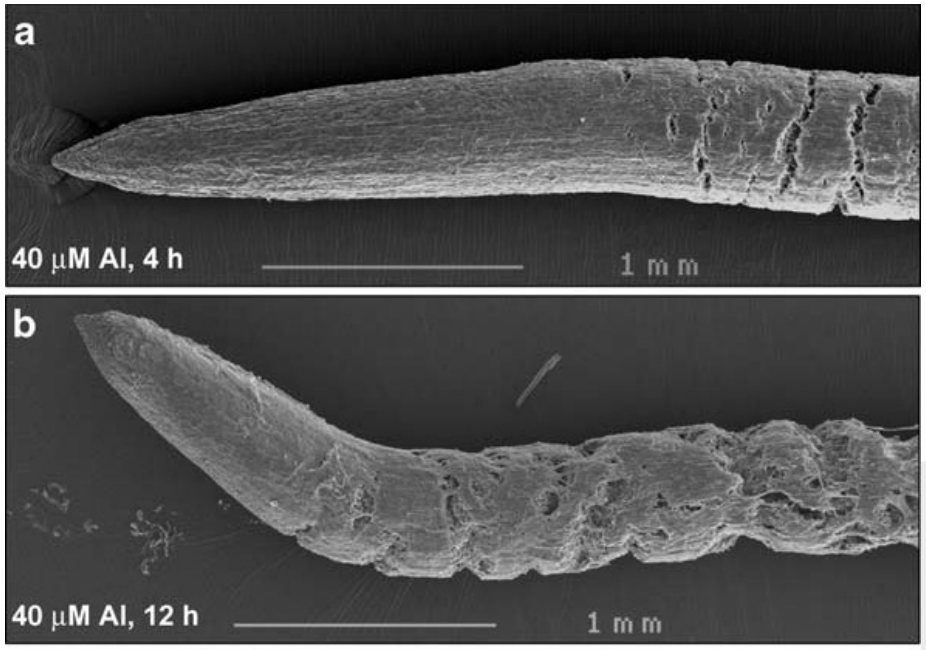
•Aluminium toxicity

Soluble Al – "the most important growth-limiting factor for plants in most strongly acid soils and mine spoils" **Foy (1984**)

Although known since 1904 that Al is the primary factor causing a reduction in plant root growth in acid soils, the mechanism by which Al is toxic remains unclear

Recent research (2014) has shown that Al exerts its toxic effects very quickly, reducing root growth in ≤ 30 min. Therefore, a crucial step in elucidating how Al exerts its toxic effects is to examine where the Al is accumulating within the roots





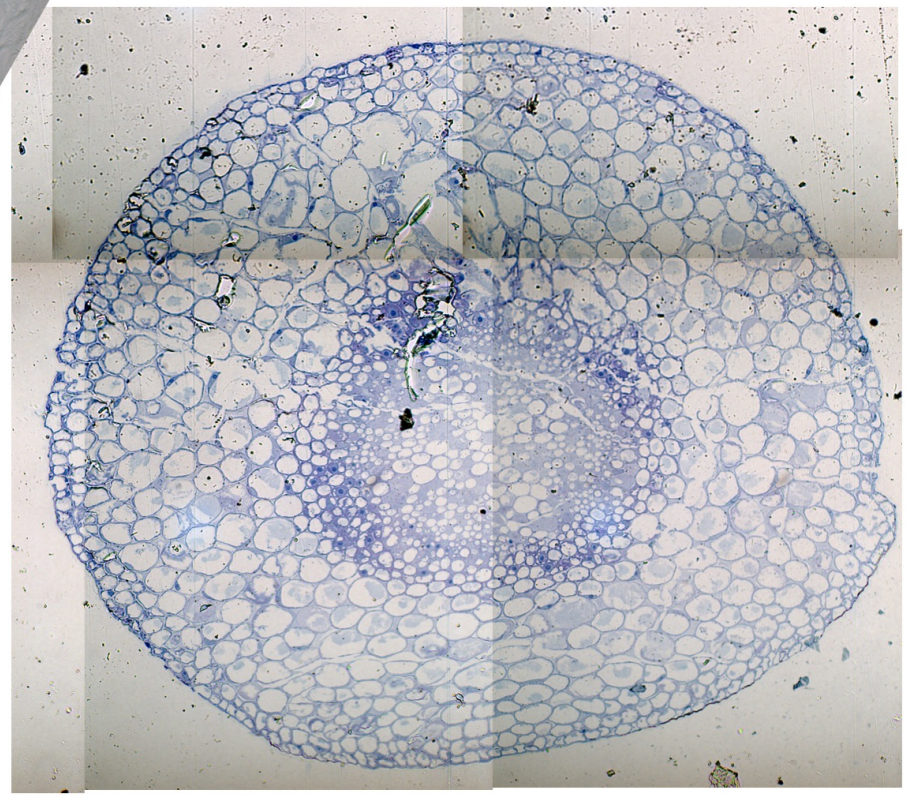
Elettra Sincrotrone Trieste

TwinMic

•Aluminum toxicity

30 minutes, 6 mm, Sample 1



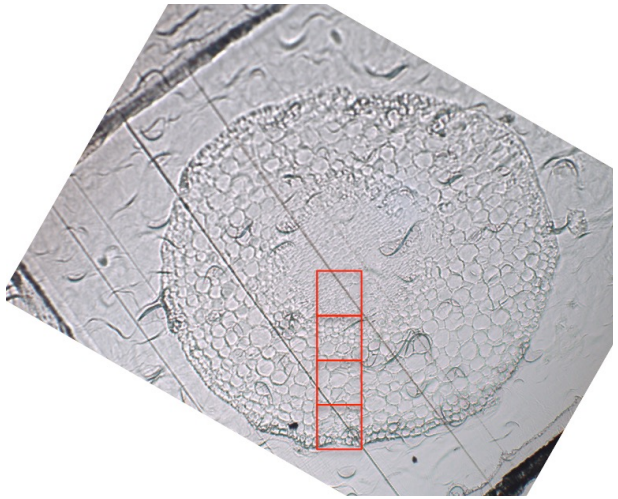


P. M. Kopittke, K. L. Moore , E. Lombi et al, "**Identification of the Primary Lesion of Toxic Aluminum in Plant Roots**" Plant Physiology, 2015, 167, 140

Elettra Sincrotrone Trieste

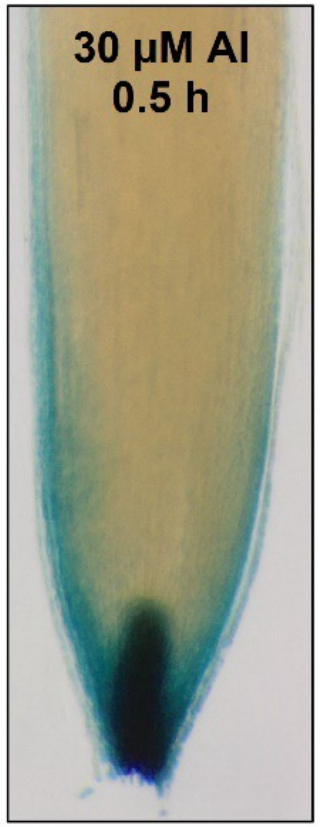
TwinMic

•Aluminium toxicity



7 µm-thick transverse cross section of soybean roots

Exposed to 30 µM Al for 0.5 h.



c) 6mm from apex

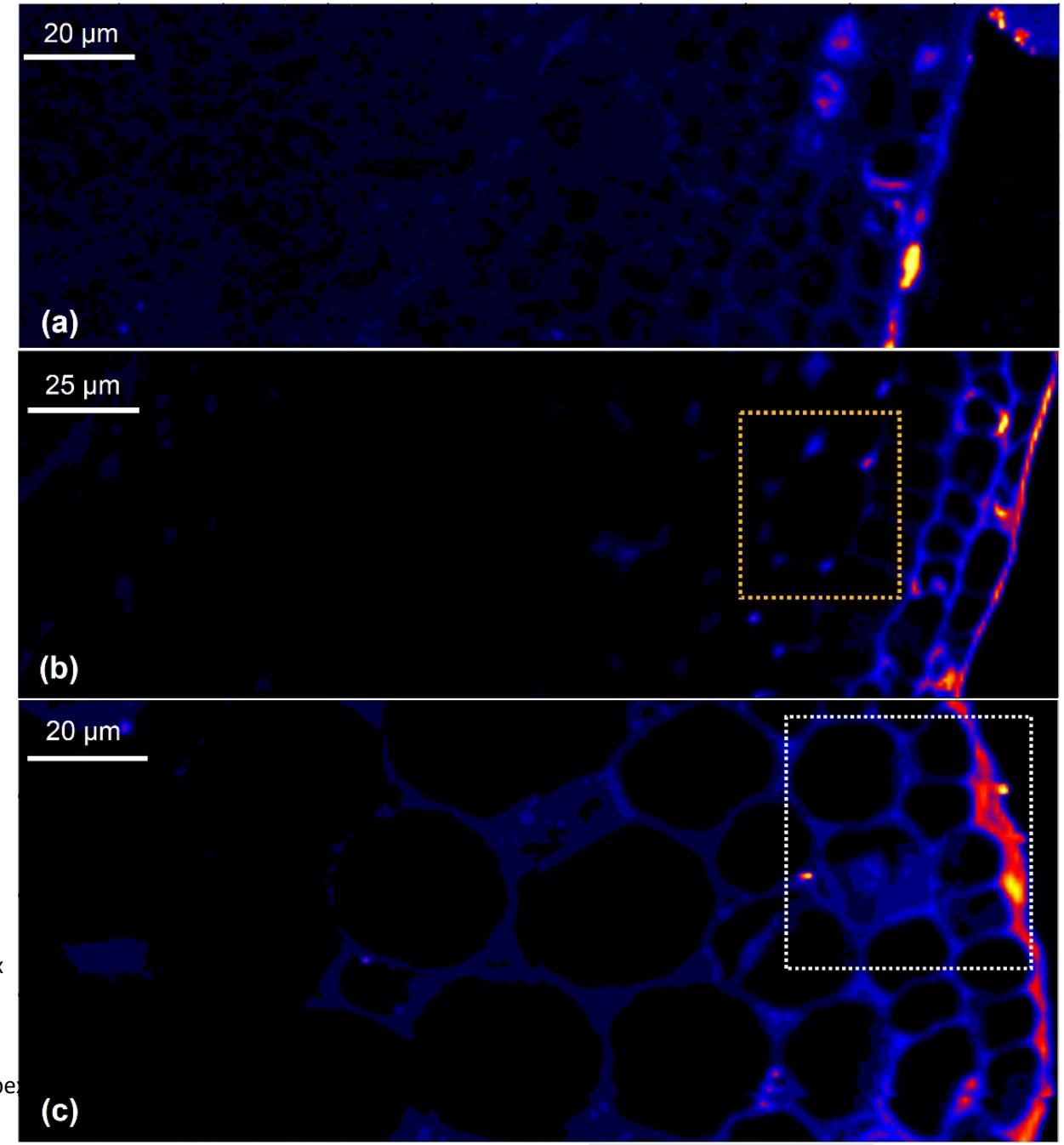
b) 2mm from Apex

a) 0.5 mm from Apex

Soluble Al – "the most important growth-limiting factor for plants in most strongly acid soils and mine spoils" **Foy (1984**)

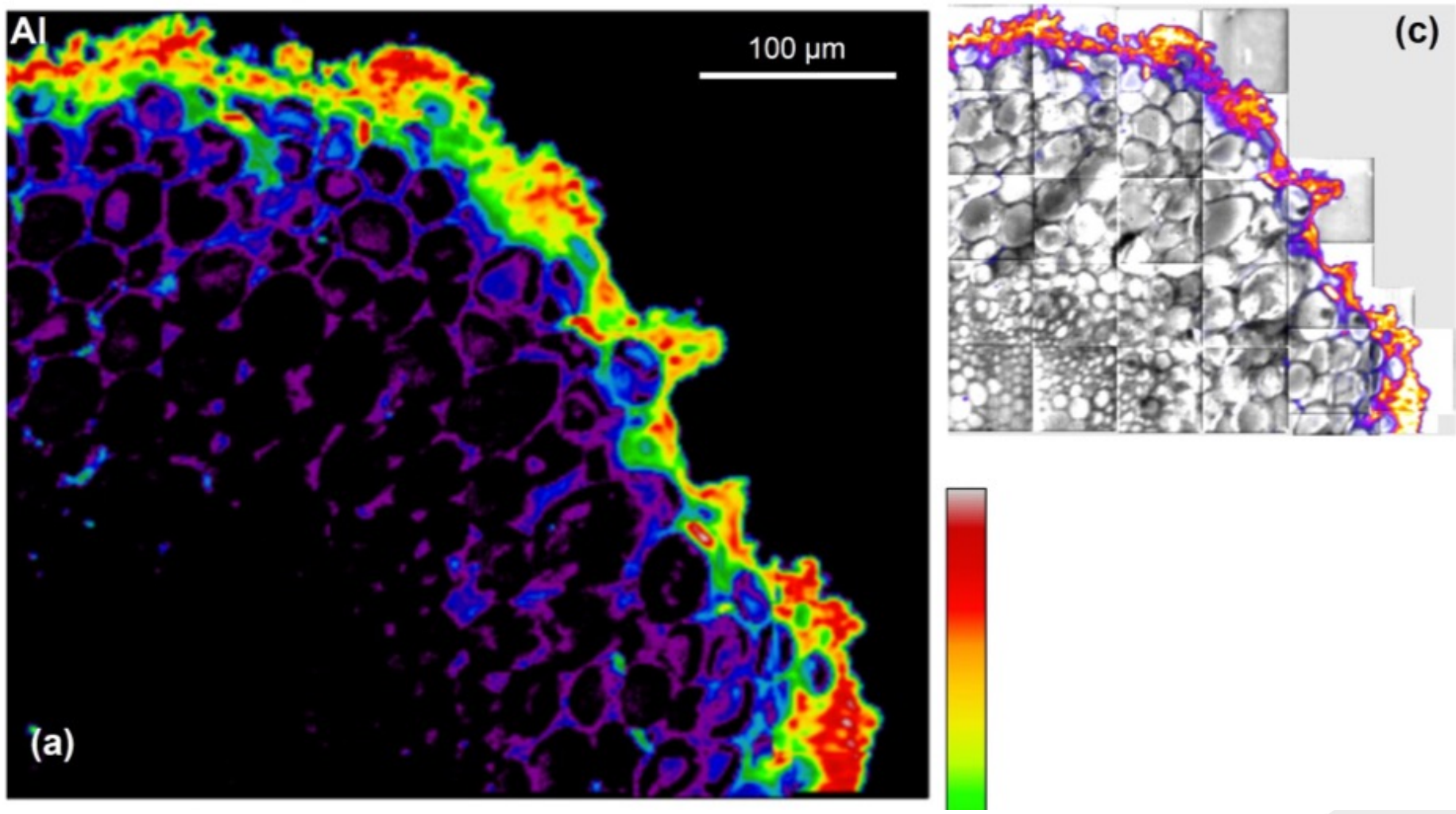
Acid soils occupy ~ 40 billion hectares (~ 30 %) of the world's ice free land area V**on Uexküll and Mutert (1995**)

In Australia alone, acid soils cost $1.5 billion p.a. in lost productivity



P. M. Kopittke, K. L. Moore , E. Lombi et al, "**Identification of the Primary Lesion of Toxic Aluminum in Plant Roots**" Plant Physiology, 2015, 167, 140

- **Soybean roots exposed to 30 µM Al for 0.5 h**



P.M. Kopittke et al "**Identification of the Primary Lesion of Toxic Aluminum in Plant Roots**" Plant Physiology 2015, 167, 140

• Al in wheat

- In wheat (Triticum aestivum), it is commonly assumed that Al is detoxified by the release of organic anions into the rhizosphere (so in the soil), but it is also possible that detoxification occurs within the apoplast and symplast of the root itself
- Rhizosphere = plant-root interface, not well definable in size or shape

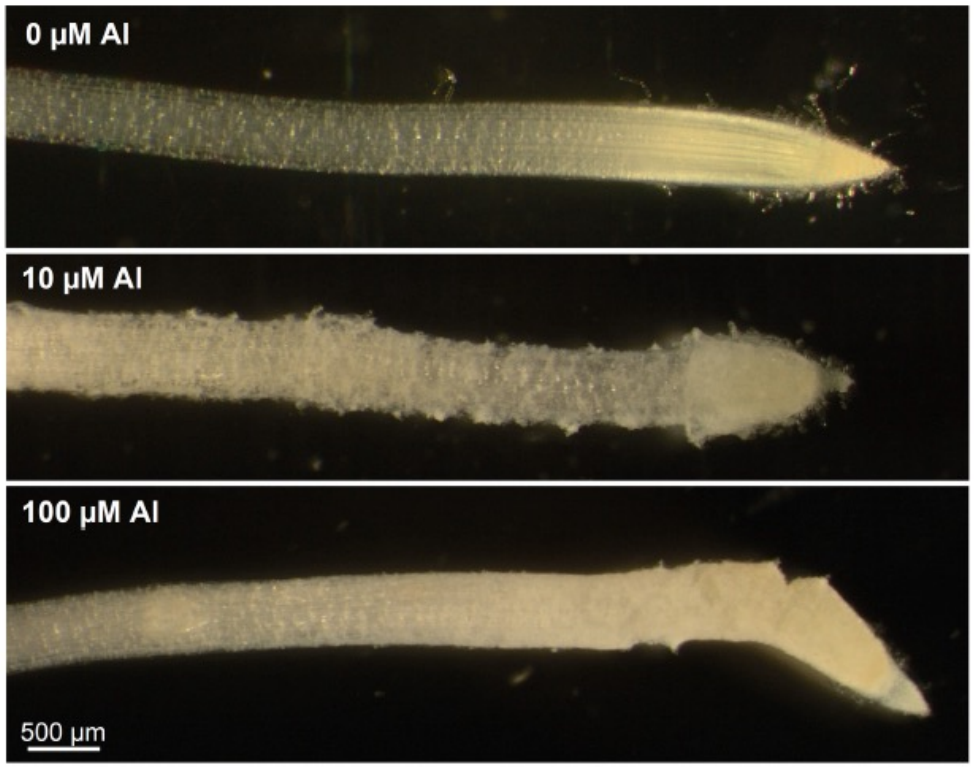


FIGURE 3 | Light micrographs showing roots of ES8 exposed to 0, 10, or 100 µM Al for 48 h. Note the tearing and rupturing evident in the outer tissues of roots exposed to 10 or 100 µM Al. The scale bar applies to all three images.

Kopittke et al. Frontiers in Plant Science 8, 1377 (2017)

Elettra Sincrotrone Trieste

TwinMic

- XRF analyses @ TwinMic

Al-sensitive (ES8)

Al-resistant (ET8)

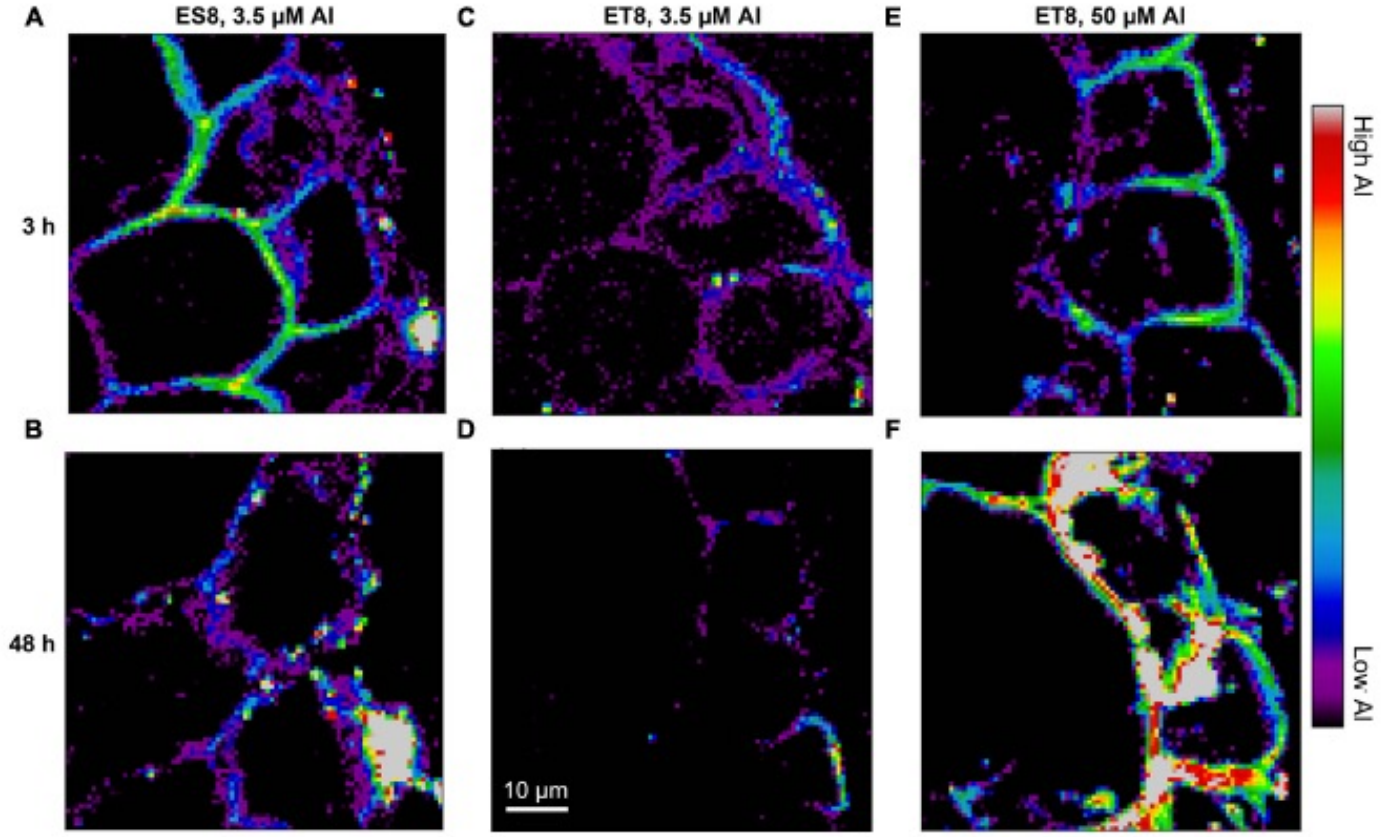


FIGURE 5 | The distribution of Al, examined using LEXRF, in 5-µm-thick transverse root sections taken 3 mm from the apex of ES8 and ET8 exposed to 3.5 or 50 µM Al for either 3 h **(A,C,E)** or 48 h **(B,D,F)**. In all cases, the rhizodermis (and exterior of the root) is on the right-hand side of the image, with only the rhizodermis and 1–2 layers of cortical cells shown. The signal intensity is presented as a color scale, with brighter colors corresponding to higher concentrations. All images were scaled to the same values, and hence intensities can be compared between images. The scale-bar in **(D)** applies to all images. See Supplementary Figure 1 for corresponding light micrographs.

- When ES8 and ET8 were grown at 3.5 mM Al, roots of ES8 accumulated more Al than did those of ET8
- when grown at Al concentrations that resulted in the same reduction in RER (root elongation rate), root tissues of ET8 tended to accumulate more Al than did those of ES8
- Al accumulated primarily in the cell wall in apical root tissues of both ES8 and ET8

- Roots ruptures form initially in the elongation where Al was found to accumulate to high concentrations. This reaffirms the importance of Al accumulation in the cell walls, thereby decreasing root elongation by rapidly inhibiting the ability of the walls to loosen.

Kopittke et al. Frontiers in Plant Science 8, 1377 (2017)

Elettra Sincrotrone Trieste

TwinMic

- XANES on Al edge (@ CLS)

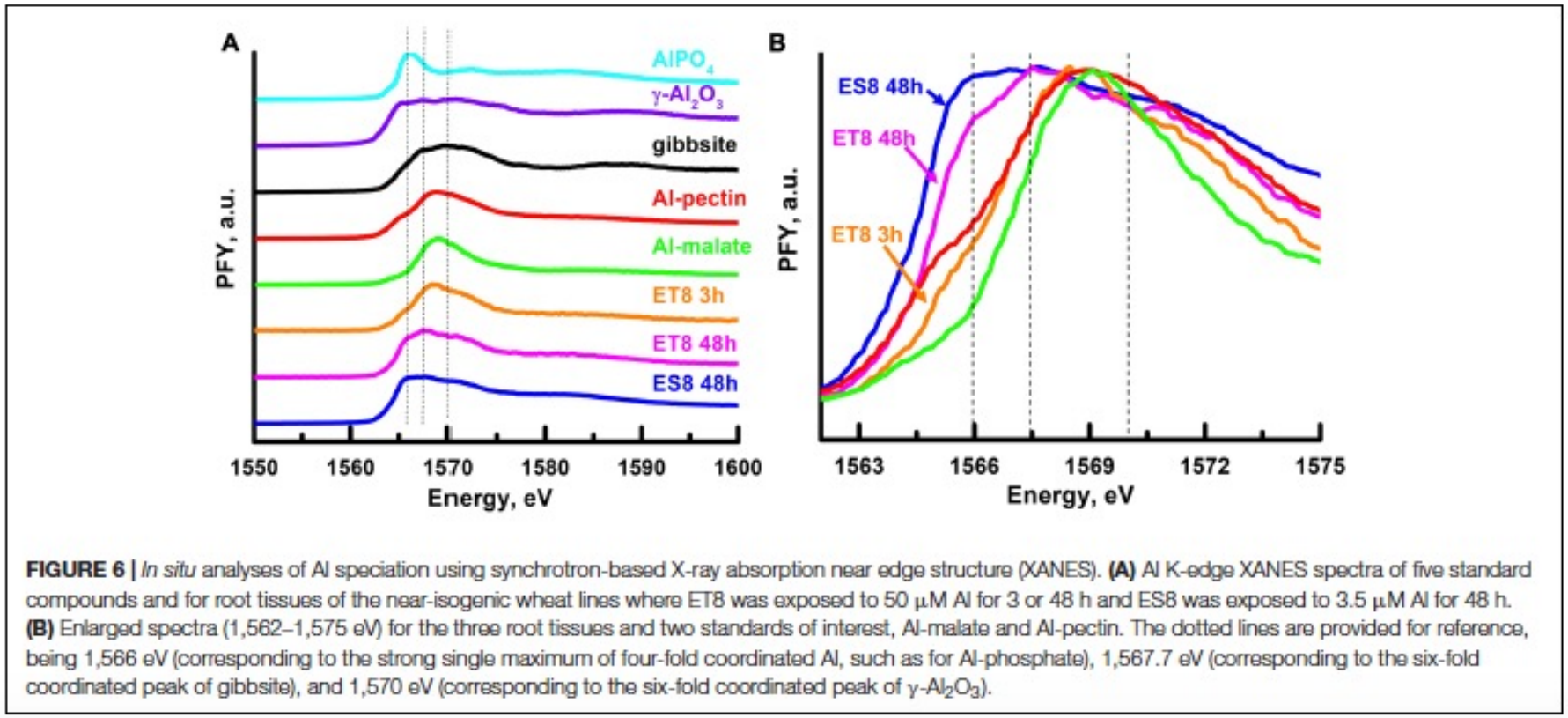
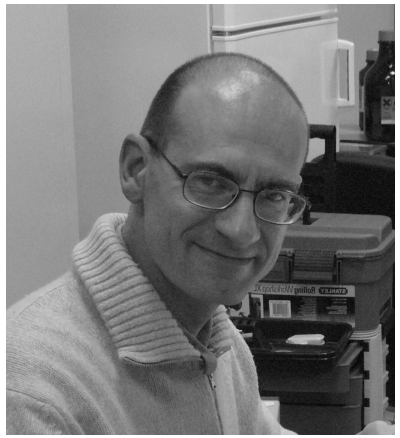


FIGURE 6 | *In situ* analyses of Al speciation using synchrotron-based X-ray absorption near edge structure (XANES). **(A)** Al K-edge XANES spectra of five standard compounds and for root tissues of the near-isogenic wheat lines where ET8 was exposed to 50 μM Al for 3 or 48 h and ES8 was exposed to 3.5 μM Al for 48 h. **(B)** Enlarged spectra (1,562–1,575 eV) for the three root tissues and two standards of interest, Al-malate and Al-pectin. The dotted lines are provided for reference, being 1,566 eV (corresponding to the strong single maximum of four-fold coordinated Al, such as for Al-phosphate), 1,567.7 eV (corresponding to the six-fold coordinated peak of gibbsite), and 1,570 eV (corresponding to the six-fold coordinated peak of γ-Al_2O_3).

- ET8 exposed for 3 h being a mixture of Al species, but mainly Al organic species including that of Al-malate and Al-pectin
- After exposure to Al for 48 h, much of the Al was four-fold coordinated (particularly for ES8, with ET8 still having a higher proportion of six-fold coordinated Al), although the exact form of this four-fold coordinated Al is not clear and further work is required.
- The complexation of Al by malate in ET8 reduces the strong binding of Al to the cell wall, and thereby reduces the damaging interactions of Al with the root cells.

Kopittke et al. Frontiers in Plant Science 8, 1377 (2017)

Electrochemistry: Development of fuel cells

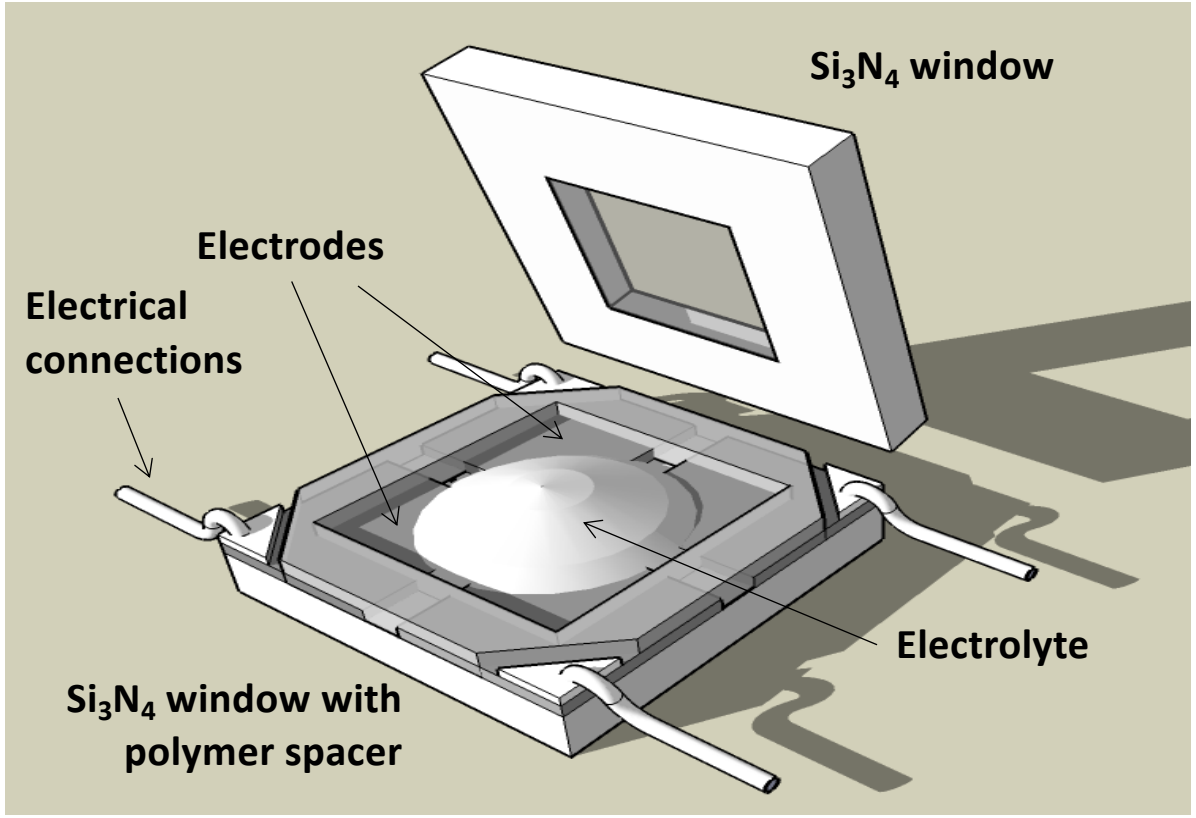


Benedetto Bozzini,
Uni Lecce/ Salento, I

Towards the development of a micro fuel-cell for in-situ spectromicroscopy

B. Bozzini et al., ChemSusChem 2010

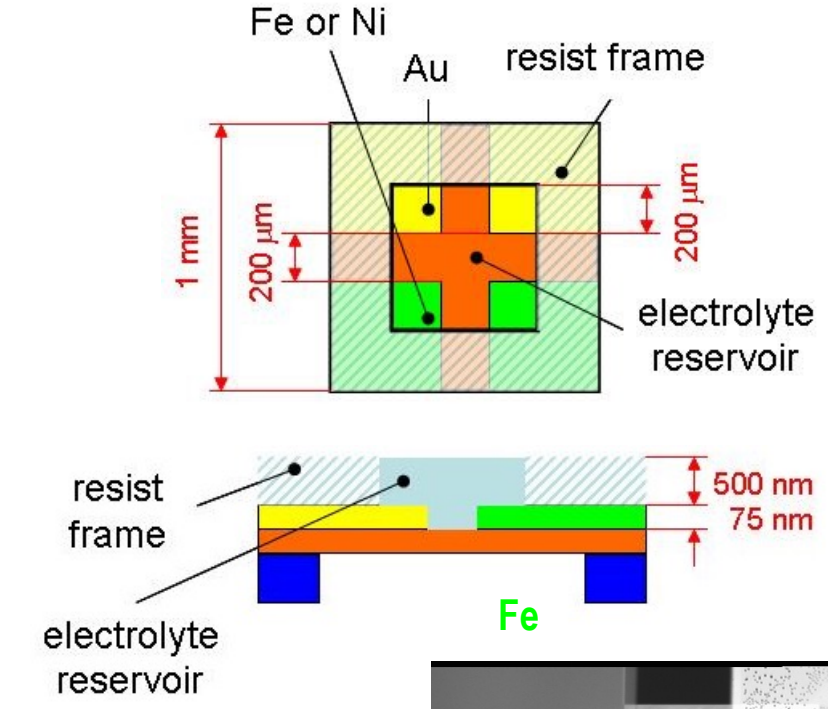
Vacuum-compatible functional electrolytic specimen cell for in-situ studies



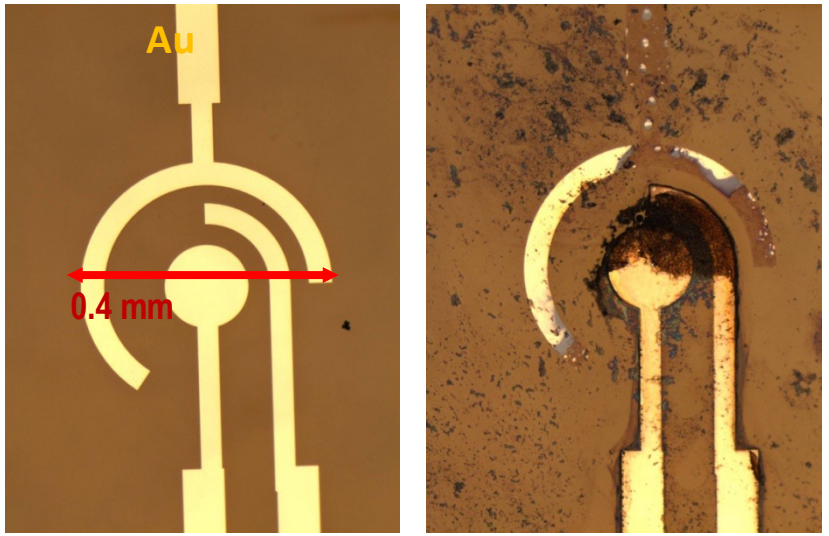
B. Bozzini, A. Gianoncelli, B. Kaulich, .M. Kiskinova, M. Prasciolu, I. Sgura, Metallic Plate Corrosion and Uptake of Corrosion Products by Nafion in Polymer Electrolyte Membrane Fuel Cells, ChemSusCHem 2010, 3, 846-850.

•Vacuum compatible Electrochemical cells

Through-mask evaporation



Electron-beam lithography

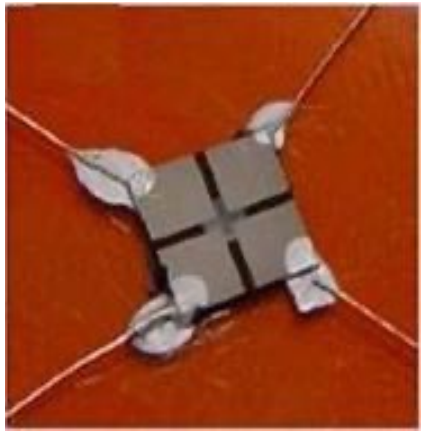


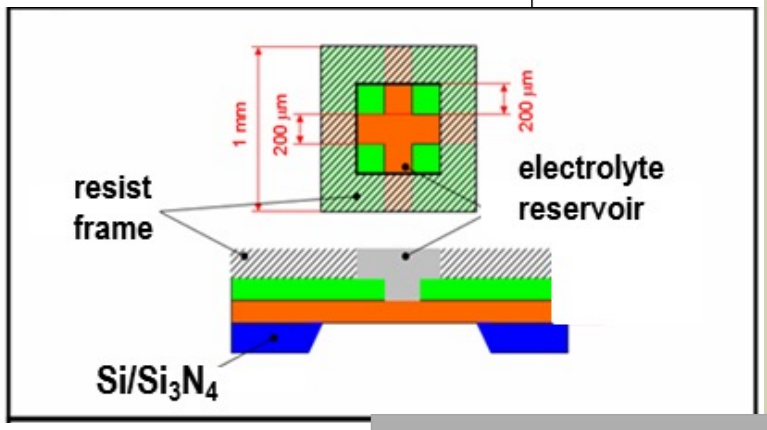
1) **Improve the current density distribution**
2) **Localisation of the electrochemical processes**

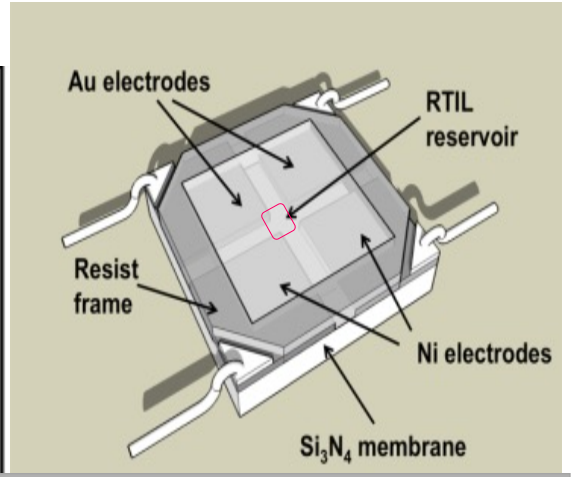
Elettra Sincrotrone Trieste

TwinMic

- **Vacuum-compatible electrolytes (ionic liquids and IL-based gels)**



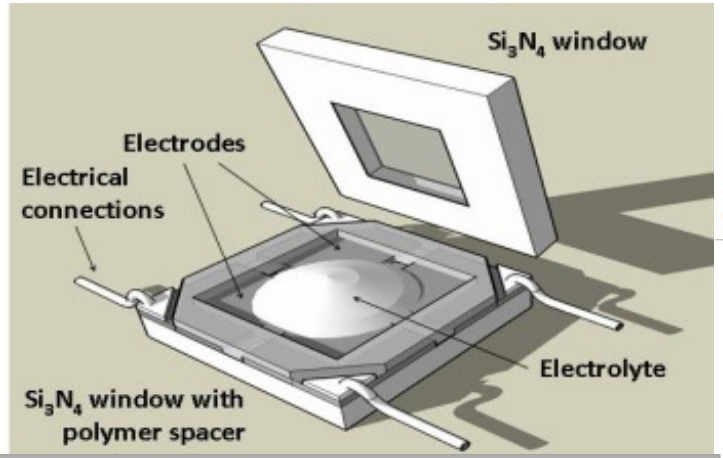




Corrosion of Ni in 1-butyl-1-methyl-pyrrolidinium bis (trifluoromethylsulfonyl) amide room-temperature ionic liquid: operated at anodic polarization of 0.5 V vs Au electrode

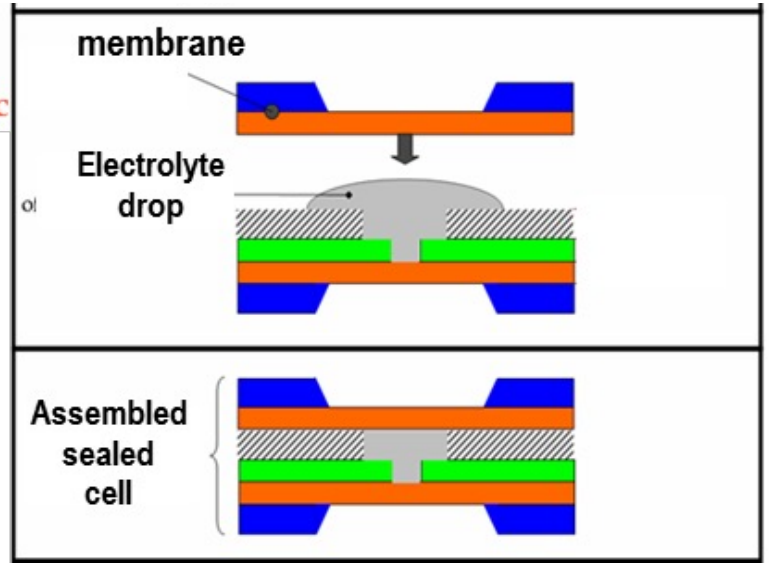
B. Bozzini et al, ChemPhysPhysChem (in press)

Non vacuum-compatible (aqueous solutions)



Metallic Plate Corrosion and Uptake of Corrosion Products by Nafion in Polymer Electrolyte Membrane Fuel Cells

B. Bozzini et al, ChemSusChem 3, 1, 2010



water solution
Nafion 0.25 %,
isopropyl alcohol 3.75 %

- **A selection of in situ STXM results**

1) Electrodeposition

(1.1) Proof of concept: Ag electrodeposition,

(1.2) Electroforming of Ni in nm-thick features,

(1.3) Mn electro-deposition from CHCl+Urea for supercapacitors.

2) PEMFC durability

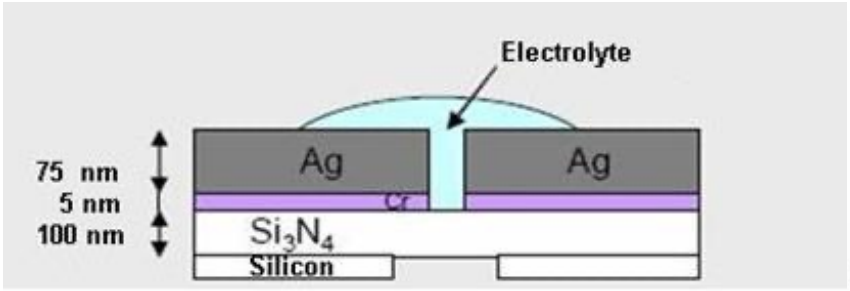
(2.1) BP corrosion in ionic liquid,

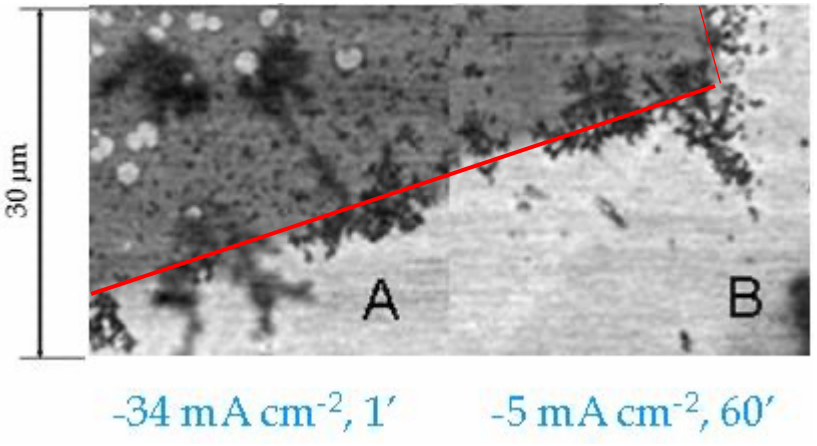
(2.2) BP corrosion and pickup of metal ions by Nafion,

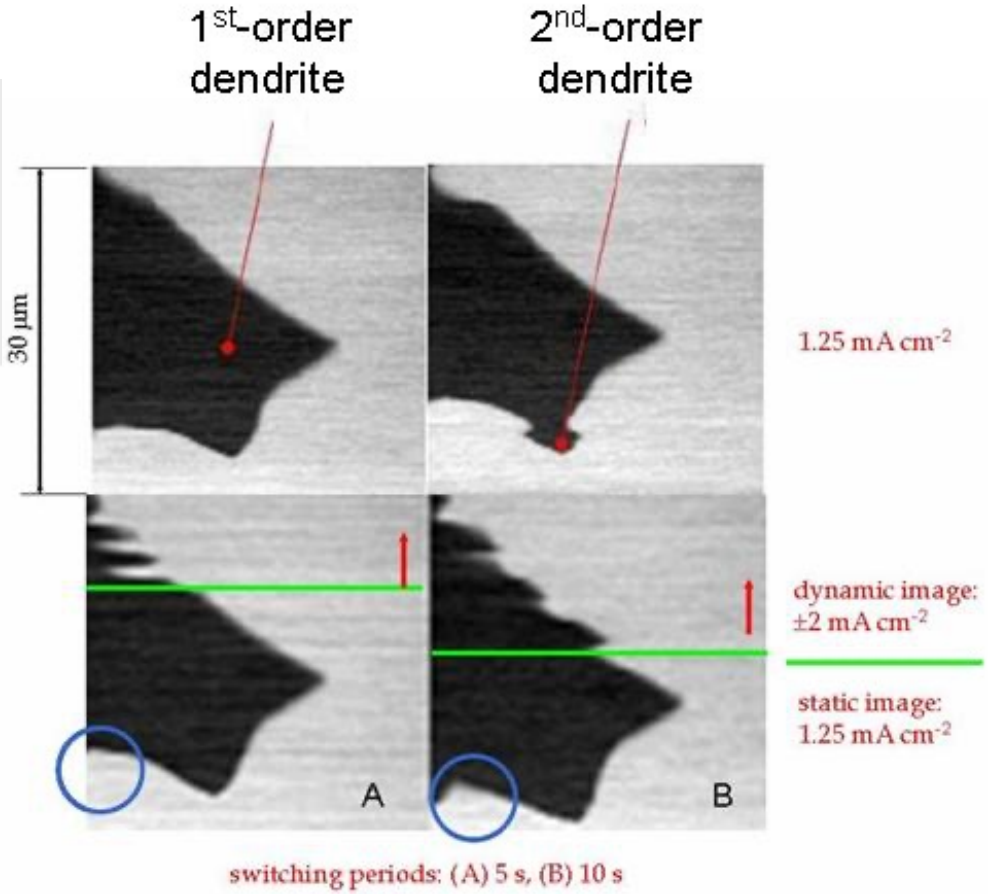
(2.3) Model anodic and cathodic half-cells (Fe/Au/Pt/Nafion + ionic liquid/fuel/O_2)

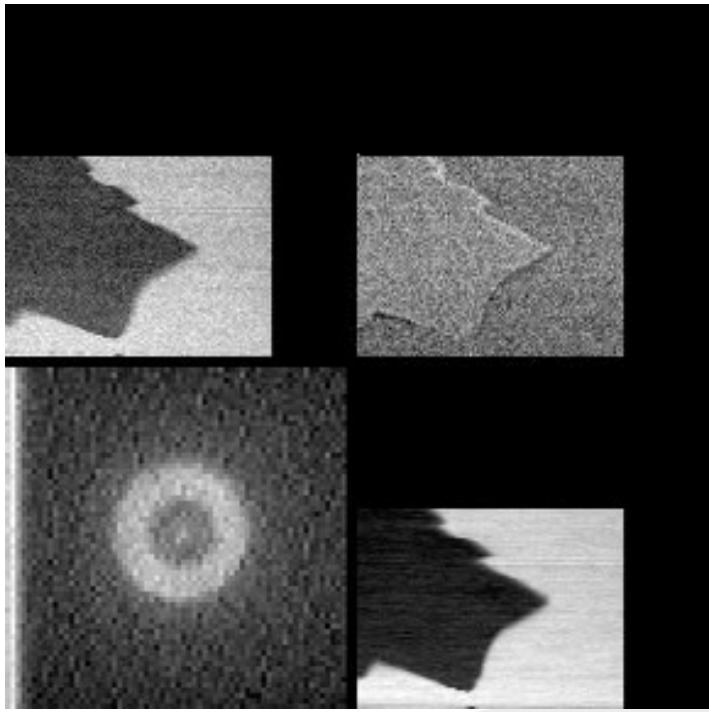
- In situ Ag electrodeposition aqueous electrolyte (sealed cell)

SXTM images









NH_4^+

$E_{h\nu}$ = 477 eV

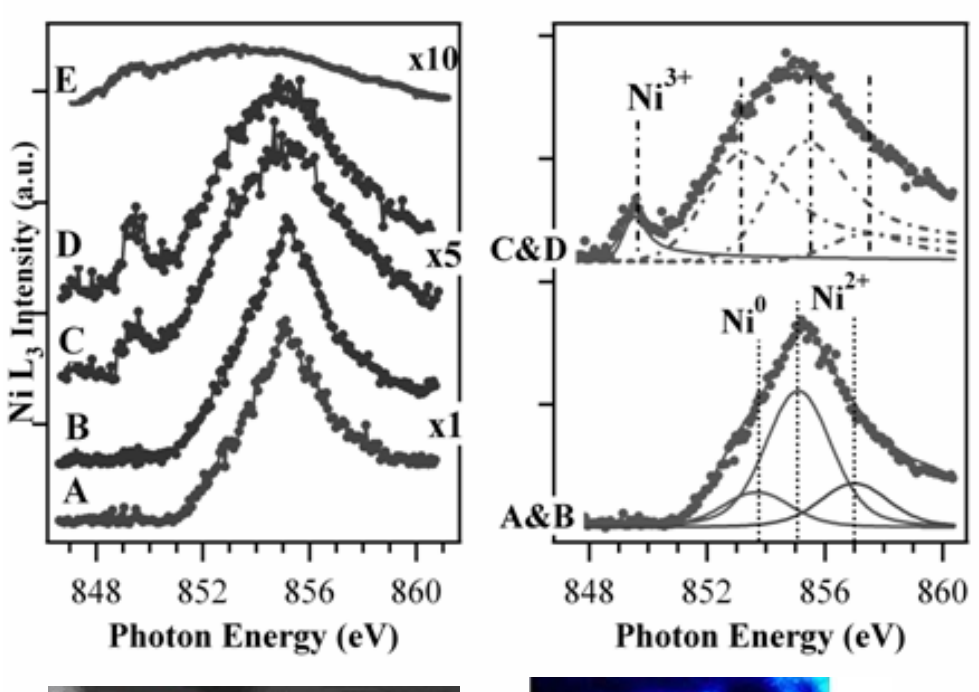
Cl^-

Bozzini et al. Electrochem. Comm. 10 (2008) 1680

Elettra Sincrotrone Trieste

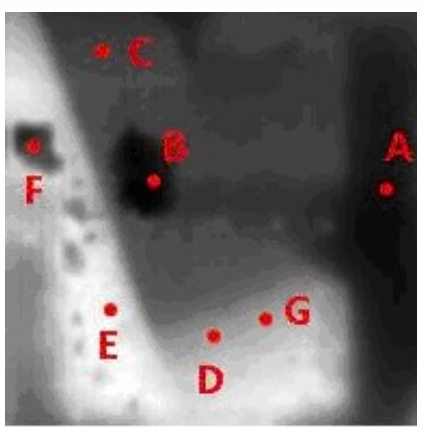
TwinMic

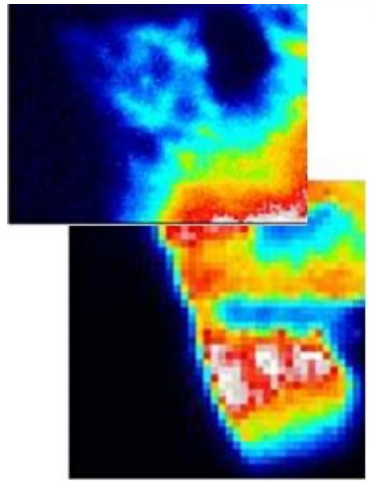
• FC durability



Bipolar plate (Ni) corrosion in ionic liquid

Ni XANES spectra





Ni XRF map

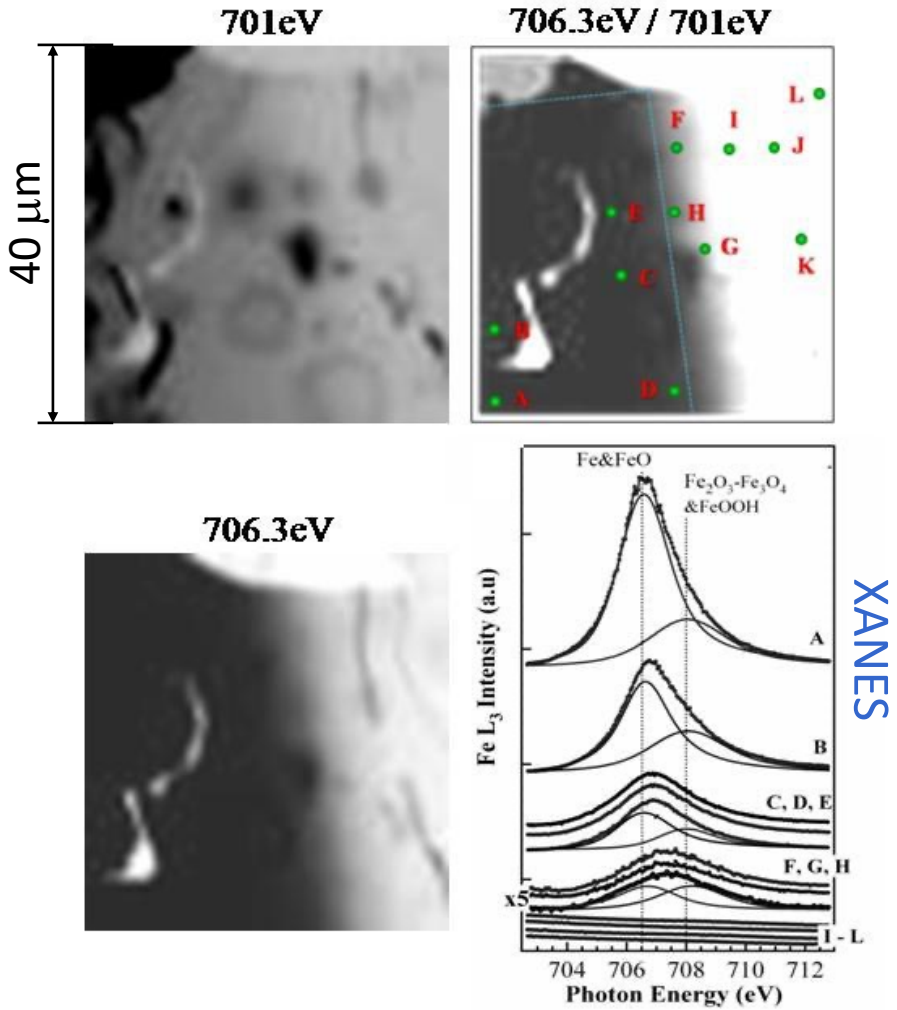
Bozzini et al. PhysChemChemPhys 13 (2011) 7968.

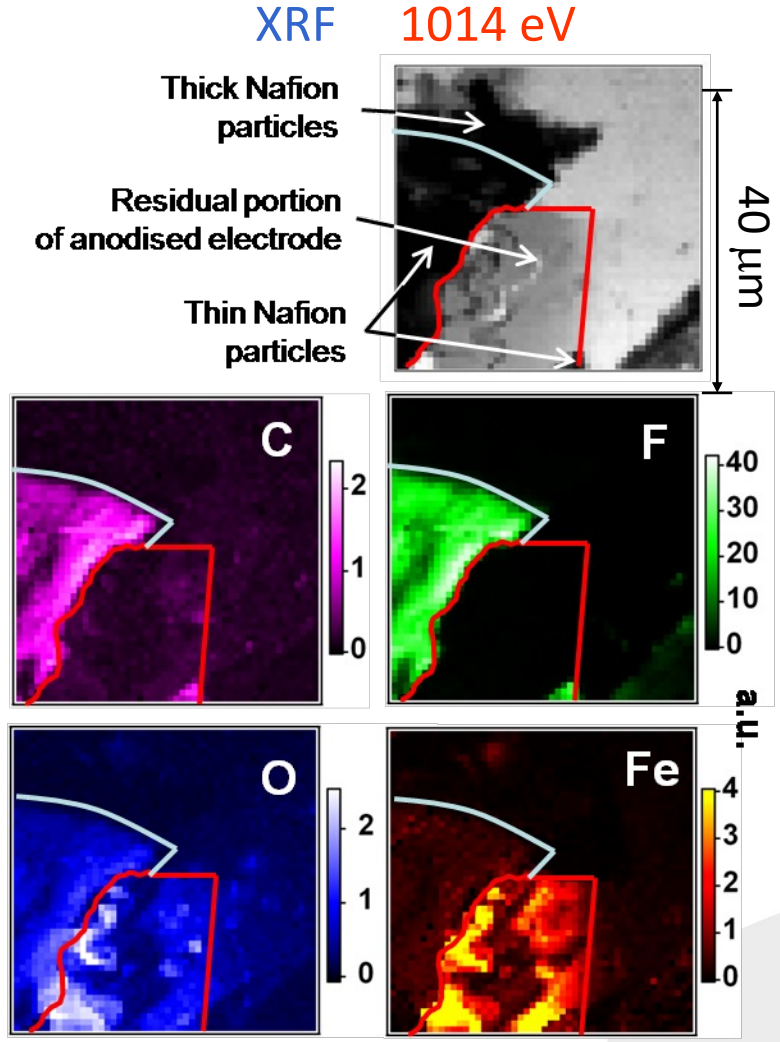
Elettra Sincrotrone Trieste

TwinMic

• FC durability

Bipolar plate (Fe) corrosion and Nafion poisoning





Bozzini et al. *ChemSusChem* , 7 (2010) 846

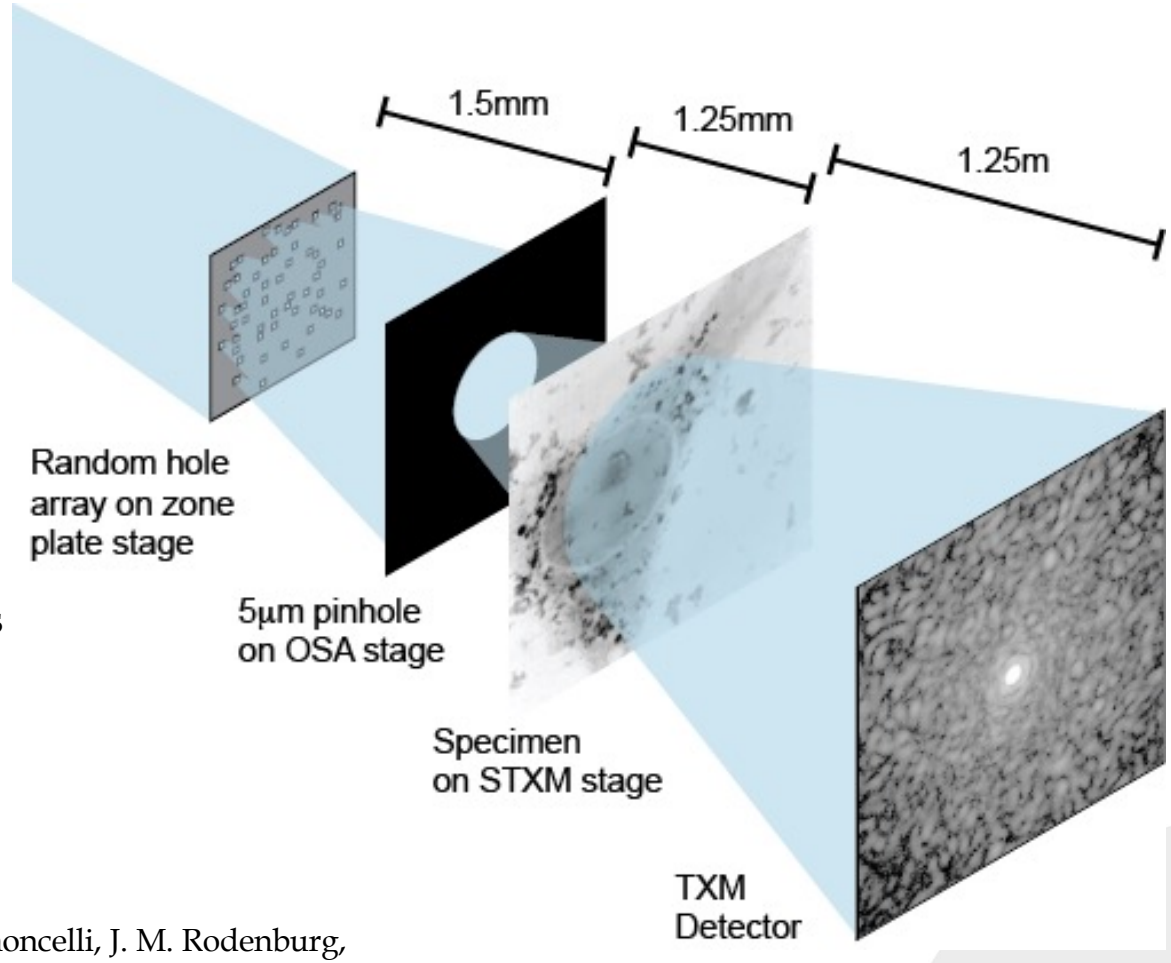
Elettra Sincrotrone Trieste

Spectro-Ptychography

Soft X-ray spectromicroscopy using ptychography with randomly phased illumination

- Illuminated area defined by a 5 μm pinhole
- Sample was scanned with raster steps ~1 μm

To spread the illumination across the detector

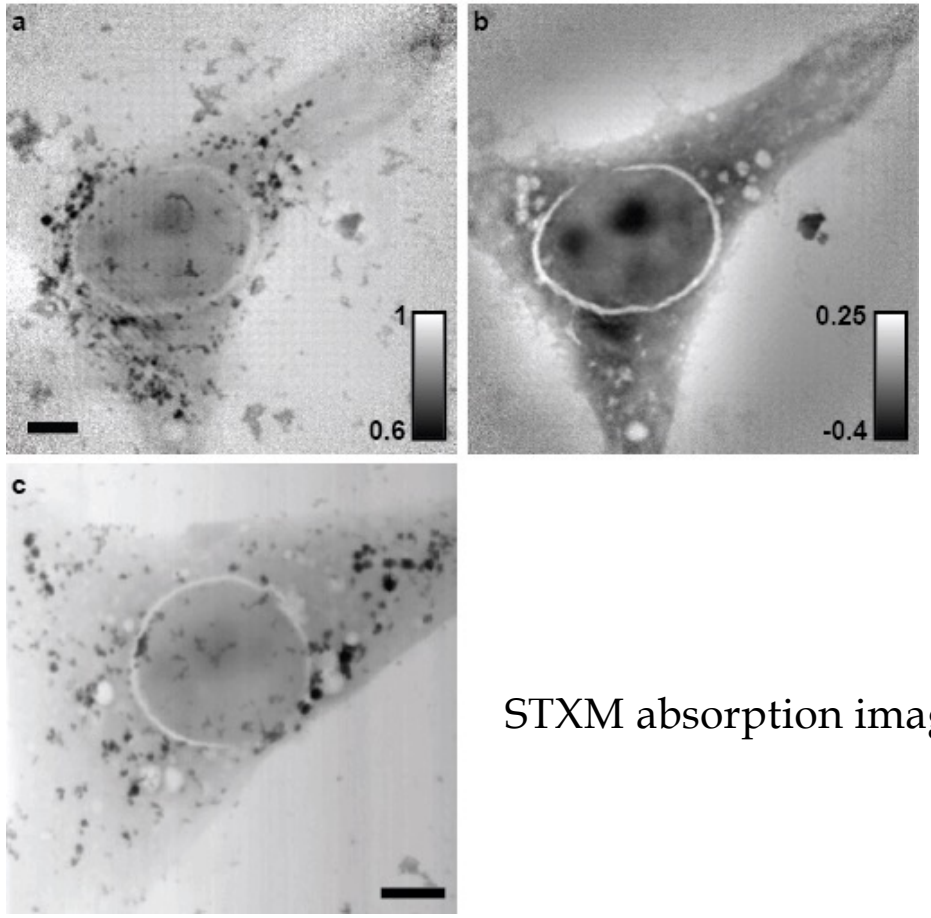


A. M. Maiden, G. R. Morrison, B. Kaulich, A. Gianoncelli, J. M. Rodenburg, *"Soft X-ray spectromicroscopy using ptychography with randomly phased illumination"*, Nature Communications 4, 1669, (2013)

Elettra
Sincrotrone
Trieste

Spectro-Ptychography

Soft X-ray spectromicroscopy using ptychography with randomly phased illumination



Balb/3T3 mouse fibroblast cells that had been exposed to cobalt ferrite ($CoFe_2O_4$) nanoparticles

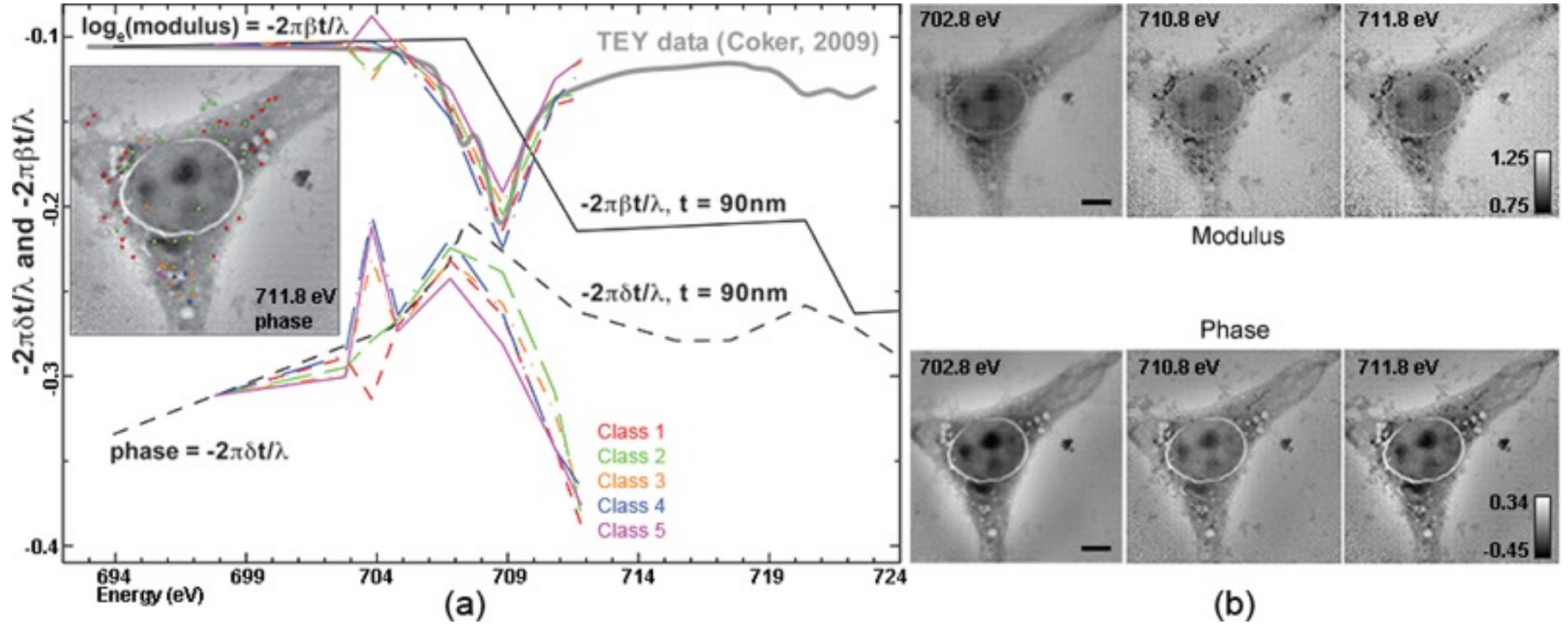
Ptychography reconstruction
using the ePIE algorithm (Uni of Sheffiled)

STXM absorption image

A. M. Maiden, G. R. Morrison, B. Kaulich, A. Gianoncelli, J. M. Rodenburg,
"Soft X-ray spectromicroscopy using ptychography with randomly phased illumination", Nature Communications 4, 1669, (2013)

Elettra
Sincrotrone
Trieste

Soft X-ray spectromicroscopy using ptychography



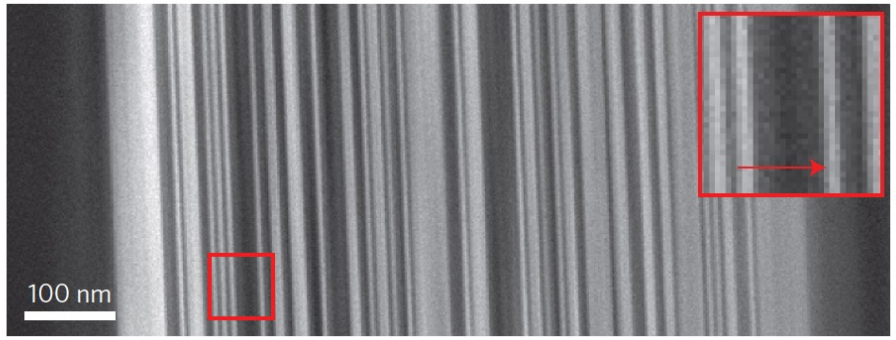
First direct measurements from cobalt ferrite nanoparticles of the phase variations across the iron L_3 edge, with the phase variations showing stronger and clearer features than the modulus data provided

A. M. Maiden, G. R. Morrison, B. Kaulich, A. Gianoncelli, J. M. Rodenburg,
"Soft X-ray spectromicroscopy using ptychography with randomly phased illumination",
Nature Communications 4, 1669, (2013)

• Ptychography @COSMIS (ALS synchrotron)

- The development of diffraction-based methods such as ptychography has, in
- principle, removed the resolution limit imposed by the characteristics of the X-ray optics

- Using soft X-ray ptychography,
- they demonstrated to be able to image 5 nm structures



Shapiro, D., Yu, YS., Tyliszczak, T. *et al.* Chemical composition mapping with nanometre resolution by soft X-ray microscopy. *Nature Photon* **8**, 765–769 (2014). https://doi.org/10.1038/nphoton.2014.207

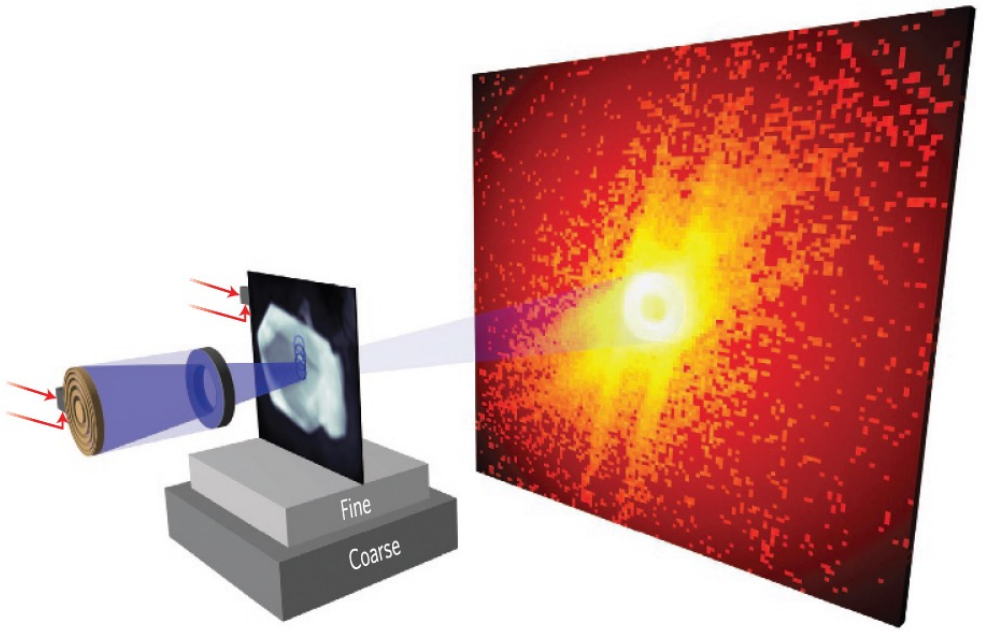
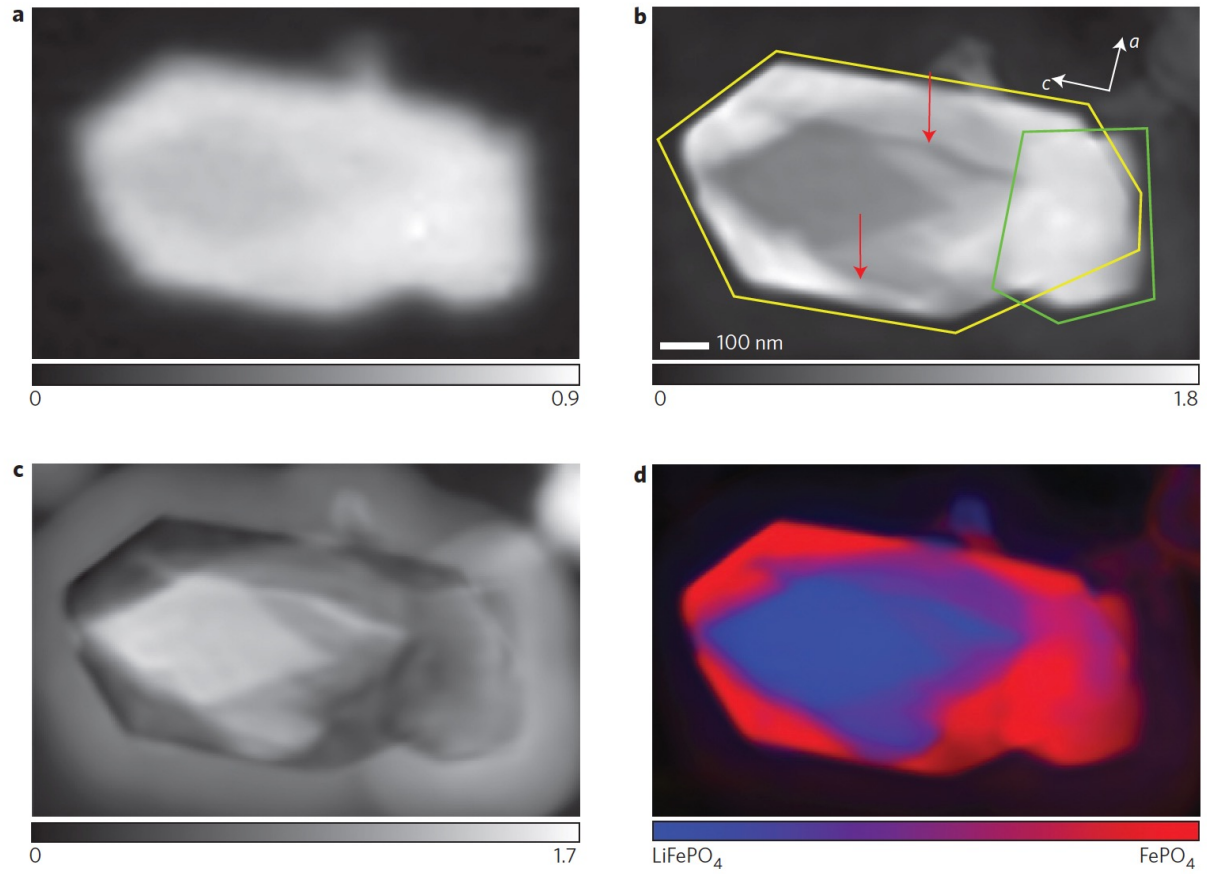
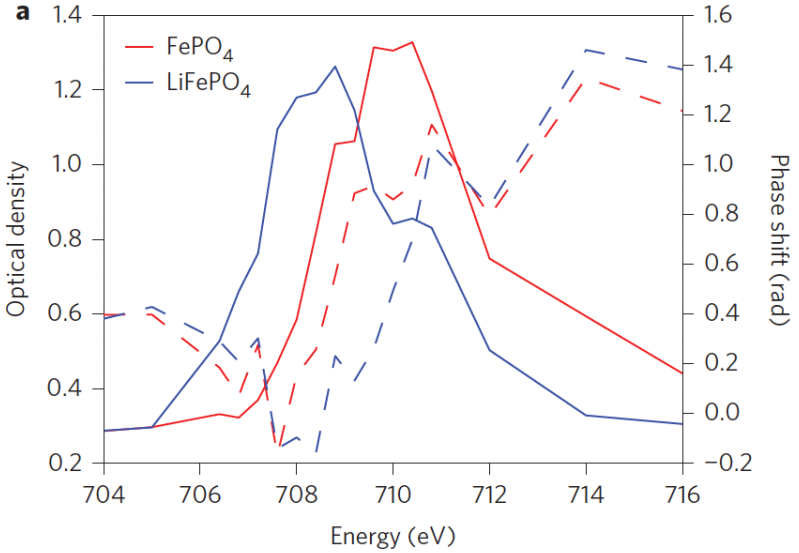


Figure 1 | Layout of the soft X-ray ptychographic microscope. A 60 nm outer-zone-width zone plate focuses a coherent soft X-ray beam onto the sample, which is scanned in 40 nm increments to ensure overlap of the probed areas. An order-sorting aperture blocks all but the first-order focus from the zone plate optic. Diffraction data are recorded on an X-ray CCD located 80 mm downstream of the sample, while the sample position is stabilized with respect to the zone plate by an interferometer (red arrows) that measures relative displacements in the scanning directions with 1.5 nm resolution. The central annulus in the diffraction pattern is the band-limited diffraction pattern of the X-ray probe, and all photons scattered outside this annulus contribute to the increased spatial resolution of the imaging system.

• Ptychography @COSMIS (ALS synchrotron)

STXM **Ptycho**





Absorption (solid lines) and phase spectra (dashed lines)

The maximum relative phase shift occurs at an X-ray energy (709.2 eV) about 0.8 eV lower than that for maximum absorption contrast (710 eV).

Figure 3 | X-ray microscopy of partially delithiated $LiFePO_4$. a,**b**, Optical density maps from STXM (**a**) and ptychography (**b**) at 710 eV, showing maximum absorption contrast between the end members. The spatial resolution of the STXM is not adequate to visualize the presence of multiple particles, which are outlined in the ptychographic image, and cracks along the crystallographic *c* axis, which are indicated by red arrows (the *a* and *c* crystallographic axes are indicated by white arrows; the *b* axis is parallel to the X-ray transmission). The crack is only on the surface and reveals an unreacted domain below. Furthermore, the ptychographic image demonstrates a mismatch between the apex of the unreacted phase and that of the crystal lattice, and an asymmetry in the unreacted domain. Pixel size, 4.0 nm. Scale bar, 100 nm. **c**, Phase of the ptychographic reconstruction at 709.2 eV, showing maximum relative phase shift between the end members. The halo around the particle is carbon contamination, which builds up with X-ray exposure and is not apparent in the absorption images. **d**, Colourized composition map calculated by principal component analysis, clustering and singular value decomposition of the full complex refractive index. Only material containing the end members is apparent. The spectra used for the fitting are shown in Fig. 4.

Shapiro, D., Yu, YS., Tyliszczak, T. *et al.* Chemical composition mapping with nanometre resolution by soft X-ray microscopy. *Nature Photon* **8**, 765–769 (2014). https://doi.org/10.1038/nphoton.2014.207

Elettra Sincrotrone Trieste

OPEN

Compressive Sensing for Dynamic XRF Scanning

George Kourousias[1]✉, Fulvio Billè[1], Roberto Borghes[1], Antonio Alborini[2], Simone Sala[1,3], Roberto Alberti[2] & Alessandra Gianoncelli[1]

SCIENTIFIC REPORTS
nature research

- Compressive Sensing is an emerging and very effective technique for reconstruction from a relatively small number of data samples without compromising the imaging quality
- In our case it allows performing scans of a dynamic nature where it is possible to skip points (sparse) and acquire with variable parameters (i.e. acquisition time)
- The same scans performed in a raster way (square or rectangular) would take much longer
- It would allow for faster imaging and therefore higher statitics
- It saves time and storage space (therefore also money)

Analyst

ROYAL SOCIETY OF CHEMISTRY

COMMUNICATION

View Article Online
View Journal | View Issue

Check for updates

Cite this: *Analyst*, 2021, **146**, 5836

Received 17th June 2021,
Accepted 6th July 2021

DOI: 10.1039/d1an01074c

rsc.li/analyst

Megapixel scanning transmission soft X-ray microscopy imaging coupled with compressive sensing X-ray fluorescence for fast investigation of large biological tissues

George Kourousias, [a] Fulvio Billè, [a] Roberto Borghes,[a] Lorella Pascolo [b] and Alessandra Gianoncelli *[a]

Elettra
Sincrotrone
Trieste

Synchrotron beamtime: how do we improve it?

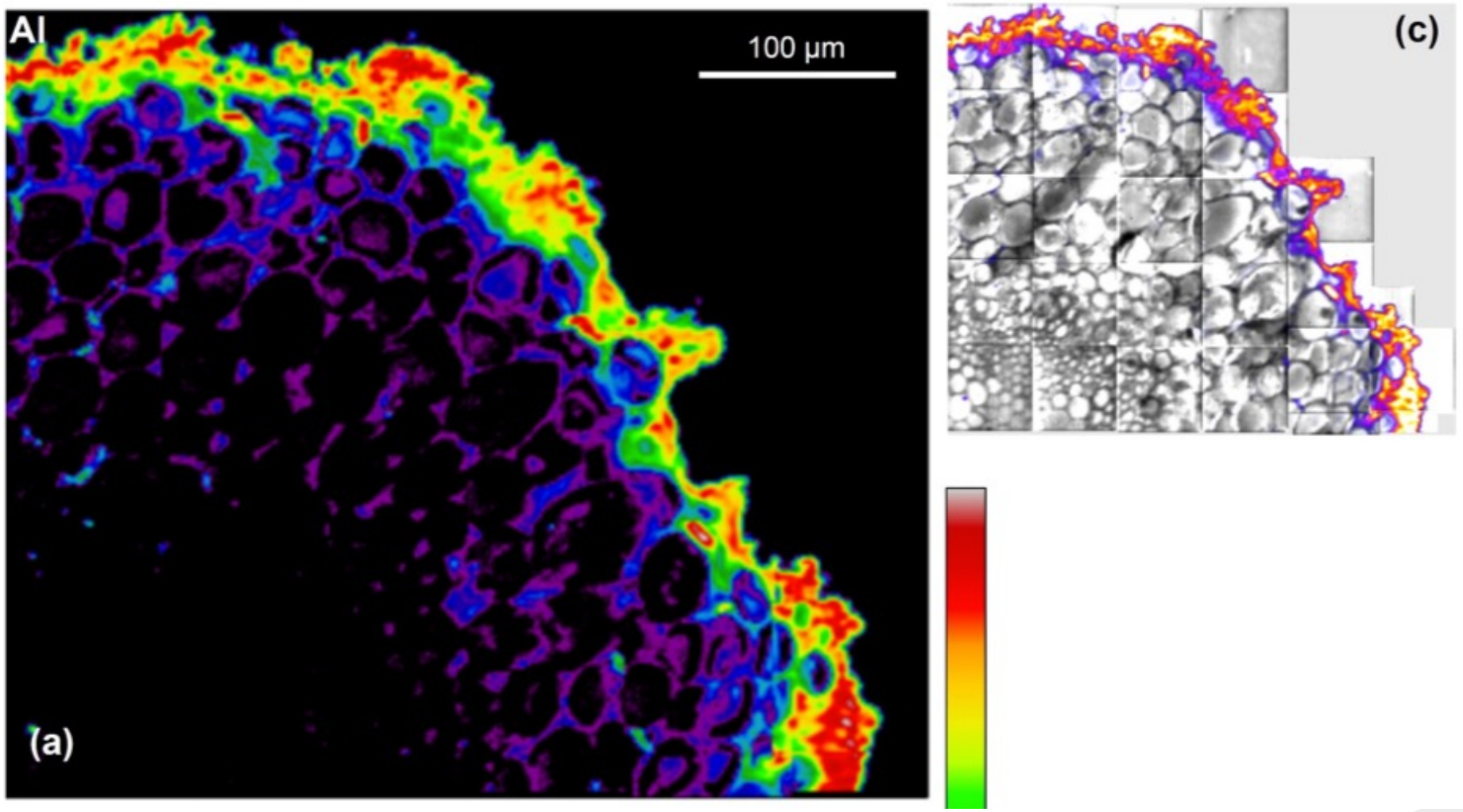
- Synchrotron time is expensive and rare (3-4-5-6 days per semester o per year)
- You want to collect as many data as meaningful as possible
- You'd like to solve your scientific question in a single beamtime

- You can speed up the measurements by having a more powerful source and/or more powerful detectors

- OR … you can develop **«smart» acquisition systems** di acquire only the meaningful data ☺

Elettra
Sincrotrone
Trieste

A good portion of the images is empty

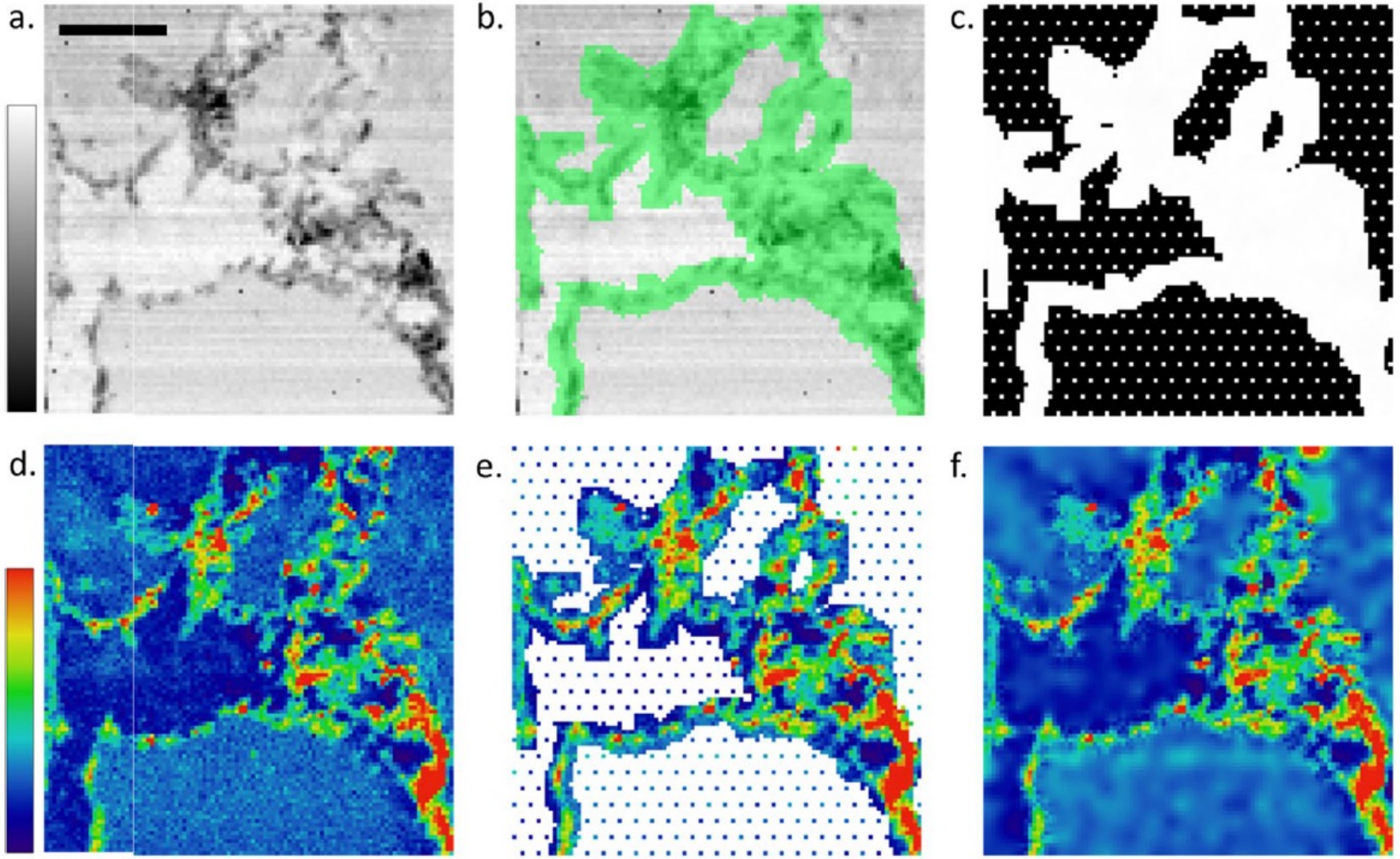


Kopittke P.M., Moore K.L., Lombi E., Gianoncelli A., Ferguson B.J., Blamey F.P.C., Menzies N.W., Nicholson T.M., McKenna B.A., Wang P., Gresshoff P.M., Kourousias G., Webb R.I., Green K., Tollenaere A. Identification of the Primary Lesion of Toxic Aluminum in Plant Roots *Plant Physiology*, Vol. 167 - 4, pp. 1402-1411 (2015)

Elettra
Sincrotrone
Trieste

First approach: a mask

Static decision which implies **motors' stability** in time

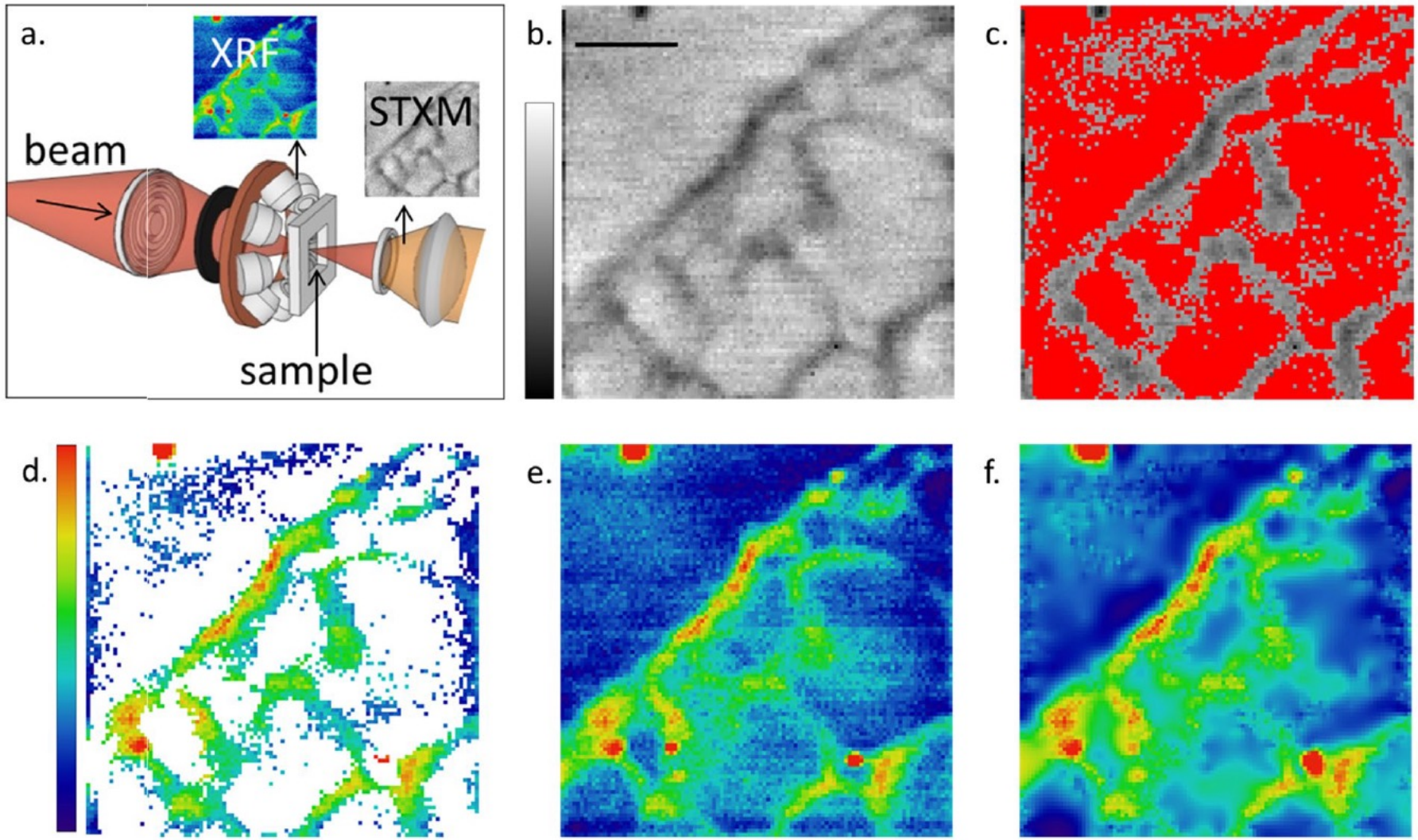


Kourousias G. et al. Scientific Reports | (2020) 10:9990 | https://doi.org/10.1038/s41598-020-66435-6

Elettra
Sincrotrone
Trieste

Second approach: absorption threshold

Dynamic decision through the signal of the available detector, for instance based on absorption threshold
which implies **beam stability** in time

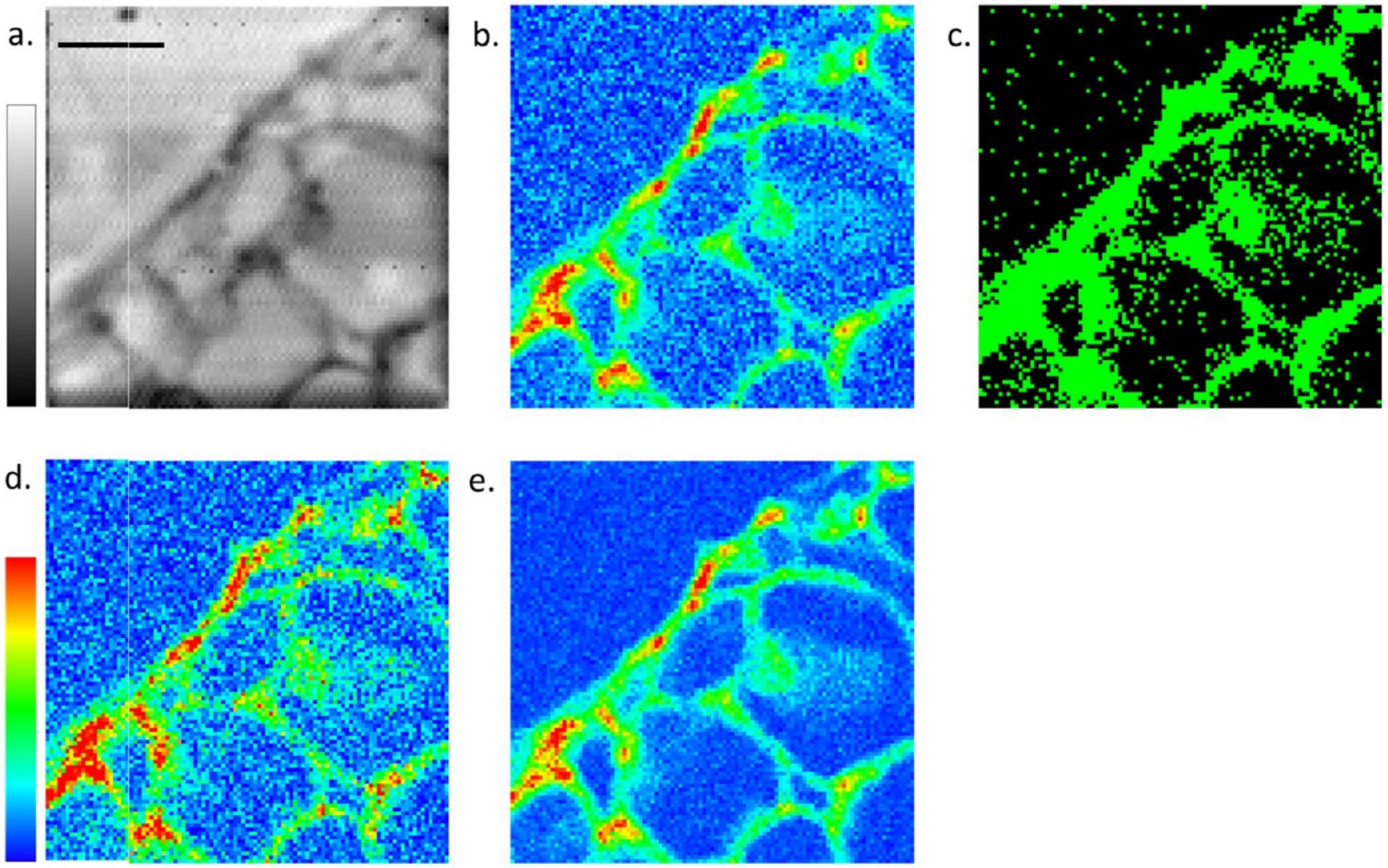


Kourousias G. et al. Scientific Reports | (2020) 10:9990 | https://doi.org/10.1038/s41598-020-66435-6

Elettra
Sincrotrone
Trieste

Third approach: XRF threshold

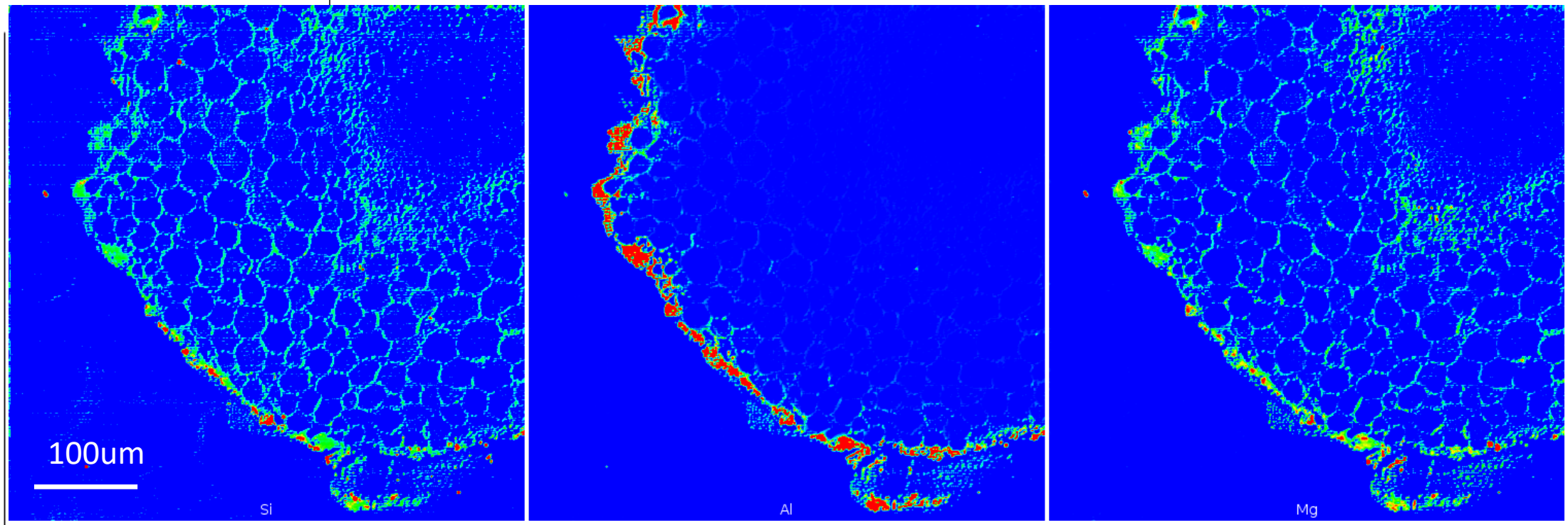
Dynamic decision through the XRF signal which implies beam stability in time



Kourousias G. et al. Scientific Reports | (2020) 10:9990 | https://doi.org/10.1038/s41598-020-66435-6

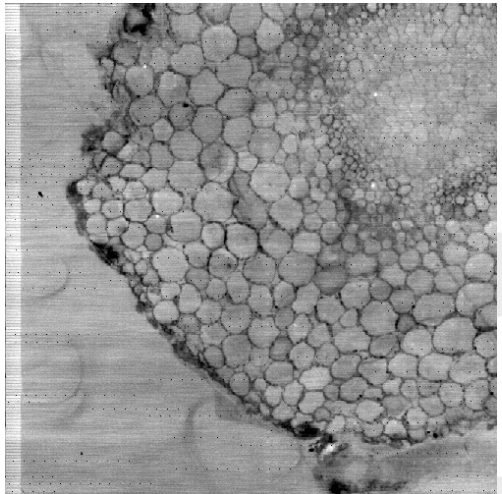
Elettra
Sincrotrone
Trieste

40% of the time



We used approach2, an absorption threshold with beam corrections

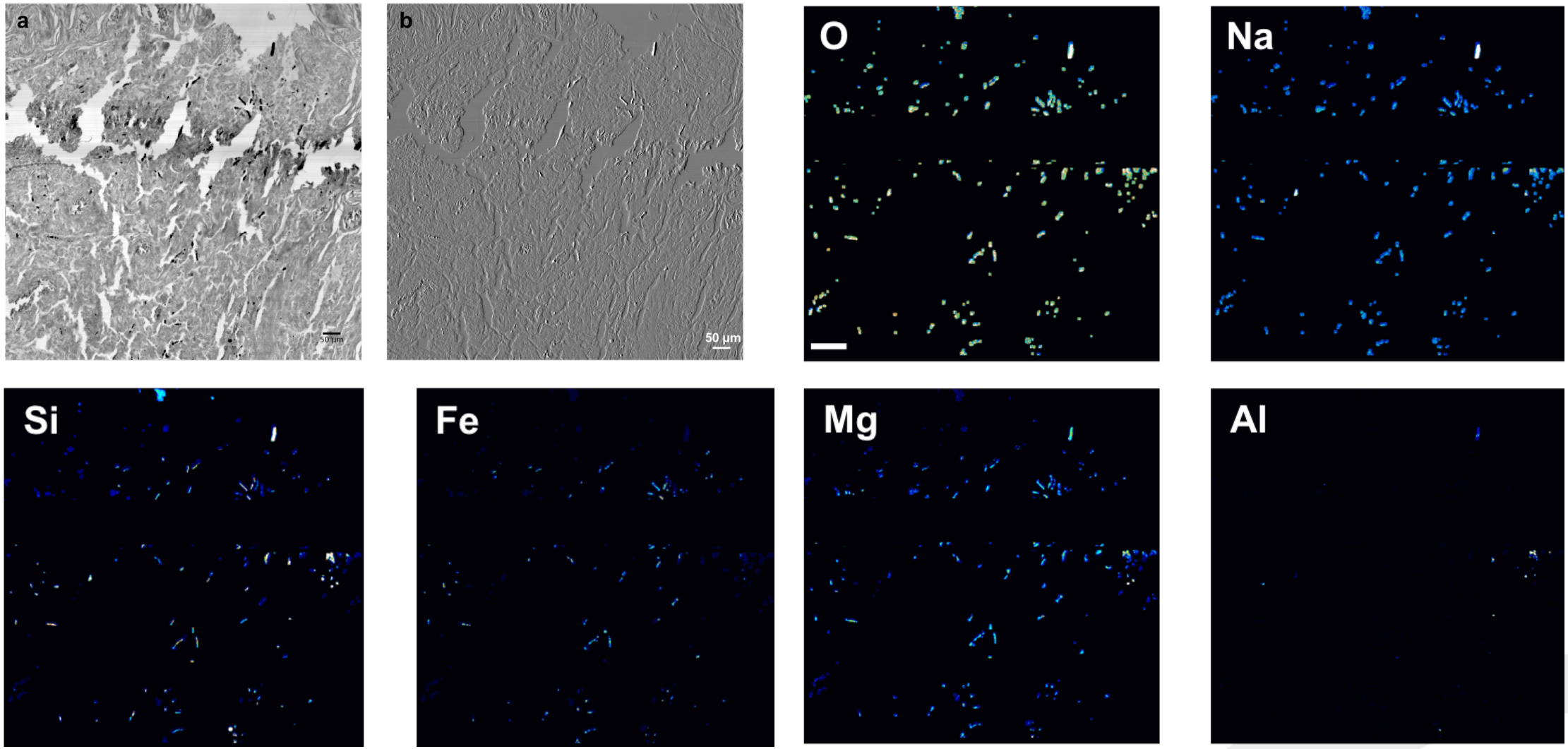
Applied also on **MegaPIXEl imaging**



Kourousias G. et al. Scientific Reports | (2020) 10:9990 | https://doi.org/10.1038/s41598-020-66435-6
Kourousias G. et al. Analyst, 146(19), 5836 (2021)

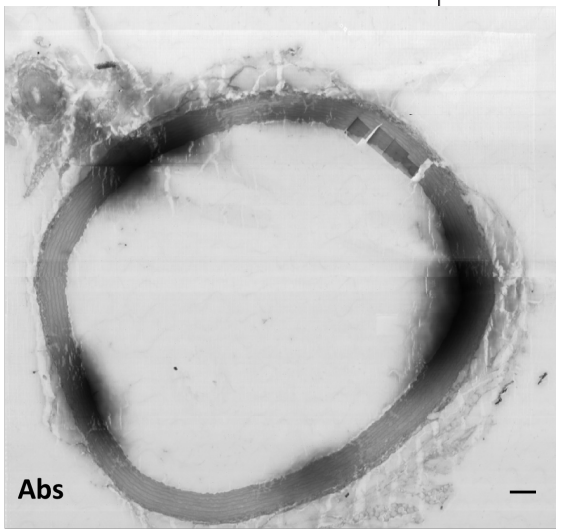
Elettra
Sincrotrone
Trieste

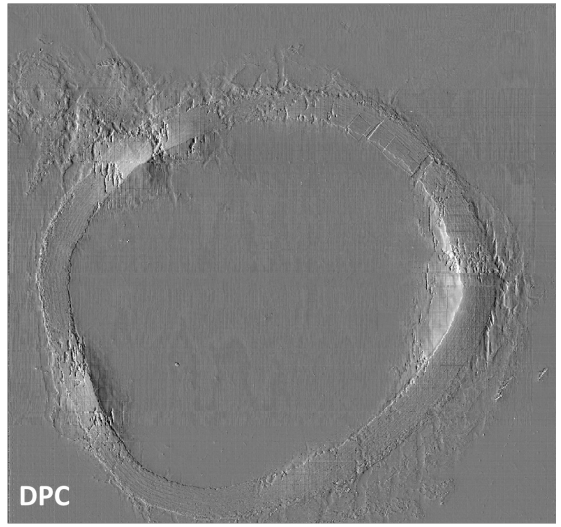
MegaPIXEL STXM + XRF mapping

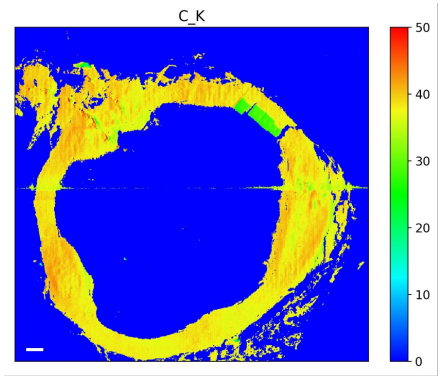


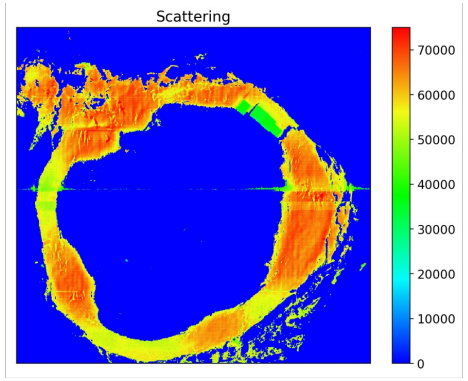
G. Kourousias, F. Billè, R. Borghes, L. Pascolo, A. Gianoncelli, A. “Megapixel scanning transmission soft X-ray microscopy imaging coupled with compressive sensing X-ray fluorescence for fast investigation of large biological tissues” *Analyst*, 1vol. 46 no. 19, pp. 5836-5842 2021.

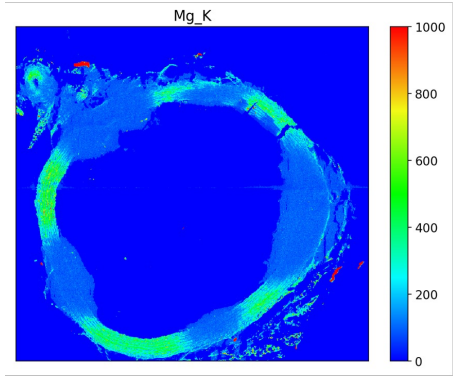
MegaPIXEL STXM + XRF mapping

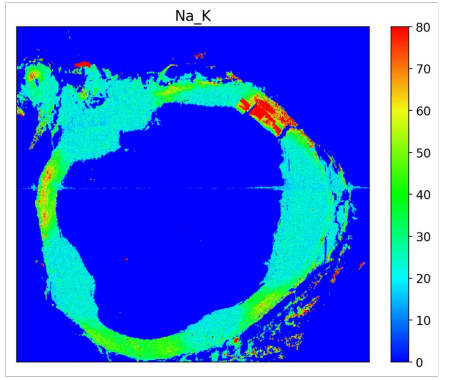


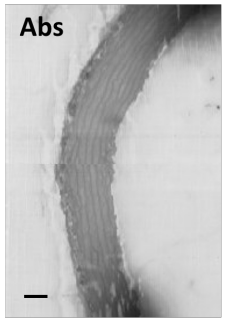




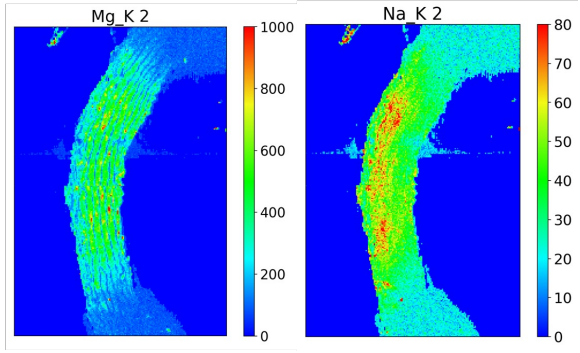












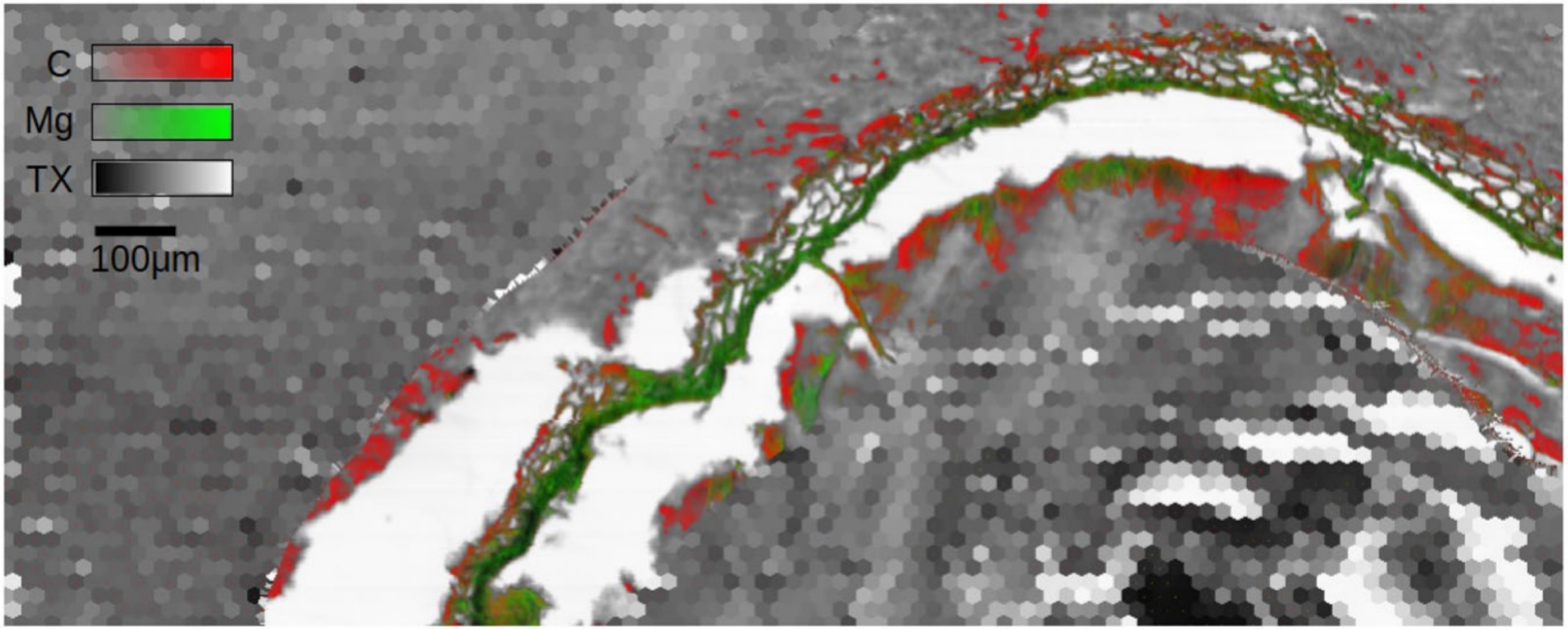
coronary artery from a rat

Scale bar is 100um

Gianoncelli A., Bonanni V., Gariani G., Guzzi F., Pascolo L., Borghes R., Billè F., Kourousias G. Soft X-ray Microscopy Techniques for Medical and Biological Imaging at TwinMic—Elettra *Applied Sciences*, Vol. 11 - 16, 7216 (2021)

Elettra
Sincrotrone
Trieste

Variable STXM resolution and selective XRF; all combinations possible



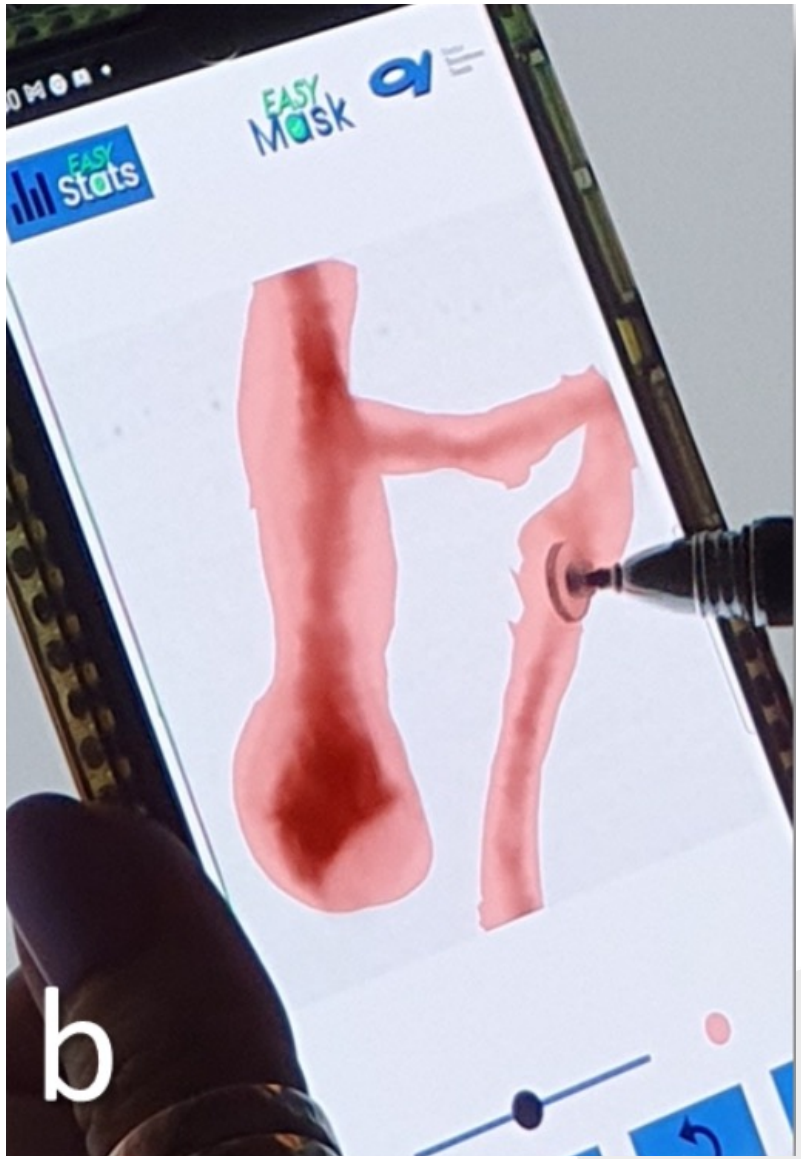
0.4MPixel Sparse scan and Masking combined with a Conditional scan and multimodal acquisition on a cane root section sample. Te STXM data (grey) (2000 µm × 800 µm) are acquired with a dense sampling (2 µm step size) along the border of the cane root section while in a sparse way (20 µm step size) in the remaining masked areas. The XRF data have been collected in a similar reduced manner (C in red, Mg in green) and are displayed overlapped with the STXM image. A traditional/complete acquisition (2 µm step size) on the total area would require a measurement time 3 times longer.

Kourousias G. et al. Scientific Reports | (2020) 10:9990 | https://doi.org/10.1038/s41598-020-66435-6

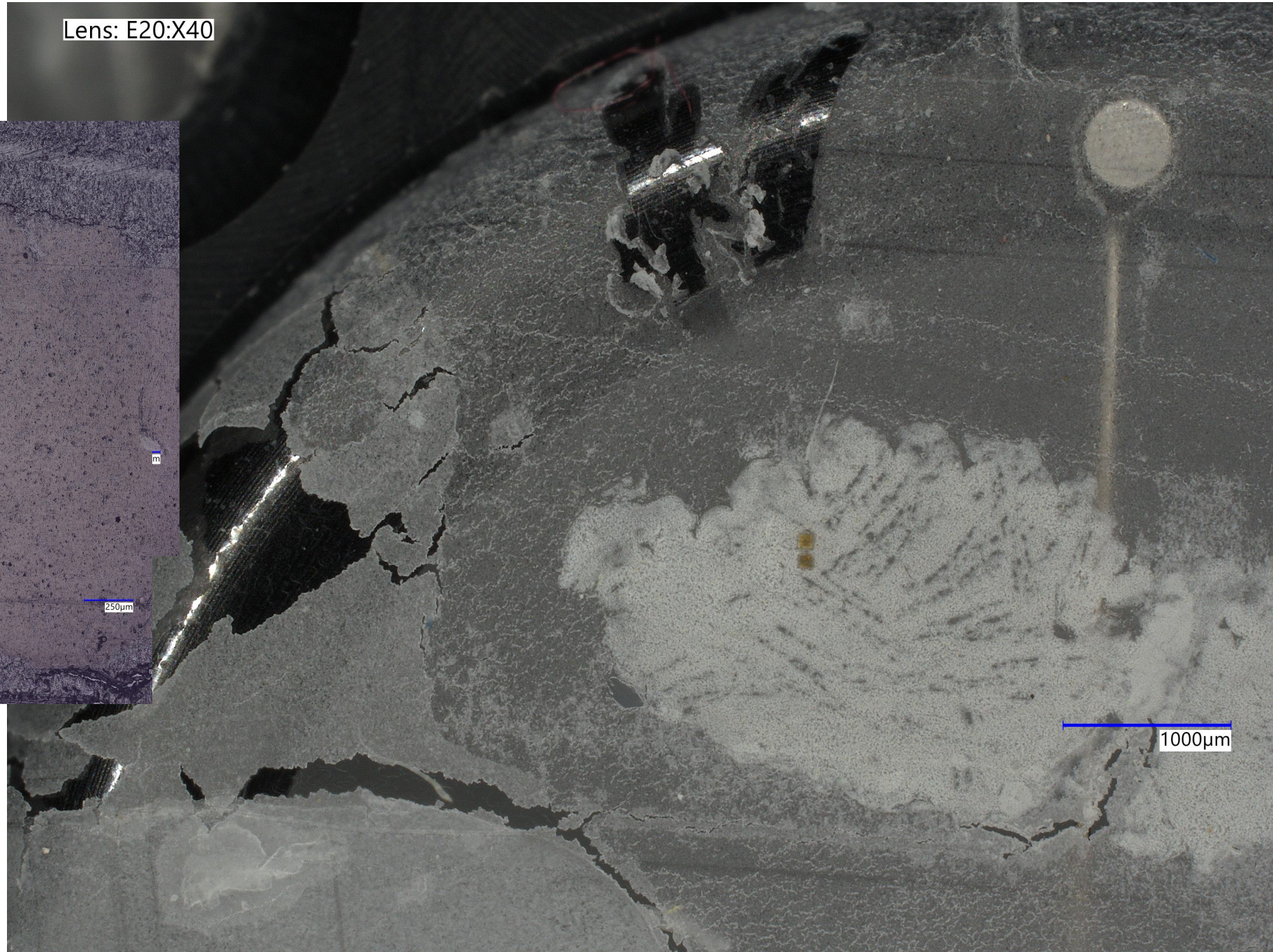
Elettra
Sincrotrone
Trieste

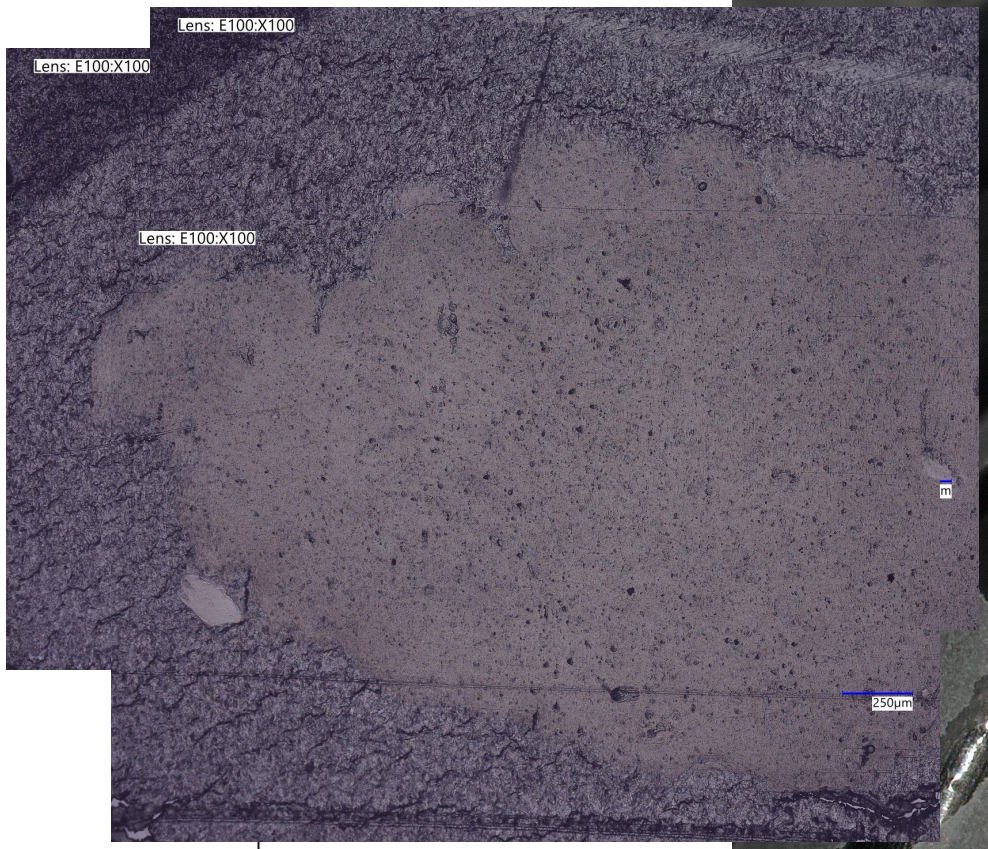
A mobile as an input device for CS workflows



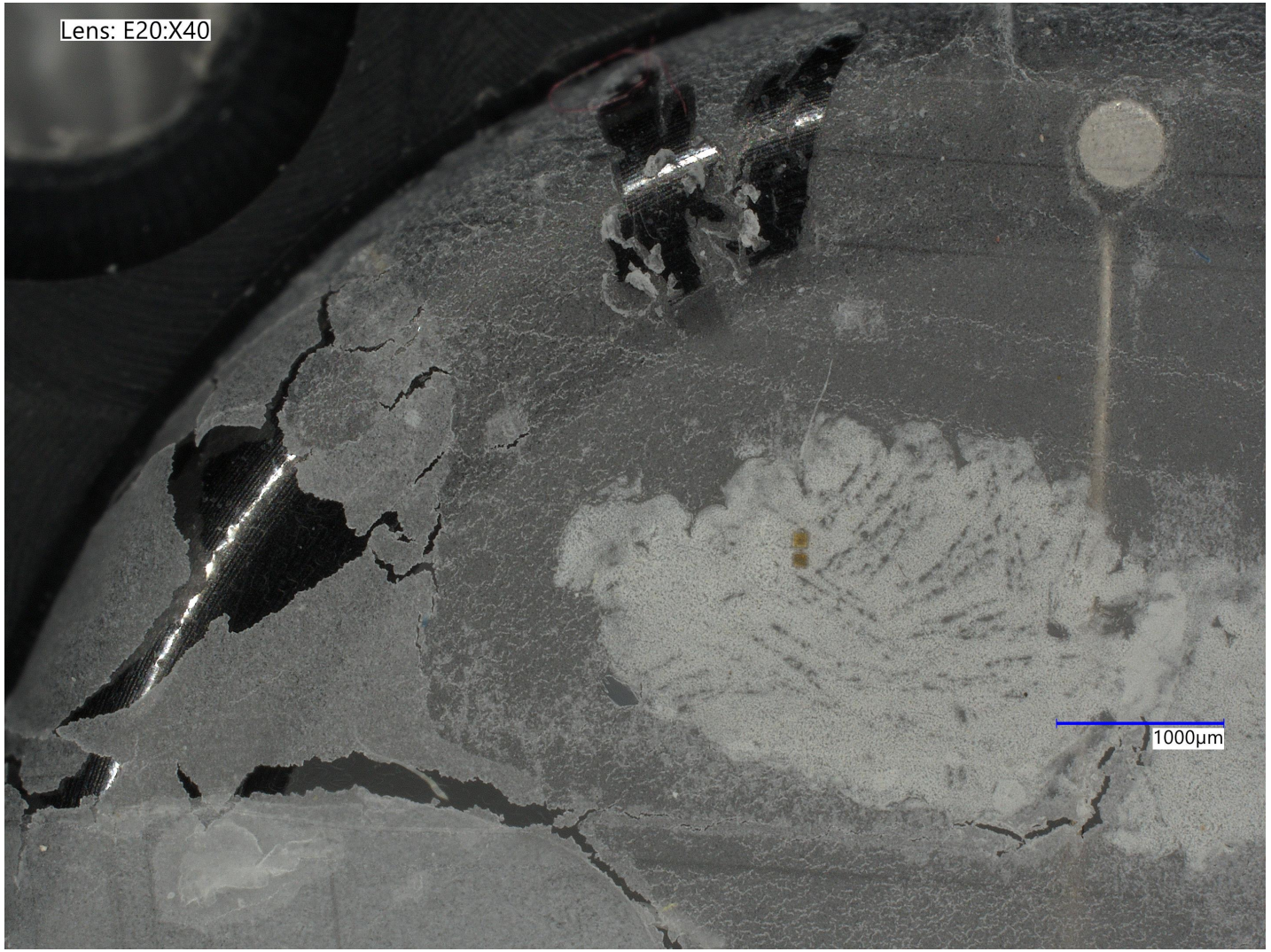


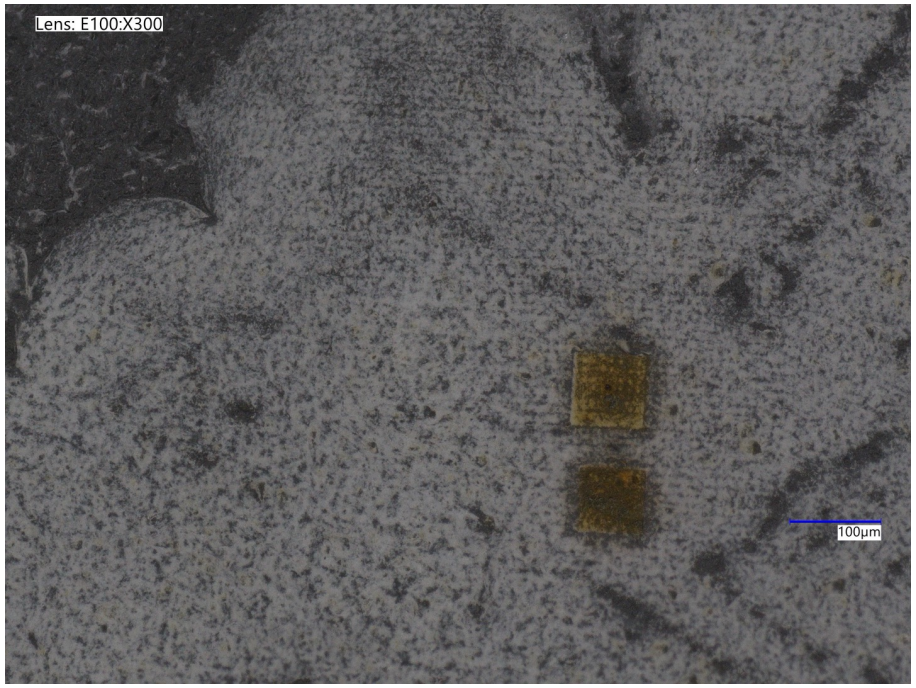
Elettra
Sincrotrone
Trieste

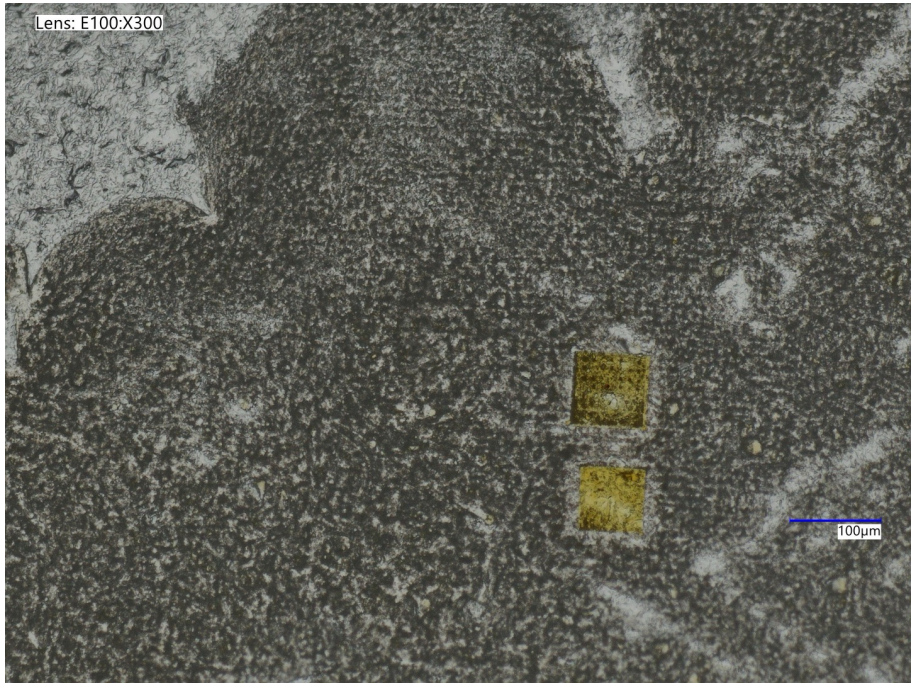




After Twinmic



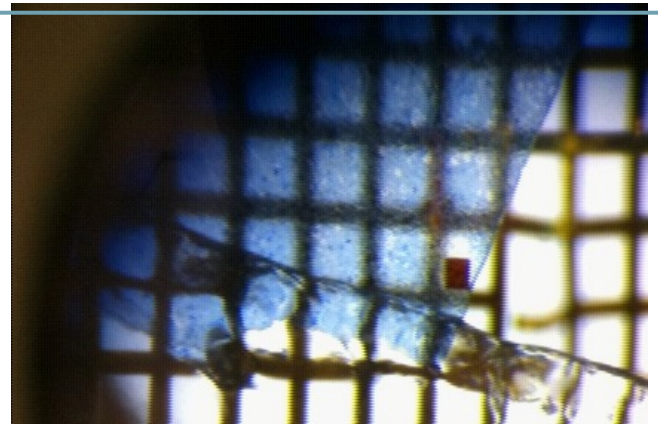


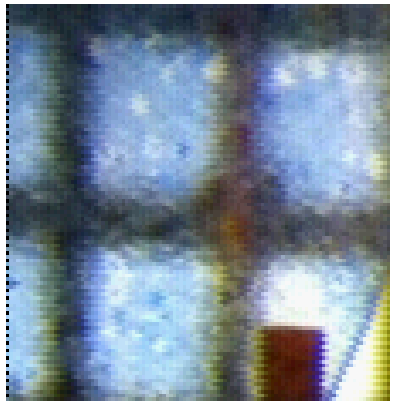


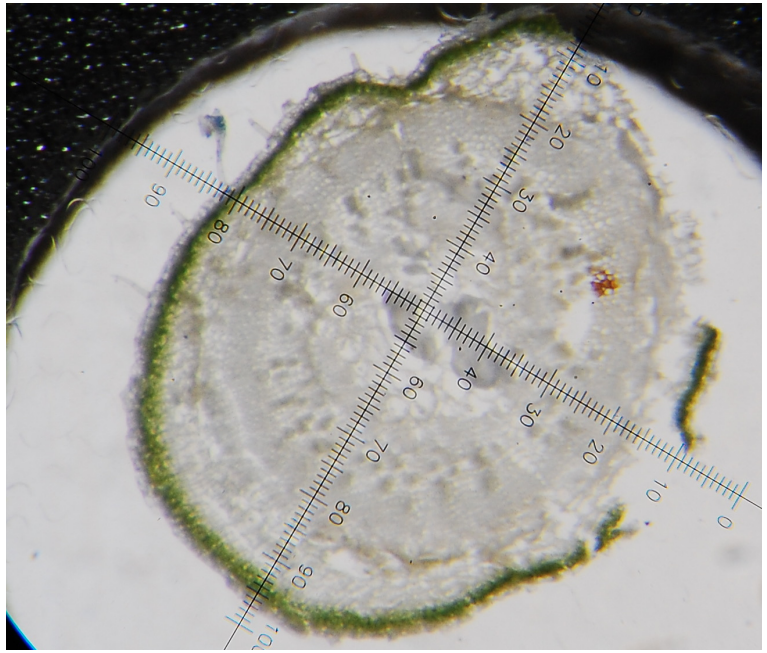
Elettra Sincrotrone Trieste

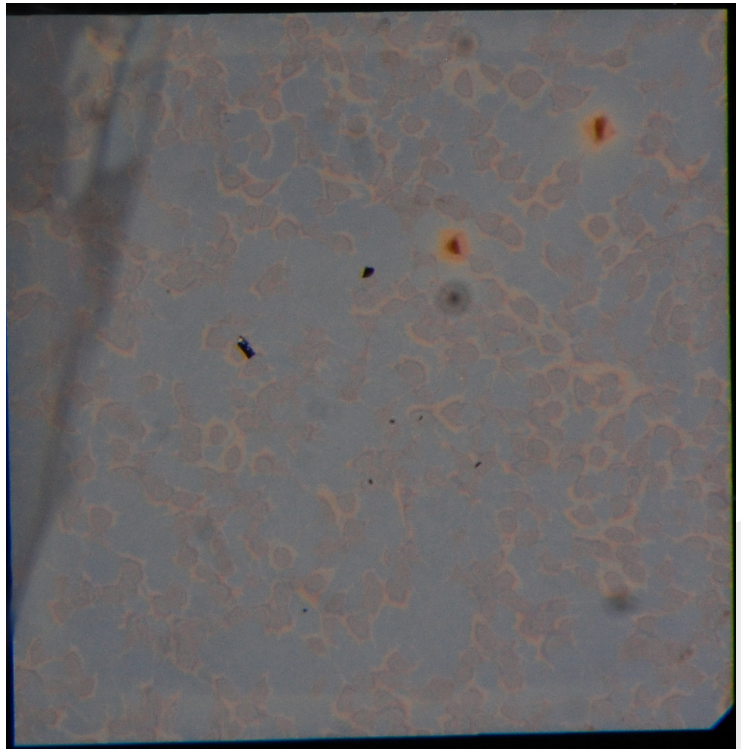
TwinMic

- **Radiation damage**







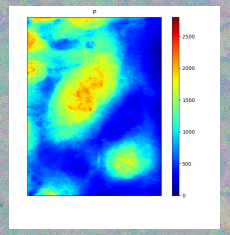


Lens: E100:X150

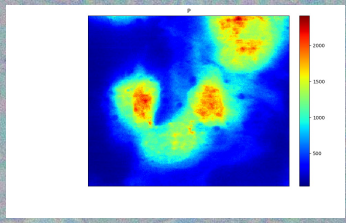
50ug\mL
pvc_2

200µm

roi_41503_48883



roi_41499_48877



roi_41491_48912

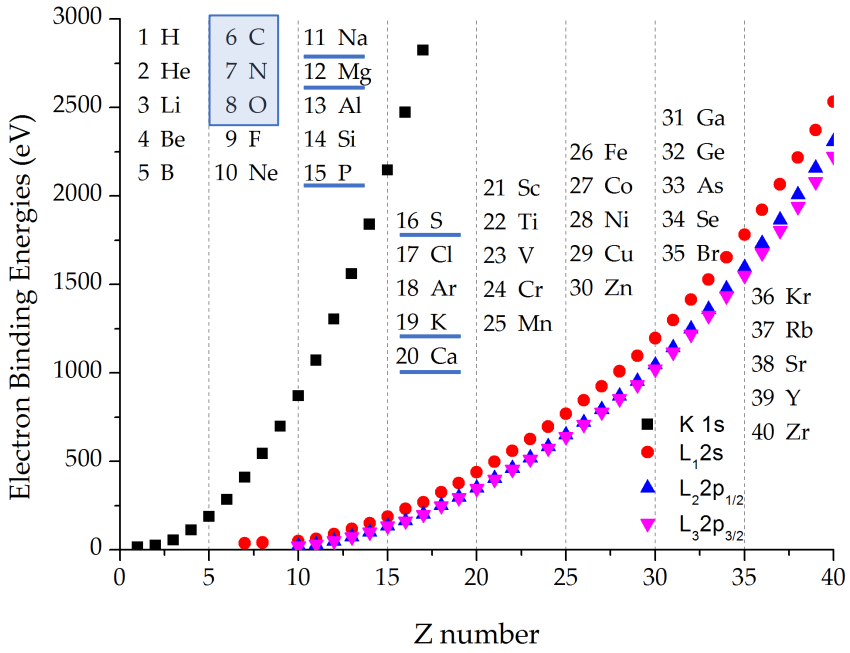
100µm

X-ray radiation damage induced by soft X-rays

• Radiation damage induced by X-rays on biological samples is one of the remaining bottlenecks for their ultrastructural characterization by X-ray microscopy techniques

• X-ray nanofocusing is a today reality but the extent to which the lateral resolution can be pushed without unacceptable bio-sample degradation is still an open question

• The problem is even more pronounced in the soft X-ray regime



Radiation damage

The very same radiation that induces damage is exploited for probing it

Radiation damage is dose dependent

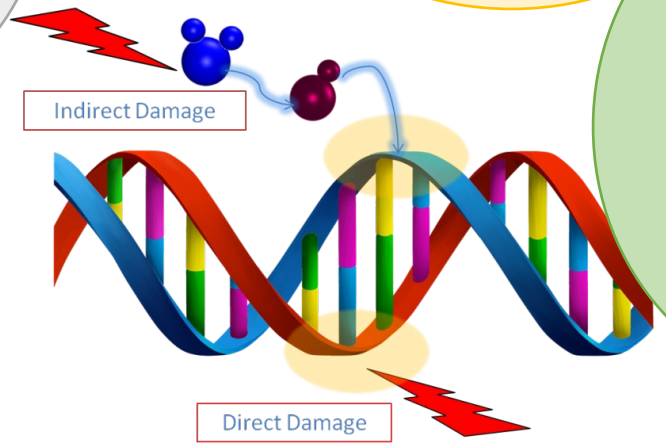
Radiation damage depends on sample preparation

Hydrated samples undergo more relevant changes with respect to fixed ones

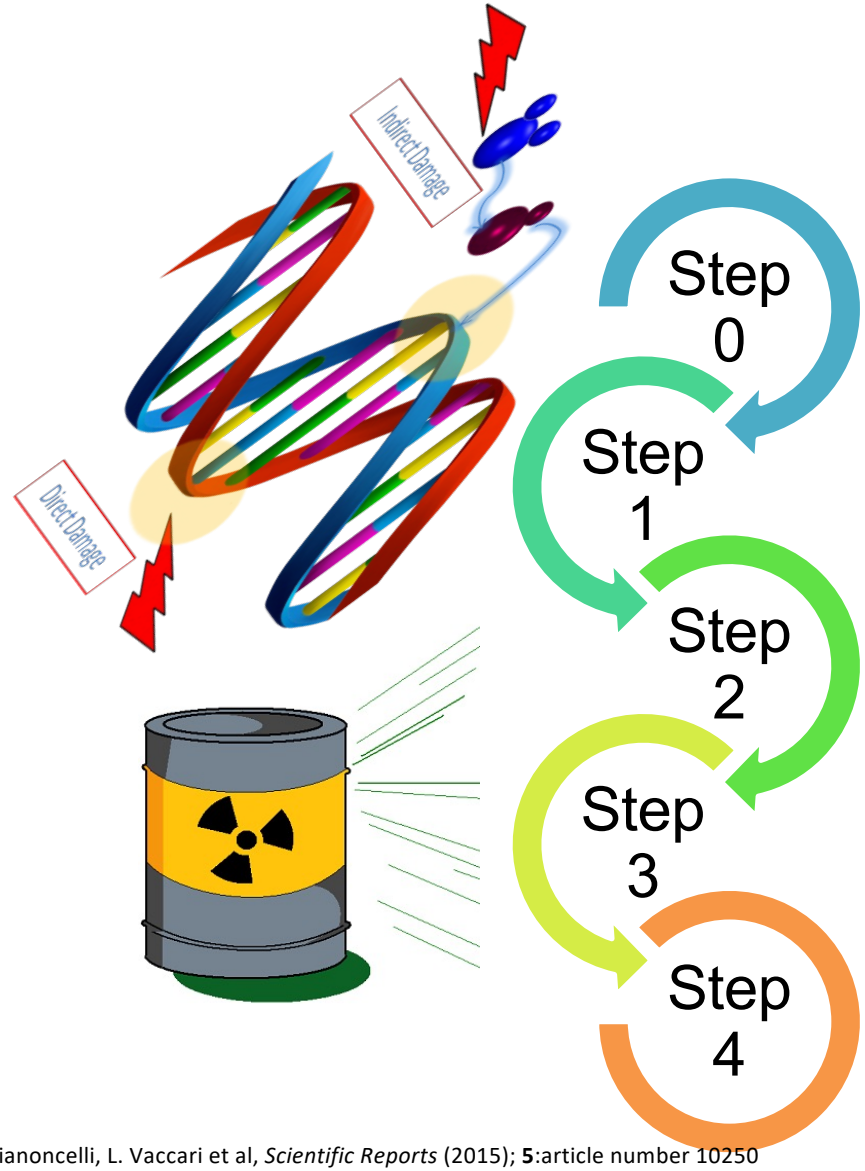
Cryo-XRM better preserves the structural integrity of bio-samples

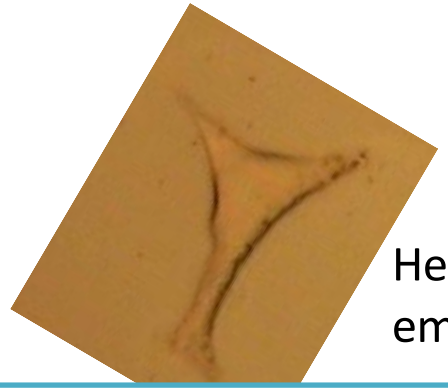
Radiolytic effects undergone by a specific molecule strongly depend on the sample architecture

Genetic material is extremely sensitive to ionizing radiation



Soft X-ray radiation damage as probed by FTIR microscopy





Hek293T cells (human embryonic kidney)

Cell growth on 100 nm Si_3N_4 membranes
Cell fixation with PFA 3.7% and overnight air drying

Cell drying in vacuum @ TwinMic
($p < 10^{-5}$ mbar) for 1:30 hour

Low Dose STXM mapping @ TwinMic 1 keV
Estimated dose: $2*10^6$ Gy

High Dose STXM mapping @ TwinMic 1 keV Estimated dose: $2*10^7$ Gy
Cumulative estimated dose: $2.2*10^7$ Gy

Very high dose STXM mapping @ TwinMic 1 keV
Estimated dose: $6*10^8$ Gy
Cumulative estimated dose: $6.2*10^8$ Gy

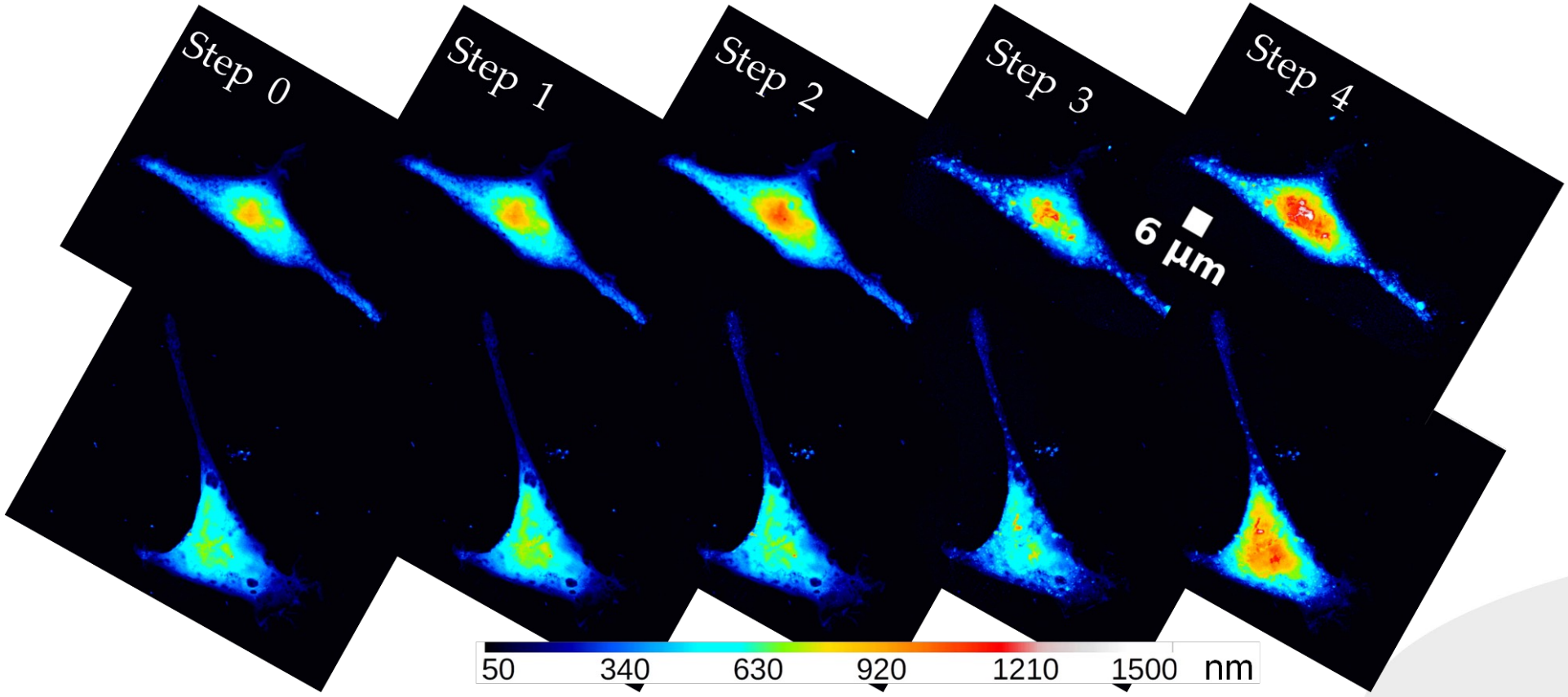
A. Gianoncelli, L. Vaccari et al, *Scientific Reports* (2015); **5**:article number 10250

Elettra Sincrotrone Trieste

TwinMic

Outcomes of AFM

- Minimal cell shrinkage
- Evident degradation/thinning of pseudopodia terminations
- Appreciable thickness variations, especially on the nuclear region at Step 4
- Outstanding topographical changes: nanometric pits and bulges increase in number and size when increasing dose

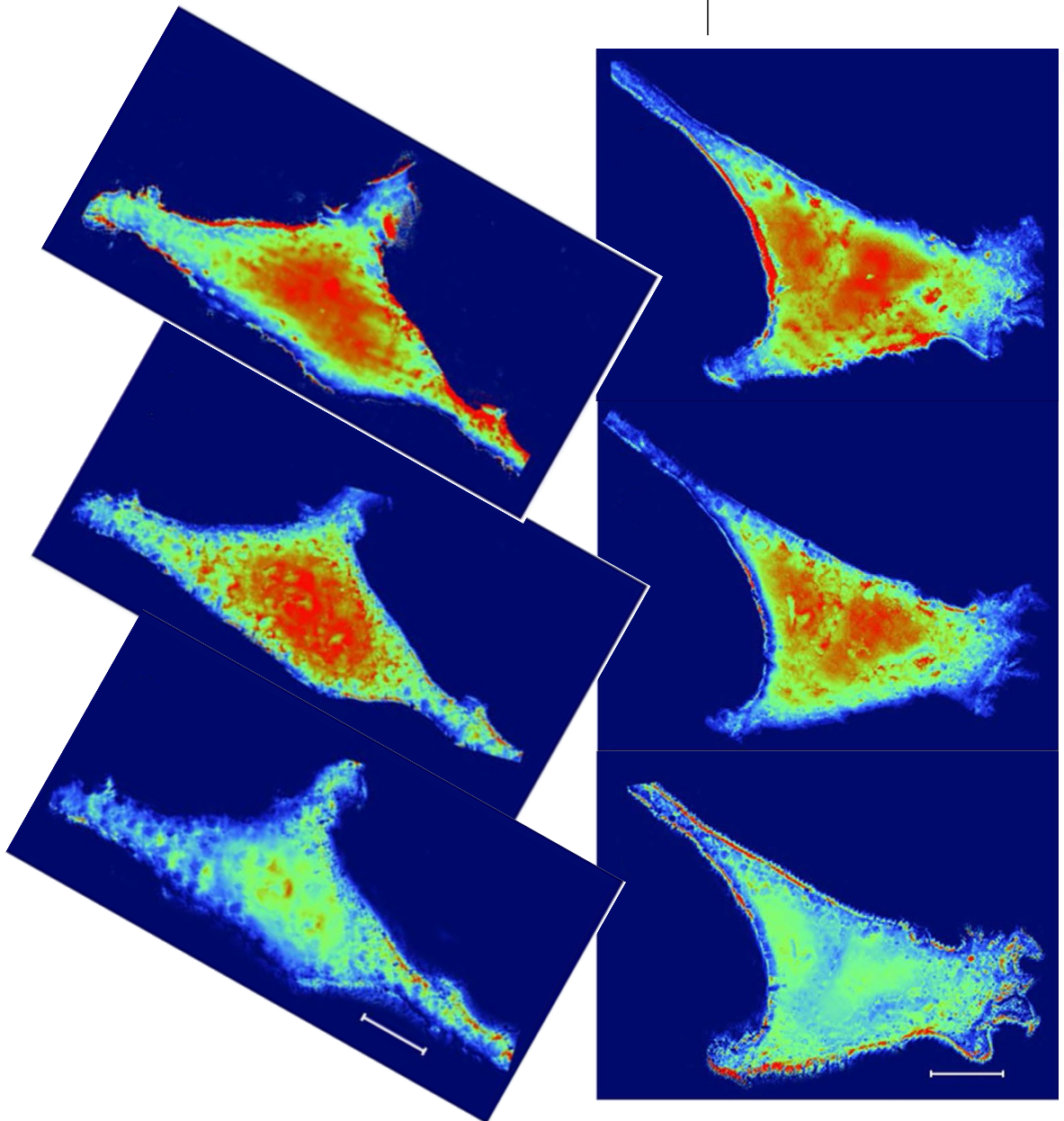


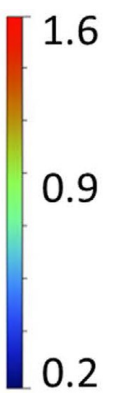
A. Gianoncelli, L. Vaccari, G. Kourousias, D. Cassese, D.E. Bedolla, S. Kenig, P. Storici, M. Lazzarino, M. Kiskinova "Soft X-Ray Microscopy Radiation Damage On Fixed Cells Investigated With Synchrotron Radiation FTIR Microscopy" **Scientific Reports** 5:10250 2015

Elettra Sincrotrone Trieste

TwinMic

Combining XRM and AFM





XRM cell images normalized over AFM cell thickness

$$\rho = -\ln \frac{(I/I_0)}{\mu * t}$$

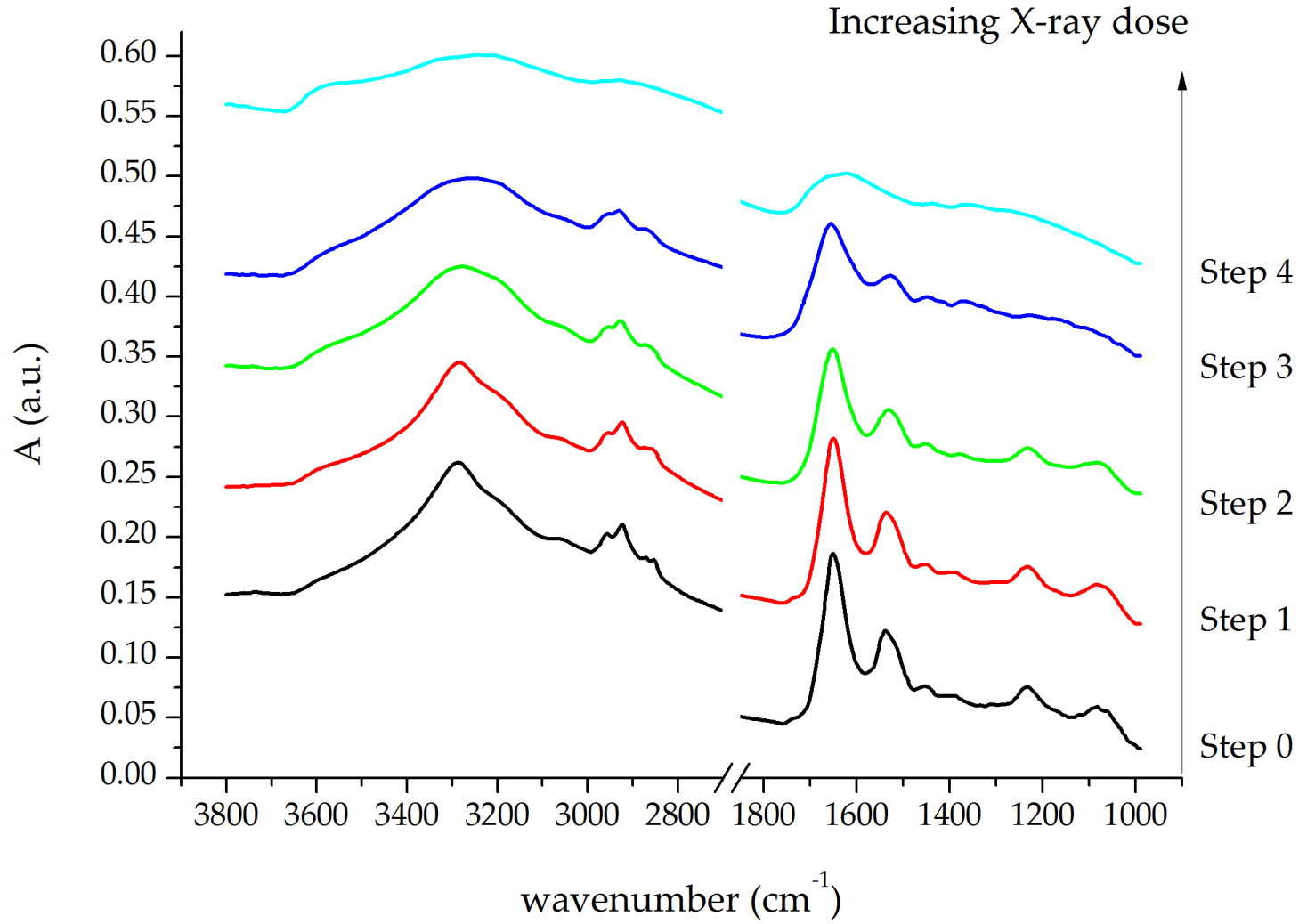
- Progressive reduction of the cell density with increasing X-ray dose

A. Gianoncelli, L. Vaccari, G. Kourousias, D. Cassese, D.E. Bedolla, S. Kenig, P. Storici, M. Lazzarino, M. Kiskinova "Soft X-Ray Microscopy Radiation Damage On Fixed Cells Investigated With Synchrotron Radiation FTIR Microscopy" **Scientific Reports** 5:10250 2015

Elettra Sincrotrone Trieste

TwinMic

FTIRM Outcomes



A. Gianoncelli, L. Vaccari, G. Kourousias, D. Cassese, D.E. Bedolla, S. Kenig, P. Storici, M. Lazzarino, M. Kiskinova "Soft X-Ray Microscopy Radiation Damage On Fixed Cells Investigated With Synchrotron Radiation FTIR Microscopy" **Scientific Reports** 5:10250 2015

Elettra
Sincrotrone
Trieste

research papers

Synchrotron JSR JOURNAL OF SYNCHROTRON RADIATION

ISSN 1600-5775

Effects of soft X-ray radiation damage on paraffin-embedded rat tissues supported on ultralene: a chemical perspective

Diana E. Bedolla,[a]* Andrea Mantuano,[b,c] Arissa Pickler,[d] Carla Lemos Mota,[c,d] Delson Braz,[d] Camila Salata,[e] Carlos Eduardo Almeida,[c] Giovanni Birarda,[a] Lisa Vaccari,[a] Regina Cély Barroso[b] and Alessandra Gianoncelli[a]*

Received 22 December 2017
Accepted 24 February 2018

- Soft X-ray radiation damage of liver and kidney tissues after different fixation procedures
- The fixatives used were as follows: 10% neutral buffered formalin (4% formaldehyde) (**F**), 2.5% glutaraldehyde in 0.1 M sodium cacodylate buffer, pH 7.2 (**G**) and Karnovsky (2.5% glutaraldehyde, 4% paraformaldehyde in 0.1 M sodium cacodylate buffer, pH 7.2) (**K**).

- G and K protocols show the least tolerance to soft X-ray radiation, while F protocol starts showing some degradation at higher radiation doses.

- Our results show that both ultralene and paraffin undergo dose-dependent radiation damage, inducing oxidation of the materials, revealed by the appearance of hydroxyl and carbonyl spectral features and by water physisorption.
- This suggests that the radiation damage process withstood by the specimens is more complex than in isolated biological tissues.

Elettra Sincrotrone Trieste

Synchrotron JSR JOURNAL OF SYNCHROTRON RADIATION

ISSN 1600-5775

Oxidation of ultralene and paraffin due to radiation damage after exposure to soft X-rays probed by FTIR microspectroscopy and X-ray fluorescence

Diana E Bedolla,[a,b]* Giovanni Birarda,[a] Sabina Giannotta,[c] Valentina Faoro,[c] Alberto Cescato,[c] Lisa Vaccari[a] and Alessandra Gianoncelli[a]

Received 25 May 2020
Accepted 6 November 2020

[a]Elettra-Sincrotrone Trieste, SS 14 Km 163.5 in Area Science Park, Basovizza, TS 34149, Italy, [b]Area Science Park, Padriciano 99, Padriciano, TS 34149, Italy, and [c]Laboratori Riuniti – Synlab, Via delle Mura 2, Trieste, TS 34121, Italy. *Correspondence e-mail: diana.bedolla@elettra.eu

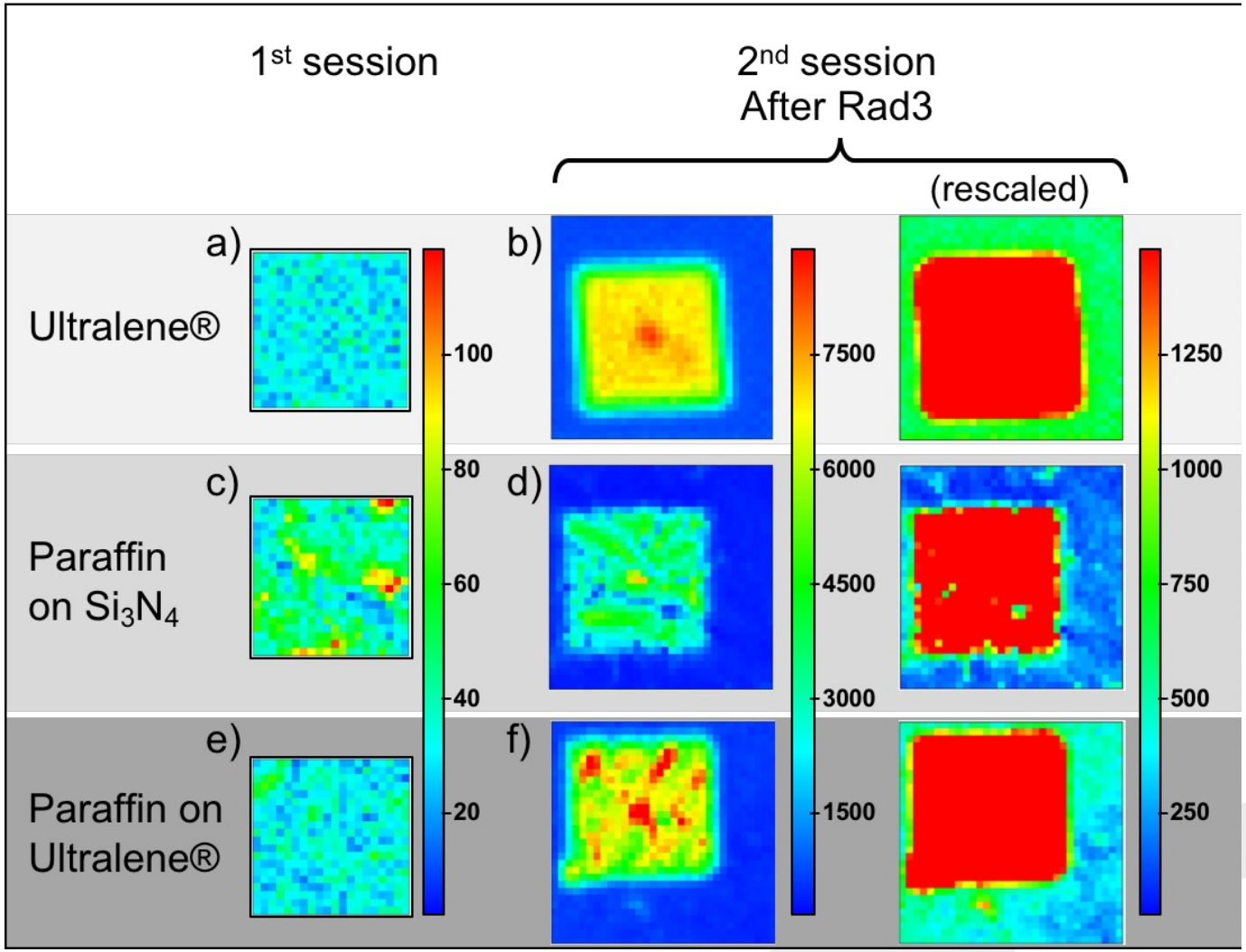
- an oxidation of both embedding medium and ultralene substrate takes place after the irradiated sample is exposed to air. This oxidation is reflected in a clear increase of C O and O—H infrared bands and on the XRF oxygen maps
- we believe that the oxidation is promoted by radicals formed in the irradiated film that further react with the environmental oxygen and water
- It appears that when still in the vacuum chambers, the highest irradiation doses cause a temporary mass loss in the exposed material – polymeric chain breaking – whereas after exposure to air, the material appears darker, less transparent, which indicates a denser state, further supporting the hypothesis of an oxidation process happening in response to air exposure
- the generation of radicals and dangling bonds requires a certain energy delivery. When this threshold is surpassed, the oxidation proceeds more rapidly and the number of oxidized species increases in time, even without further exposure

Oxygen increase after exposure to air

Ultralene and paraffin on ultralene seem to be more prone to be affected, while Si3N4 is less affected

Upon exposure, it has been observed that the long aliphatic chains break. This leads to the generation of radicals that can diffuse into the film, further damaging the intact polymeric chains. Chain rupture can also generate dangling bonds that can be subsequently oxidized when exposed to air.

The trend increases with dose and time



Elettra Sincrotrone Trieste

JOURNAL OF SYNCHROTRON RADIATION

ISSN 1600-5775

Soft X-ray induced radiation damage in thin freeze-dried brain samples studied by FTIR microscopy

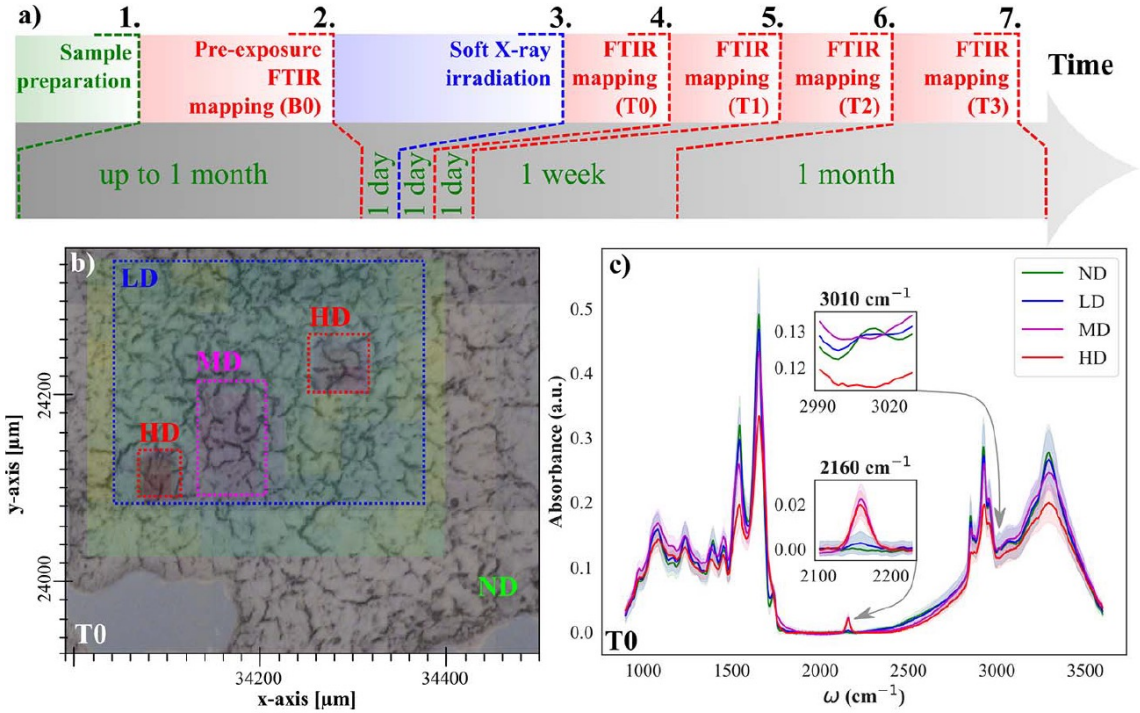
Artur D. Surowka,[a,b]* A. Gianoncelli,[a] G. Birarda,[a] S. Sala,[a] N. Cefarin,[a,c] A. Matruglio,[d] M. Szczerbowska-Boruchowska,[b] A. Ziomber-Lisiak[e] and L. Vaccari[a]

[a]Elettra-Sincrotrone Trieste SCpA, SS 14, km 163.5, Basovizza, TS 34149 Trieste, Italy, [b]AGH University of Science and Technology, Faculty of Physics and Applied Computer Science, al. Mickiewicza 30, Krakow 30-059, Poland, [c]IOM-CNR Laboratorio TASC, c/o Area Science Park, Basovizza, Trieste, Italy, [d]Department of Chemical Engineering, University College London, London, United Kingdom, and [e]Chair of Pathophysiology, Faculty of Medicine, Jagiellonian University, ul. Czysta 18, Kraków 31-121, Poland. *Correspondence e-mail: asurowka@agh.edu.pl

Received 30 January 2020
Accepted 21 July 2020

- The freeze-dried tissue samples were found to be affected by general degradation of the vibrational architecture, though these effects were weaker than those observed in paraffin-embedded and hydrated systems reported in the literature.

- In addition, weak, reversible and specific features of the tissue–Si_3N_4 interaction could be identified for the first time upon routine soft X-ray exposures, further highlighting the complex interplay between the biological sample, its preparation protocol and X-ray probe



Elettra Sincrotrone Trieste

Reversible effect on Si3N4 and SiC

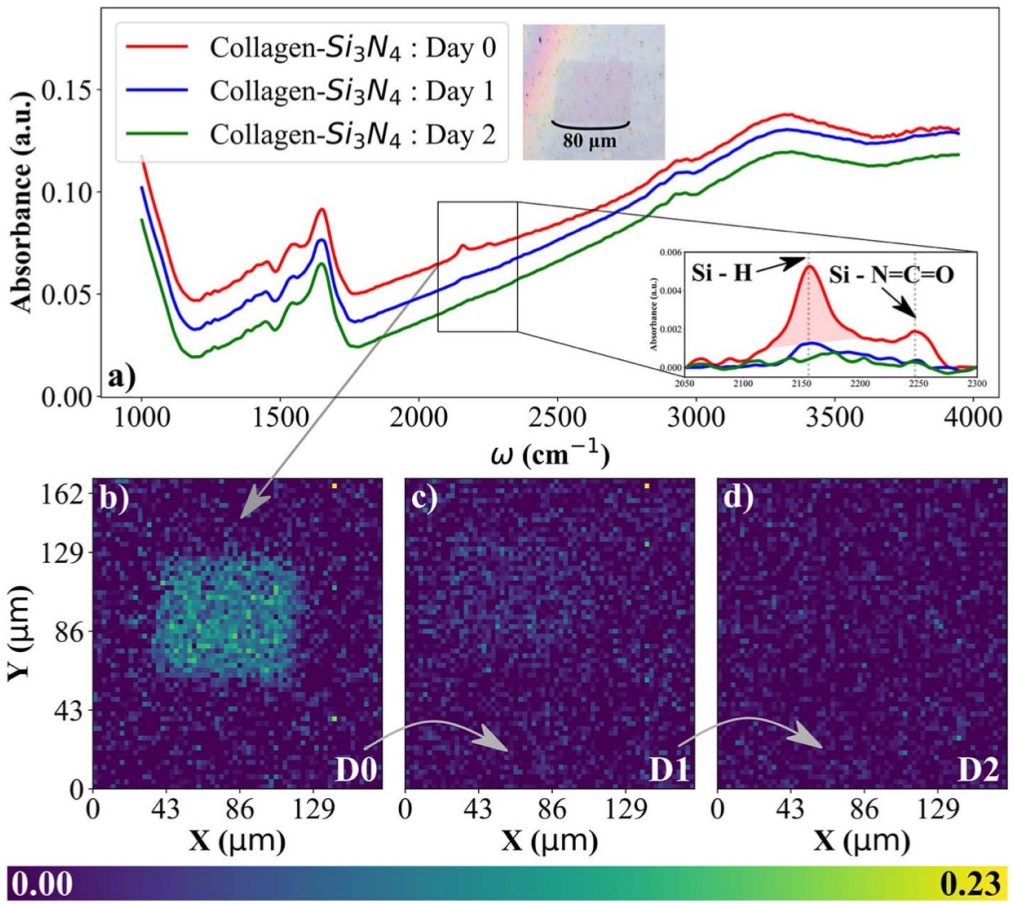


Figure 4

(*a*) Average, time-dependent FTIR spectra of the collagen–Si_3N_4 system (the insets show the optical image of the sample and zoom-in of the 2050–2300 cm^{-1} spectral range); chemogram image for the integrated (2120–2200 cm^{-1}) peak area of the Si—H band: (*b*) right after; (*c*) day after; (*d*) two days after the HD irradiation.

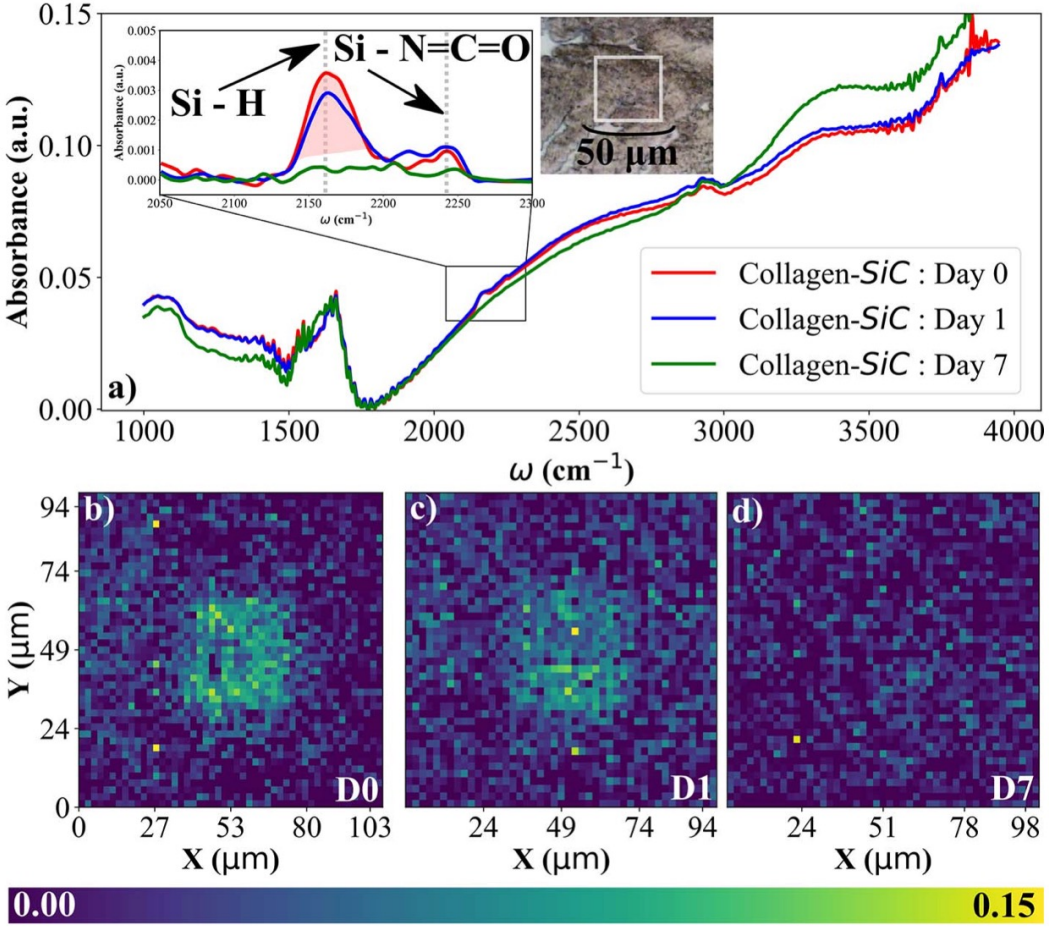


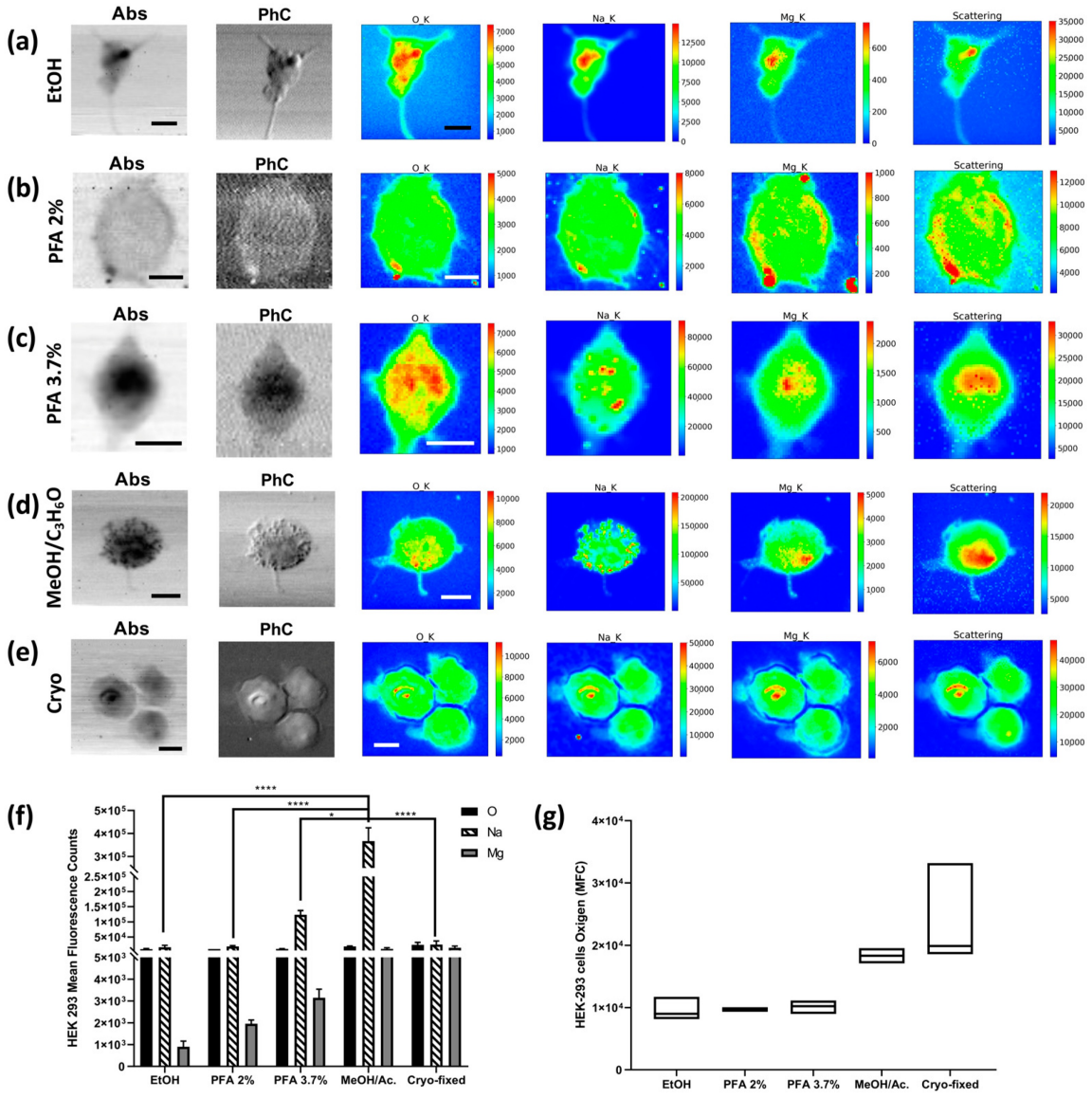
Figure 5

(*a*) Average, time-dependent FTIR spectra of the collagen–SiC system, truncated to the 2050–2300 cm^{-1} spectral range; chemogram image for the integrated (2120–2200 cm^{-1}) peak area of the Si—H band: (*b*) right after; (*c*) a day after; (*d*) seven days after the HD irradiation.

Elettra Sincrotrone Trieste

TwinMic

- **Sample preparation affects reulsts**

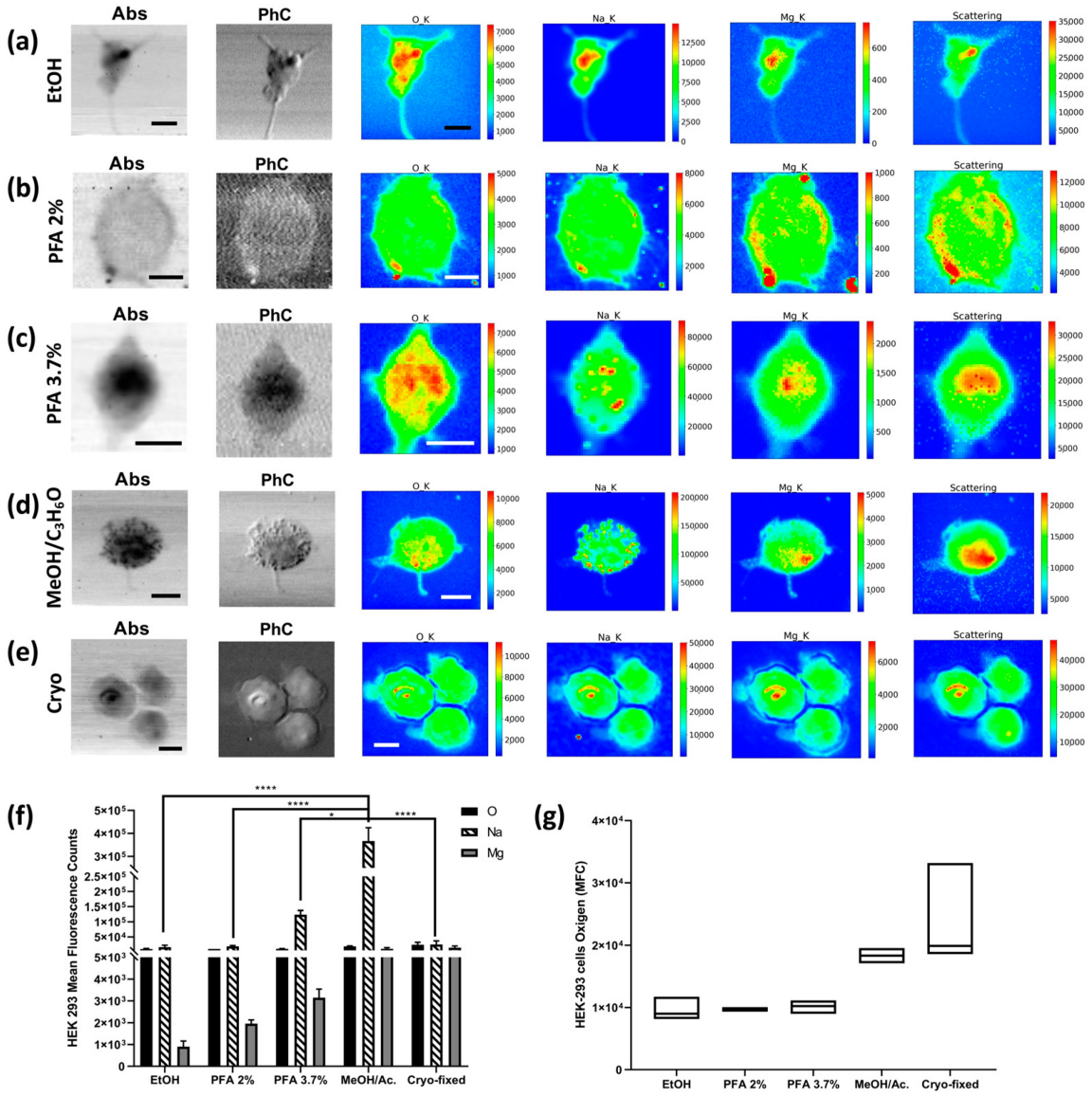


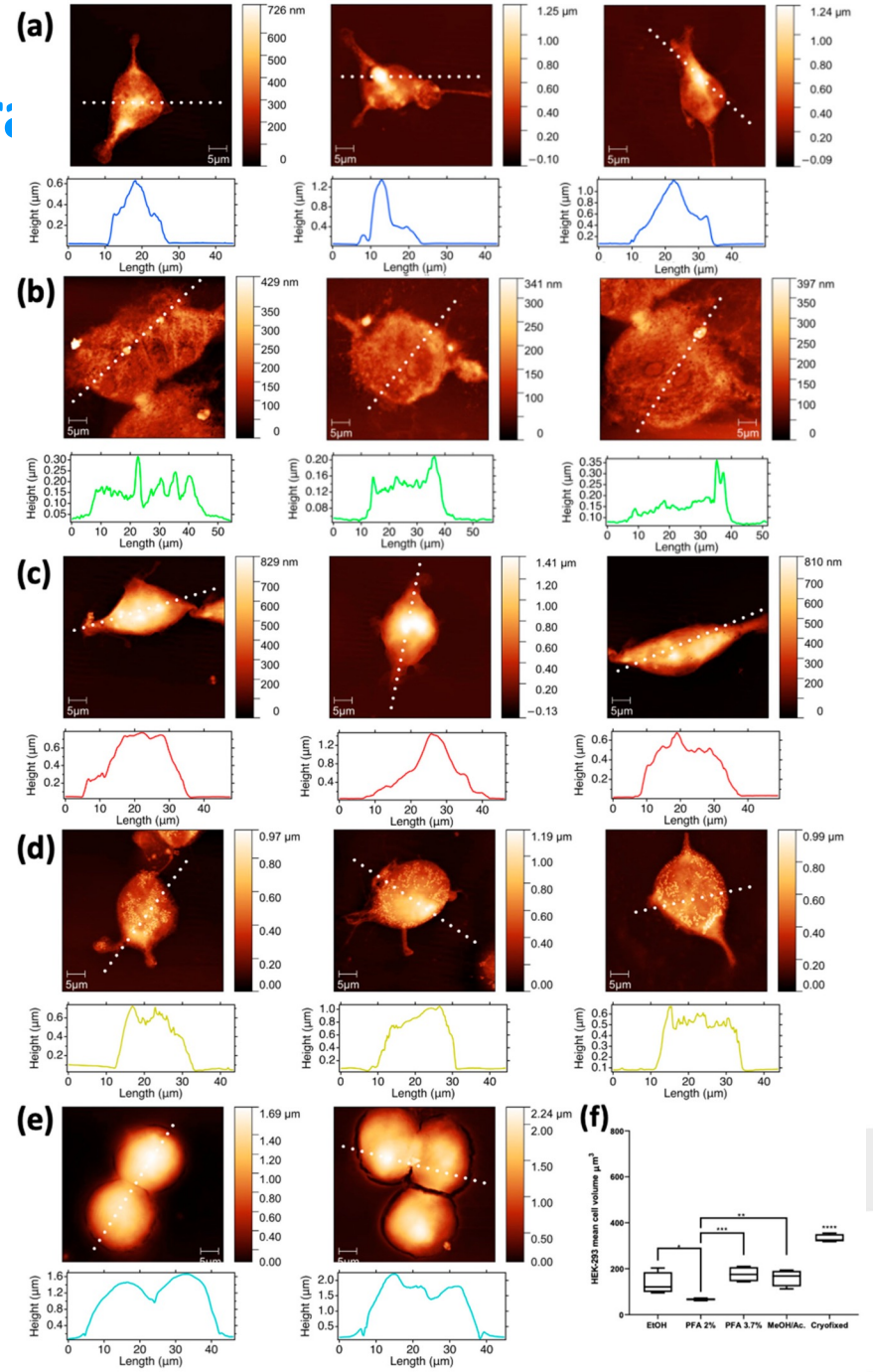
Merolle, L. et al. Impact of Sample Preparation Methods on Single-Cell X-ray Microscopy and Light Elemental Analysis Evaluated by Combined Low Energy X-ray Fluorescence, STXM and AFM. *Molecules* **2023**, *28*, 1992. https://doi.org/10.3390/molecules28041992

Elettra Sincrotrone Trieste

TwinMic

• Sample prepara



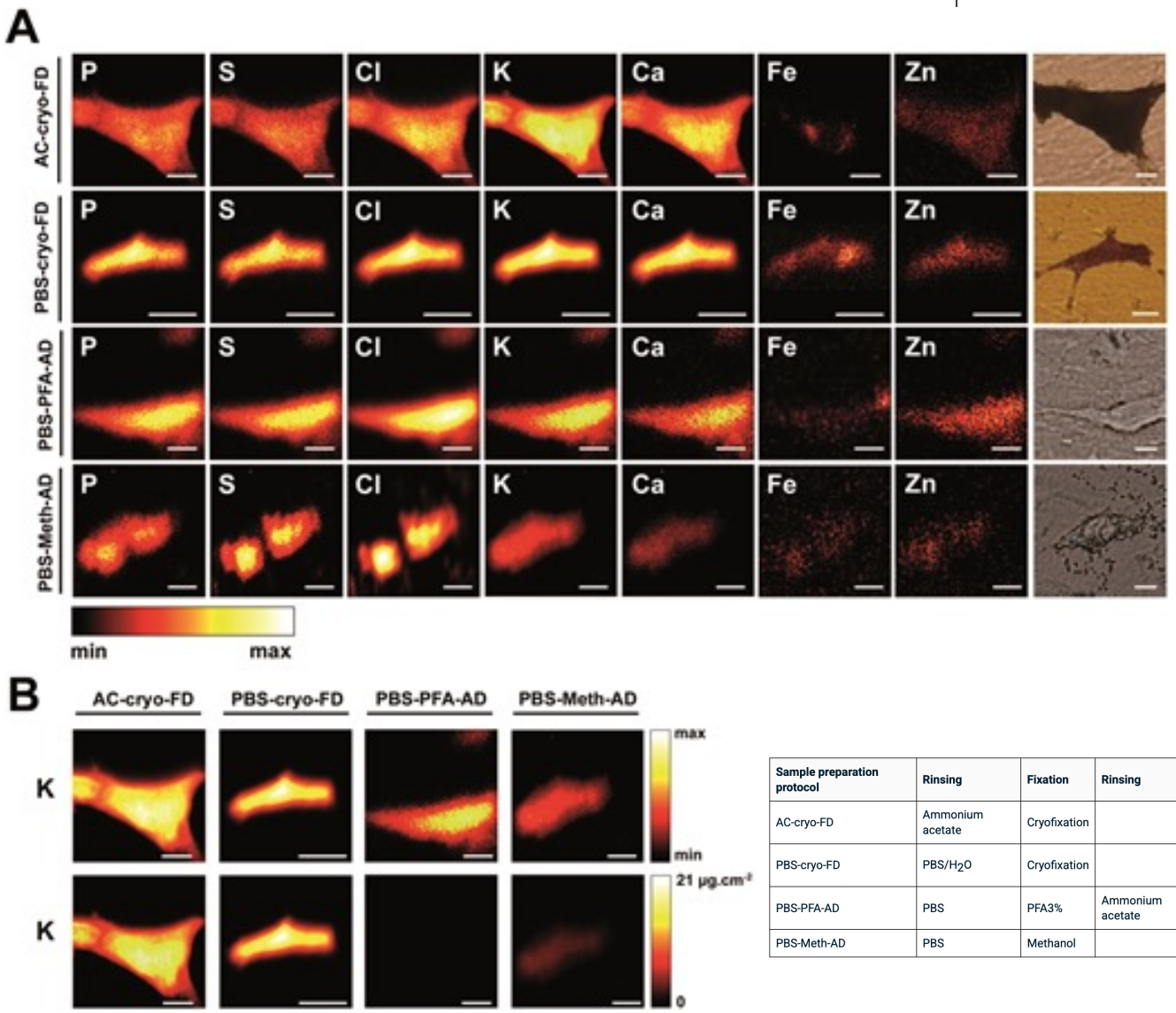


Merolle, L. et al. Impact of Sample Preparation Methods on Single-Cell X-ray Microscopy and Light Elemental Analysis Evaluated by Combined Low Energy X-ray Fluorescence, STXM and AFM. *Molecules* **2023**, *28*, 1992. https://doi.org/10.3390/molecules28041992

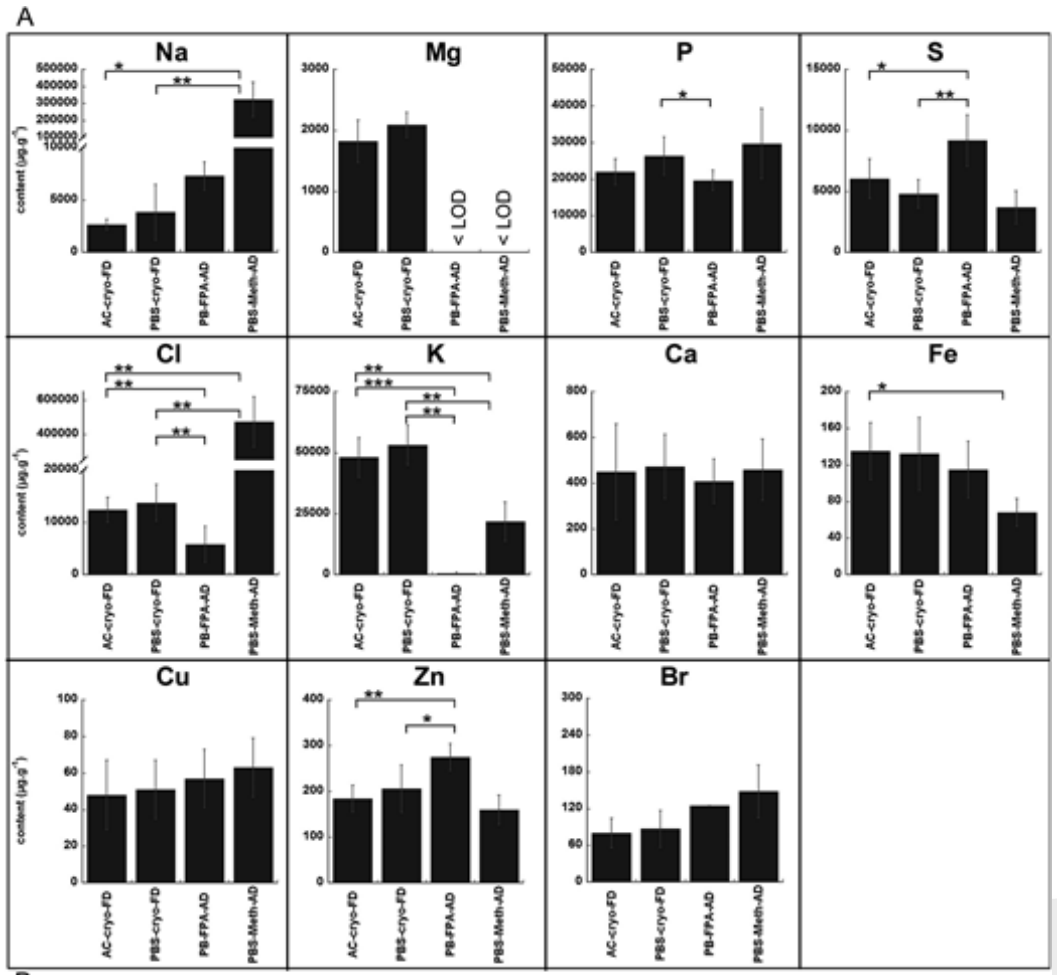
Elettra Sincrotrone Trieste

TwinMic

• Sample preparation affects reulsts



Sample preparation protocol	Rinsing	Fixation	Rinsing	Drying
AC-cryo-FD	Ammonium acetate	Cryofixation		Freeze-drying
PBS-cryo-FD	PBS/H_2O	Cryofixation		Freeze-drying
PBS-PFA-AD	PBS	PFA3%	Ammonium acetate	Air
PBS-Meth-AD	PBS	Methanol		Air



B

	AC-cryo-FD	PBS-cryo-FD	PBS-PFA-AD	PBS-Meth-AD
K/Na	18.24	13.88	0.09	0.07
Cl/K	0.26	0.26	9.22	21.80

L. Perrin et al.; Evaluation of sample preparation methods for single cell quantitative elemental imaging using proton or synchrotron radiation focused beams. *J. Anal. At. Spectrom.* 2015; 30 (12): 2525-2532.

Elettra Sincrotrone Trieste

Summary and challenges

- X-ray spectro-microscopy has proven to be a valuable tool for exploring morphologically complex matter, including bio-systems at cellular and sub-cellular level.
- A limited number of samples can be analysed due to the relatively difficult access to synchrotron facilities
- Correlative research is essential (FTIR, PIXE, EM, lab-related bulk analysis & others)
- Multimodal imaging is a plus
- Improving efficiency of synchrotron imaging (higher number of samples, faster imaging…)
- Radiation damage
- Sample preparation may affect the reults

Elettra
Sincrotrone
Trieste

Acknowledgements

Current colleagues:
Milan Zizic
Valentina Bonanni

Federica Zingaro

Maya Kiskinova

Scientific Computing:
Georgios Kourousias
Fulvio Bille'

Past colleagues:
Gianluca Gariani
Simone Sala
Diana Bedolla
Matteo Altissimo
Majid Kazemian
David Jersersek
Burkhard Kaulich

L. Pascolo, G. Ricci et al. (Burlo Hospital, Trieste)
K. Vogel-Mikus et al. (Josef Stefan Institute, Ljubljana, Si)
M. Bordiga (OGS, Trieste)
A. Santucci et al. (University of Siena)
A. Marcello (ICGEB)
G. Ceccone, P. Marmorato et al. (JRC, Ispra)
L. Merolle et al. (Reggio Emilia Hospital)
R. Barroso, G, Sena Souza et al. (University of Rio de Janeiro, Brazil)
S. Raneri (University of Pisa)
G. De Giudici, D. Medas (University of Cagliari, Cagliari, Italy)
E. Lombi (Uni of South Australia, Australia)
P. Kopittke (Uni of Queensland, Australia)
E. Malucelli, S. Iotti, S. Lagomarsino (Uni Bologna, Italy)
M. Marmiroli (University of Parma, Parma, Italy)
C. Poitry-Yamate (EPFL, Switzerland)
M. Jones, G. Van Riessen (La Trobe University, Melbourne, Australia)
G.R. Morrison et al (University College London, UK)
B. Bozzini et al (Politecnico di Milano, Milano, Italy)
D. Paterson, M de Jonge (Australian Synchrotron, Melbourne, Australia)
A. Surowka (Crakow University, Poland)

and many many others...

Elettra
Sincrotrone
Trieste



www.elettra.eu